Exploiting Metabolic Vulnerabilities In Solid Tumors Treated With ABL Kinase Allosteric Inhibitors

by

Jillian Hattaway Luttman

Department of Pharmacology & Cancer Biology
Duke University

Date:_______________________
Approved:

____
Ann Marie Pendergast, Supervisor

____
Donald McDonnell

____
Chris Newgard

____
Nancie MacIver

____
Deborah Muoio

____
Jen-Tsan Ashley Chi

Thesis submitted in partial fulfillment of
the requirements for the degree of Doctor
of Philosophy in the Department of
Pharmacology & Cancer Biology in the Graduate School
of Duke University

2021

Exploiting Metabolic Vulnerabilities In Solid Tumors Treated With ABL Kinase Allosteric Inhibitors

by

Jillian Hattaway Luttman

Department of Pharmacology & Cancer Biology
Duke University

Date:_______________________
Approved:

____
Ann Marie Pendergast, Supervisor

____
Donald McDonnell

____
Chris Newgard

____
Nancie MacIver

____
Deborah Muoio

____
Jen-Tsan Ashley Chi

An abstract of a thesis submitted in partial
fulfillment of the requirements for the degree
of Doctor of Philosophy in the Department of
Pharmacology & Cancer Biology in the Graduate School of
Duke University

2021

Abstract

Metastases are common and devastating complications linked to ~90% of cancer deaths. Therapy-resistance is a major challenge for the treatment of cancer cell metastasis as metastatic cells metabolically rewire to survive cytotoxic therapies and adapt to new environments. Understanding and effectively targeting these metabolic changes opens an entirely new therapeutic avenue for combating cancer by defining cancer-related metabolic vulnerabilities. Using a CRISPR/Cas9 loss-of-function screen and RNA-sequencing analysis, the studies presented herein identify two metabolic vulnerabilities that arise following ABL allosteric inhibitor treatment to target metastatic and therapy-resistant cancer cells. First, we identify a novel combination therapy of ABL kinase allosteric inhibitors with lipophilic statins that impairs growth of clinically relevant therapy-resistant and brain metastatic lung cancer cells *in vitro* and in *in vivo* using mouse models. We found that ABL allosteric inhibitors impair mitochondria function without altering glycolytic capacity, leading to sensitization to statin therapeutics, and enhanced synergy to promote cancer cell death by combination therapy. Further, we found that ABL inhibitors are sensitized to statins due to the ability of statin therapeutics to inhibit the isoprenoid pathway, specifically protein geranylgeranylation. These results reveal a potential striking clinical benefit as synergy was not noted upon combination with standard of care therapeutics, gefitinib and

docetaxel, and identify a new treatment strategy for patients refractory to first-line therapeutics or with metastases to difficult to treat organs like the brain.

We have also characterized a novel ABL signaling axis as ABL inhibition was shown to deplete SLC7A11 protein levels in cancer cells. SLC7A11 is the catalytic subunit of system xCT and enables cystine import for cell detoxification and concomitant glutamate export. By depleting cancer cells of SLC7A11, cell detoxification processes are limited and excretion of toxic glutamate levels into the tumor microenvironment decrease. These data suggest that ABL regulation of this pathway could extend survival and relieve harmful symptoms in patients experiencing primary and secondary metastatic tumors. Collectively, our findings reveal metabolic vulnerabilities that can be targeted in cancer cells through treatment with ABL allosteric inhibitors, leading to improved patient survival and quality of life.

Contents

List of Tables

List of Figures

Acknowledgements

I would like to thank my mentor, Ann Marie Pendergast, for her support and encouragement during my growth as a graduate student and scientist. I would like to acknowledge the members of the Pendergast lab for helpful and thought-provoking discussions. Particularly, I would like to acknowledge the important contributions of Jacob Hoj and Kevin Lin to the project detailed in Chapter 2. I would like to thank members of the MacIver, McDonnell and Eroglu laboratories for graciously sharing reagents and scientific advice. I would like to thank Nancie MacIver, Donald McDonnell, Chris Newgard, Ryan Soderquist, and Wen Liu for helpful discussions. In addition, I would like to thank my thesis committee members, Donald McDonnell, Chris Newgard, Nancie MacIver, Deborah Muoio, Jen-Tsan Ashley Chi, and Ann Marie Pendergast. I would like to thank the funding resources that have supported this research: National Science Foundation Graduate Research Fellowship under Grant No. DGE 1644868 and a grant from the Duke Proteomics and Metabolomics facility.

Lastly, I would like to thank my family and friends who have supported me tremendously during my PhD. Having them by my side and their support has encouraged me to complete my PhD and I am tremendously thankful. Particularly, I am grateful to my amazing husband Harrison for his constant patience, encouragement, and love. I am also thankful for my mother who never stopped encouraging me even while undergoing multiple surgeries and radiation treatment for brain cancer during my PhD. Her ever-present love and her battle with cancer helped fuel my passion and drive. This dissertation is dedicated to both of them.

1. Introduction

Sections from this chapter are published in *Cell Communication and Signaling*, 2021

1.1: Background on solid tumor metastasis

Metastasis is the process whereby cancer cells spread from the primary tumor to surrounding tissues and distant organs (1-3). Metastases are common and devastating complications linked to ~90% of cancer deaths (4). Despite being a significant factor affecting patient overall survival, the mechanisms behind this process remain poorly understood. The progression of the metastatic cascade begins with invasion of primary tumor cells into surrounding tissue, intravasation of cancer cells into the blood stream, migration through the circulatory system, extravasation into a distal organ, and colonization at distant sites (5). To successfully achieve these feats, cancer cells must activate gene regulatory networks that enable and drive these processes so that they can evade the immune system and survive in new environments.

As cancer cells adapt to new environments, they will genetically and metabolically rewire to survive in these new niches. This makes the treatment of metastases difficult as their genetic and metabolic profiles are disparate from the primary tumor allowing them to evade cancer therapies, which often leads to treatment relapse (6, 7). Additionally, other forms of adjuvant care such as surgery and radiation can be difficult to perform due to the anatomically diffuse localization of metastases. Thus, further understanding into the rewiring that occurs as cancer cells travel to distal sites will enable new therapies to treat these devastating complications. This dissertation will provide an overarching description of known metabolic perturbations in tumors and highlight exciting new findings to treat patients with these cancerous lesions.

1.2 Metabolic rewiring in solid tumors

Metabolic reprogramming is a hallmark of cancer development that occurs following direct or indirect activation of oncogenic mutations as well as in response to chemotherapy, radiation, and immunotherapy (8). In fact, recent work has found that the current metabolic state of cancer cells can help predict how well tumors respond to various forms of therapies (9-12). Often, the microenvironments in which cancer cell metastases reside are nutrient poor causing these cells to shift their metabolic needs and energy processing centers to adapt to their new microenvironment. In general, cancer cells acquire simple nutrients such as sugars, lipids, and proteins from the extracellular space to fuel biosynthetic pathways. These metabolites are catabolized through core metabolic pathways to produce biosynthetic intermediates necessary for cancer growth. Four core metabolic pathways in cancer cells are: glycolysis, the TCA cycle, fatty acid synthesis, and protein catabolism. These four fundamental pathways and their susceptibility to oncogenic rewiring will be reviewed in more detail.

1.2.1 Glycolysis

One of the first examples that cancer cells reprogram their metabolism was observed by Otto Warburg in the 1920s when he found that cancer cells undergo glycolysis under normal oxygen states (13). Generally, glycolysis is a metabolic pathway activated under states of hypoxia, when oxygen levels are low, forcing cells to rely on glucose for energy. Glycolysis begins with glucose uptake from the extracellular environment leading to production of two molecules of pyruvate and ATP from one glucose molecule through oxygen-independent enzymatic reactions (14). The ability of cancer cells to undergo glycolysis in the presence of oxygen has been termed "aerobic glycolysis" (14).

This phenomenon was originally believed to occur because of impaired mitochondrial function in cancer cells, but more recent studies have debunked these claims finding that mitochondrial metabolism is indeed intact. Rather, it is believed that cells undergo aerobic glycolysis because glycolysis-derived ATP is generated much faster than ATP made through oxidative phosphorylation, and excess glycolytic intermediates feed into the pentose phosphate pathway resulting in NADPH and ribose-5-phosphate production (15). Both, NADPH and ribose-5-phosphate are essential for the synthesis of lipids and nucleic acids.

Oncogenic mutations increase the glycolytic pathway by either increasing expression of glucose transporters or increasing the activity of glycolytic enzymes (8). The PI3K/Akt pathway acts as a master regulator of glycolysis by promoting the expression of glucose transporter 1 (GLUT1) as well as GLUT1 translocation to the cell surface (16, 17). Akt also potentiates the activity of hexokinase (HK), a rate-limiting enzyme of the glycolytic pathway that phosphorylates glucose molecules allowing for their movement through the pathway, as well as phosphofructokinase (PFK) enzyme, which catalyzes the key irreversible step of glycolysis (18, 19).

The MYC oncoprotein plays a key role in cancer cell glycolysis as it can directly bind to a classical E-box sequence and activate transcription of a large majority of glycolytic genes (20). MYC can modulate glucose uptake by increasing expression of *SLC2A1* as well as lactate export through inducing expression of *MCT1* and *MCT2 (21, 22)*. Further, glycolytic enzymes such as HK2, GAPDH, and ENO1, are transcriptionally upregulated by MYC (20). MYC was also shown to regulate alternative splicing of pyruvate kinase preferentially promoting processing of *PKM2* over *PKM1* (23). PKM2 has been shown to cause cells to undergo aerobic glycolysis while PKM1 induces oxidative phosphorylation (23).

HIF-1α is a transcription factor that is canonically known for its ability to regulate cellular adaptive responses to hypoxia. Genetic alterations in cancer cells as well as hypoxic stimuli promote HIF-1α expression (24). In addition to its ability to maintain cell fitness in the presence of low oxygen levels, HIF-1α can increase glycolytic activity in cells by inducing transcription of glycolytic enzymes and transporters. HIF-1α stimulates expression of hexokinases 1 and 2, phosphoglycerate kinase 1, and the glucose transporters GLUT1 and GLUT3 (25). HIF-1α also upregulates lactate dehydrogenase A allowing for lactate breakdown into pyruvate and NADH for energy utilization (26-30).

Additionally, HIF-1α can shunt cell metabolism away from the mitochondria by phosphorylating pyruvate dehydrogenase kinases which in turn causes inhibitory phosphorylation of pyruvate dehydrogenase (31). Inhibition prevents pyruvate dehydrogenase from processing pyruvate for entry into the mitochondria as fuel for the citric acid cycle (TCA). It is believed that this inhibitory mechanism helps maintain NADH levels for energy utilization. NADH is oxidized in the mitochondria to fuel the electron transport chain and is regenerated as NAD for glycolysis (32). When this process shuts down, NADH is instead used to convert pyruvate into lactate and NAD is generated following lactate secretion into the extracellular space. By shutting down mitochondrial metabolism, HIF-1α can maintain cellular reliance on glycolytic cycle and cell redox levels. HIF-1α-dependent modification of mitochondrial metabolism has been shown to be beneficial for tumor growth in pancreatic cancers (33).

The oncogenic signaling protein Ras has also been shown to be a master regulator of cancer cell metabolism. Oncogenic activation of RAS can directly and indirectly activate glycolytic enzymes. Ras can directly increase aerobic glycolysis by promoting GLUT1 mRNA expression leading to enhanced glucose import (34, 35). Further, Ras can enhance glycolytic flux by increasing expression of HK2, PFKFB3, and MCT1 (36, 37). Thus, Ras can control cancer cell glycolysis by regulating these key processes: glucose import and phosphorylation, fructose-1,6- bisphosphate production, and lactate export. In an indirect manner, RAS can also modulate glycolysis through upregulating HIF-1α protein synthesis through the RAS/RAF/MEK/ERK signaling cascade (38, 39).

1.2.2 Mitochondrial metabolism

Despite the high glycolytic rates of most cancer cells, mitochondrial metabolism generates the majority of ATP and is necessary for cancer cell proliferation and tumorigenesis (14, 40, 41). Mitochondrial ATP production is supplied not only by pyruvate from glycolysis but also fatty acids and amino acids which serve as substrates for the citric acid cycle (TCA). Fatty acids are broken down through beta-oxidation to generate acetyl-CoA and reducing molecules NADH and FADH2 (14). NADH and FADH2 are used by the electron transport chain (ETC) to facilitate the hydrogen pump to produce ATP. Branched chain amino acids like isoleucine, valine, and leucine are converted into acetyl-CoA for entrance into the TCA cycle (42). The amino acid glutamine undergoes a process called glutaminolysis where it is converted into glutamate and subsequently α-ketoglutarate to fuel the TCA cycle (43). The flexibility of the TCA cycle to rely on multiple metabolic inputs allows cancer to adapt to changing environments during tumor growth and progression.

Cancer cells have an increased basal mitochondrial respiration rate in comparison to non-oncogenic counterparts. Because of this, mitochondria produce more reactive oxygen species (ROS) than normal cells and this helps facilitate activation of oncogenic signaling pathways such as PI3K, MAPK/ERK, HIF, and NF-κB (44-46). Oncogenic mutations and the tumor microenvironment contribute to this increased rate of ROS production and it has been shown that increased ROS levels enable tumor progression (47). Interestingly, treatment with antioxidants has been shown to decrease the growth of some tumors (47-49).

Activation of oncogenes and loss of tumor suppressors can have direct or indirect consequences on mitochondria function or metabolism during tumor formation. Several oncogenic mutations that can affect mitochondrial activity include PI3K/Akt/mTOR, Myc, p53, and BCL2. PI3K/Akt/mTOR activation can redirect carbon flux from glucose molecules into biosynthetic pathways that reprogram citrate metabolism in the mitochondria and increases anabolic mitochondrial metabolism (50). Additionally, mTOR can upregulate glutaminolysis to increase α-ketoglutarate uptake in the TCA cycle by inhibiting SIRT which activates glutamate dehydrogenase (51). Expression of mitochondrial SHMT (SHMT2) partially restores survival of c-Myc-null cells, as discovered during a functional screen of Myc-responsive cDNAs in cells deplete of Myc (52). SHMT2 breaks down serine into one-carbon units and glycine, and has been shown to be required for efficient cell respiration as products of SHMT2 help assemble complex I of the ETC (53). Myc can also upregulate expression of GLUT1 to increase glucose transport and GLS for glutamine metabolism.

p53 has also been shown to affect mitochondrial function in part by regulating α-ketoglutarate levels, as loss of p53 decreases α-ketoglutarate while expression of wild-type p53 increases α-ketoglutarate in pancreatic cells (54). Additionally, increased expression of α-ketoglutarate in p53 deplete cells antagonizes malignant growth. p53 null cells also have increases in the anti-apoptotic protein BCL2 (55). BCL2 can prevent activation of downstream apoptotic proteins like Bax and Bak and inhibit mitochondrial-induced cell death (56). Expression of wild-type p53 in p53 null cells caused a shift in this balance and a decrease in BCL2 levels, while subsequently increasing Bax levels and initiating cell death (55). BCL2 can also directly affect oxidative phosphorylation as inhibition of BCL2 in acute myelogenous leukemia stem cells reduced mitochondrial respiration and eradicated quiescent stem cells (57).

1.2.3 Lipid synthesis

Tumorigenesis is associated with rapid production of fatty acids for membrane biosynthesis. Increased levels of saturated fatty acids in the cell membranes protects against oxidative stress (58). Lipid synthesis requires acetyl-CoA and NADPH. Often, cancer cells will rely on glucose for acetyl-CoA sources, but glutamine and acetate have also been shown to provide alternative sources of acetyl-CoA (59, 60). Citrate can also be converted into acetyl-CoA by acetyl-CoA carboxylase (ACLY). To synthesize fatty acids, acetyl-CoA will be processed by acetyl-CoA carboxylase (ACC) to make malonyl-CoA which will then be used by fatty acid synthase (FASN) to assemble long chain fatty acids. Malonyl-CoA can also be diverted for production of cholesterol, a type of lipid that contains a sterol group, which has been shown to enable tumor growth.

The SREBP family of transcription factors, SREBP-1 and SREBP-2, are considered master regulators of lipid homeostasis. SREBP-1 regulates genes that either catalyze or promote fatty acid synthesis (61). When lipid levels are high, SREBP-1 is sequestered in the endoplasmic reticulum, but, when lipid levels decrease, SREBP-1 is released from the endoplasmic reticulum and can travel into the nucleus to activate target gene expression. SREBP-1 promotes transcription of ACLY, ACC, and FASN, which are frequently upregulated in cancer cells and inhibition of these components effects tumorigenesis (62-65). SREBP-2 is primarily responsible for the activation of genes in cholesterol biosynthesis (66).

Uptake of lipids and fatty acids from the extracellular environment can also occur simultaneously to intracellular lipid biosynthesis to support membrane synthesis. Low-density lipoprotein receptor (LDLR) is responsible for taking up cholesterol-carrying lipoproteins and inhibition of LDLR can decrease tumor progression (67). Further, expression of oncogenes can affect both lipid synthesis and uptake. Oncogenic expression of PI3K or Ras can upregulate SREBP-1 expression through activation of mTORC1 causing enhanced lipogenesis (68). High levels of mTORC1 are associated with increased mRNA and protein of SREBP-1 as well as activation of several SREBP-1 transcriptional targets (50). Both SREBP-1 and LDLR are activated by epidermal growth factor receptor (EGFR) in gliomas and cancer cells are sensitive to fatty acid and cholesterol synthesis inhibitors (69).

1.2.4 Glutaminolysis

Glutaminolysis is the production of α-ketoglutarate from glutamine. It is a necessary process as α-ketoglutarate is used as an anaplerotic substrate in the TCA cycle, meaning that α-ketoglutarate will help restore the supply of carbon to offset the release of intermediates for anabolism, and α-ketoglutarate produces reducing agents for oxidative phosphorylation (70). To produce α-ketoglutarate, glutamine is first converted into glutamate by glutaminases encoded by the *GLS* and *GLS2* genes (71). Subsequently, glutamate undergoes catalysis into α-ketoglutarate either through oxidative deamination by glutamate dehydrogenase (GDH) in the mitochondria or by transamination in either the cytosol or the mitochondrion. Glutamate is also a precursor to production of the antioxidant glutathione and also serves as a source of amino groups for nonessential amino acids.

Myc driven cancer cells are highly sensitive to glutamine depletion. Myc drives glutamine uptake and stimulates expression of GLS enzymes (72). Elevated expression of GLS enzymes in tumors has been shown to be directly correlated with growth rate and malignancy (73-75). Glutamine deprivation in Myc transformed cancer cells causes reduction in TCA cycle intermediates and TCA cycle flux, decreased ATP levels, and apoptosis (76, 77). Silencing of GLS enzymes produced similar phenotypes to glutamine depletion. *KRAS*-driven pancreatic cancer cells also rely on glutamine for growth and redox balance (78).

1.3 Pharmacological targeting of metabolic pathways

Effectively targeting metabolic pathways in tumors has been the focus of a growing field of cancer therapy. Finding the exact therapeutic window in which to treat and the appropriate drug combination that also minimizes toxicity to the patient has remained a major challenge. However, some metabolic therapies have shown promise while others need to undergo further assessment.

Inhibitors against key glycolytic enzymes have been developed and used in preclinical studies with mixed efficacy. Many drugs have shown promising antitumor phenotypes but exhibit off targets effects due to expression of their target proteins in non-transformed cells. Among drugs that have shown promising results in clinical trials are lonidamine and 3-BrPA. Lonidamine is a HKII inhibitor (Figure 1). HKII is a rate-limiting enzyme responsible for the first step of glycolysis where glucose is converted into glucose-6-phosphate (15). Lonidamine has completed phase III clinical trials, but its success has been limited by significant pancreatic and hepatic toxicities (79). 3-BrPA is a 3-bromopyruvate analog of pyruvate with specificity against GAPDH (80, 81) (Figure 1). 3-BrPA can inhibit GAPDH causing the production of NADH to become depleted and cellular redox balance to become skewed (82, 83). 3-BrPA is currently in Phase I clinical trials.

Despite the poor vascularization and oxygen availability within the core of many tumors, tumor cells still use mitochondrial respiration as the ETC has been shown to function optimally even at oxygen levels as low as 0.5% (84-86). Thus, inhibitors for the ETC can have efficacy despite oxygen availability. One of the most successful drugs to date is metformin. Metformin is a mitochondrial ETC complex I inhibitor that has been tested in multiple clinical trials in combination with standard of care therapies for anticancer treatment (87) (Figure 1). Metformin is believed to regulate tumor growth through two different mechanisms. The first possible mechanism is its ability to decrease circulating insulin levels, which is important as insulin has been shown to be mitogenic (88). Alternatively, metformin could also be eliciting anti-tumor effects by inhibiting complex I of the ETC. This mechanism may be the most relevant as metformin has had mixed effectiveness in tumor models as tumors expressing lower levels of organic cation transporters (OCTs), metformin intracellular transporters, are less sensitive to metformin treatment (42). Thus, profiling tumors for the expression of OCTs may facilitate prediction of their responsiveness to metformin treatment.

Two other drugs that impair mitochondrial metabolism that are currently undergoing clinical trial testing are venetoclax and telaglenastat (Figure 1). Venetoclax is a BCL-2 inhibitor that has shown efficacy in cancers, such as acute myeloid leukemias, that are reliant on BCL-2 for survival (42). It is currently in phase III clinical trials. Telaglenastat is a glutaminase inhibitor and impairs conversion of glutamine into glutamate (42). Currently, it is in phase II clinical trials and is being tested in combination with the mTOR inhibitor Everolimus or the multi-tyrosine kinase inhibitor Cabozantinib for patients with advanced or metastatic renal cell carcinoma (NCT03163667 and NCT03428217).

Many inhibitors have been developed to target lipid synthesis, uptake, and oxidation, but the most successful in clinical trials to date are TVB-2640 and statins (Figure 1). TVB-2640 is the only FASN inhibitor that has advanced to clinical trials and is currently in phase II clinical trials for patients with KRAS mutant breast and non-small cell lung cancers (NCT03179904 and NCT03808558). Statins are FDA-approved inhibitors that target HMGCR and inhibit cholesterol production (89). Preclinical studies have shown anticancer capabilities of statins, but studies in patients where these drugs have been used in combination with standard of care therapies have had mixed results (90).

Current attempts to clinically target glutaminolysis have focused on inhibiting the enzymes encoded by the glutaminase genes *GLS* and *GLS2*. Various inhibitors targeting theses enzymes cause decreased cancer growth in preclinical studies (91-95). Of these inhibitors, CB-839, is currently in phase I/II clinical trials for patients with colorectal, lung, and metastatic sold tumors (NCT04265534, NCT03965845, NCT03263429, NCT03047993, NCT02861300). Further work will be needed to understand the correct drug combinations and therapeutic windows for the described metabolic inhibitors in order to harness their full anticancer abilities.

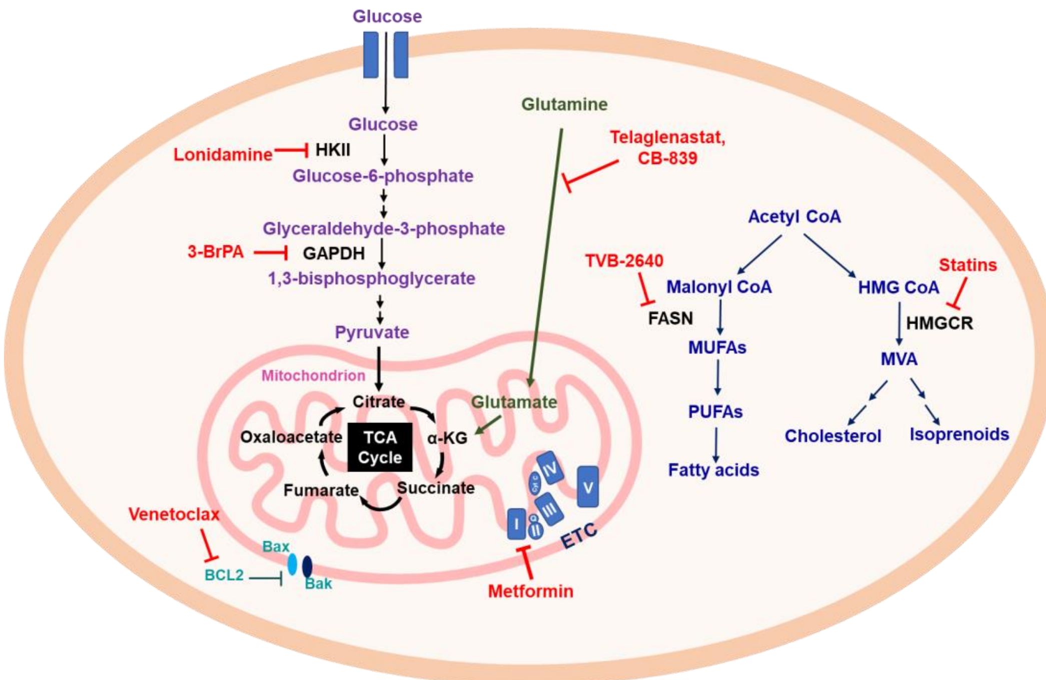

Figure 1: Diagram of metabolic pathways with FDA-approved inhibitors. FDA inhibitors (shown in red) and their target enzymes in the following metabolic pathways: glycolysis, mitochondrial metabolism, glutaminolysis, fatty acid production, and cholesterol synthesis.

1.4 The Abelson family of non-receptor tyrosine kinases

Tyrosine kinases regulate a vast array of cellular signaling networks necessary for processes such as survival, growth, migration, and invasion. Regulation of these processes is required for proper mammalian development and cellular homeostasis (96). The Abelson (ABL) family of tyrosine kinases ABL1 (c-ABL) and ABL2 (ABL-related gene, ARG) regulate diverse cellular processes during development and normal homeostasis, but ABL kinases are aberrantly activated during tumor progression, metastasis, tissue injury responses, inflammation, neural degeneration and other diseases (97-106). ABL kinases are activated by diverse stimuli including but not limited to growth factors, adhesion receptors, chemokines, oxidative stress, and DNA damage (107). Upon activation, ABL kinases can alter the cytoskeletal network necessary for cell migration, adhesion, polarity, phagocytosis and motility (108). In solid tumors, activated ABL kinases can promote invadopodia formation, invasion, and diverse cellular processes implicated in the epithelial-mesenchymal transition (EMT) and subsequent steps in the metastatic cascade.

ABL1 was initially identified as a driver of leukemia in mice and humans (109, 110). Subsequently, ABL1 and ABL2 were shown to promote solid tumor progression and metastatic dissemination (99, 101, 106, 111-113). In the context of solid tumors, ABL kinases are upregulated due to enhanced gene expression and/or enzymatic activation by oncogenic drivers, such as receptor tyrosine kinases (RTKs) and chemokine receptors (107). Upon activation, ABL kinases can potentiate cancer cell survival, proliferation, migration, and invasion, depending on the cellular context. In this review, we will focus on the role of ABL kinases in regulating downstream targets implicated in EMT as well as distinct cellular processes required for metastatic dissemination. Recent reports have revealed that inhibition of the ABL kinases can decrease tumor outgrowth and impair metastatic spread, indicating the potential use of ABL kinase inhibitors for the treatment for some solid tumors with activated ABL kinases (97, 99-101, 105, 106, 112, 114-117).

1.4.1 Structure and regulation of ABL kinase function and activity

ABL kinases are a family of non-receptor tyrosine kinases (nRTKs) consisting of two paralogs, ABL1 and ABL2 (Figure 2A). ABL1 was first discovered as the cellular homolog of the Abelson murine lympho-sarcoma virus (A-MuLV) (109). It was later discovered that constitutive activation of ABL1 upon fusion with the breakpoint cluster region (BCR) generated the BCR-ABL1 oncoprotein responsible for driving several forms of human leukemia (110). ABL2 was later identified using a sequence homology search (118). While the oncogenic ABL proteins exhibit constitutively active kinase activity, the endogenous ABL kinases cycle between inactive and active conformations dependent on intra-and inter-molecular interactions (Figure 2B).

The amino (N)-terminal domain of the ABL kinases contains highly conserved regulatory SRC homology (SH) 3 (SH3) and SH2 domains, followed by the kinase or SH1 domain. While the SH3-SH2-SH1 cassette is shared by 19 of the 22 human non-receptor tyrosine kinases (nRTKS), the SH3-SH2-SH1 domains of human ABL1 and ABL2 are more highly conserved (92%) to each other than the corresponding domains of any other nRTKs and their closest respective paralogs or orthologs (119). SH3 domains canonically bind proline-rich peptides that form left-handed polyproline type II helices (120). SH3 domains exhibit a wide-array of ligand (PxxP) specificities that have been broadly divided into two major classes: class 1 which bind a (K/R)xxPxxP motif and class 2 which bind a PxxPx(K/R) motif (120). The consensus binding motif of the ABL SH3 domain is divergent from both class 1 and class 2 with a target sequence of PPx(F/W/Y)xPPP(A/G/I/LV) (121). Further, recent work revealed that the ABL2 SH3 domain can bind a proline-independent sequence (122).

SH2 domains canonically bind tyrosine phosphorylated peptides. The ABL SH2 and SH1 have co-evolved to exhibit a similar consensus binding motif (VYxxP) (119). The SH3 and SH2 domains are preceded by an amino (N)-terminal CAP region and together these sequences engage in intra and intermolecular interactions that modulate tyrosine kinase activity. There are two major splice variants of the ABL kinases with alternative start sites (1A- short isoform, 1B- long isoform; numbering in this review uses 1B) (123). A glycine residue exists in the 1B isoform that becomes myristoylated, and the myristoyl moiety binds to a pocket in the C-lobe of the kinase domain to stabilize the inactive kinase conformation (124). Activation of ABL kinases by diverse stimuli leads to disruption of intramolecular interactions and phosphorylation of downstream targets (Figure 2B).

The carboxy (C)-terminal domain of the ABL kinases is encoded by a single exon (Figure 2A). While the N-terminal CAP-SH3-SH2-SH1 domains are highly conserved (90%), the C-terminal domains are divergent (29%), suggesting potential unique functions of ABL1 and ABL2 (118). Both kinases have three conserved class 2 PxxP located adjacent to the SH1 domain which mediate binding to proteins containing SH3-binding domains (125). The ABL1 protein localizes to the nucleus and cytoplasm and encodes three K/R-rich nuclear localization signals (NLS) and a nuclear export signal (NES) allowing its entrance and egress from the nucleus (Figure 2A). In contrast, ABL2 lacks these domains and is retained in the cytoplasm (126, 127). ABL1 contains globular (G)-actin and filamentous (F)-actin binding domains, while ABL2 contains two F-actin binding domains and a microtubule-binding domain (128-131). The presence of these C-terminal sequences endows the ABL kinases with a unique capacity to integrate diverse stimuli to dynamic changes in the actin and microtubule cytoskeletons.

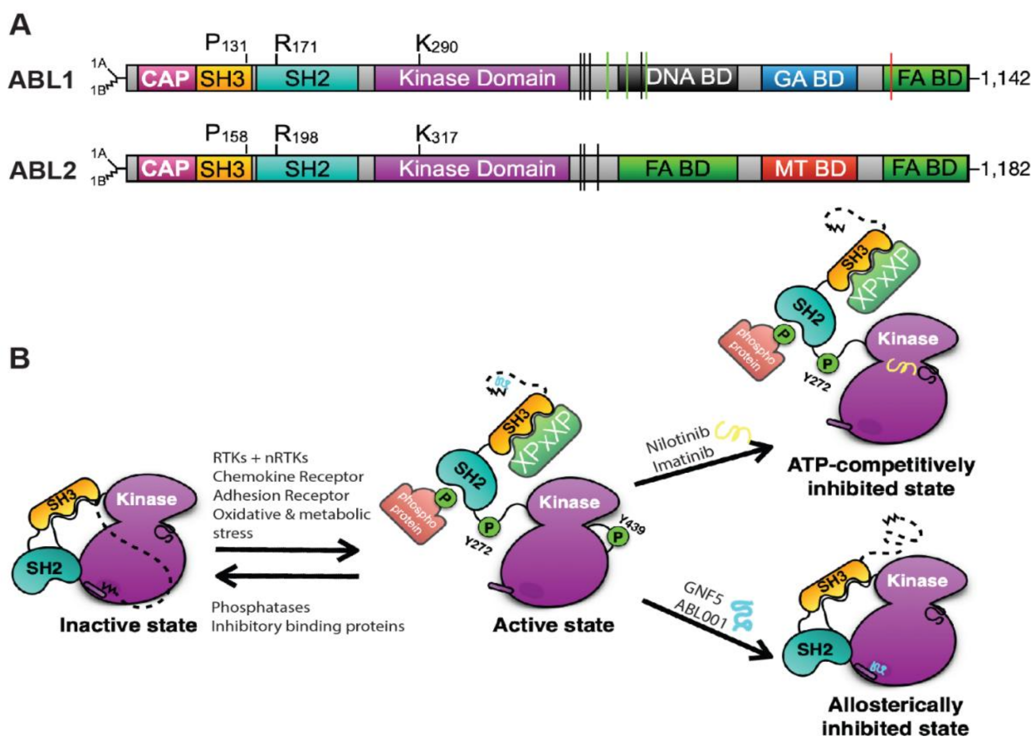

Figure 2: Representation of the ABL structural domains and regulation of ABL kinase activity. **A)** There are 2 major splice variants of *ABL1* and *ABL2*, the 1A isoforms (straight line) and the 1B isoforms (jagged line); numbering uses the 1B isoform. The amino (N)-termini of the ABL kinases contain the SRC homology 3 (SH3), SH2 and SH1 (tyrosine kinase) domains. The carboxyl C-termini of the ABL kinases are divergent with only a conserved filamentous (F)-actin-binding domain (BD) between both paralogs. ABL1 has a globular (G)-actin-binding domain and a DNA-binding domain, whereas ABL2 has a second internal F-actin-binding domain and a microtubule (MT)-binding domain. ABL1

has three nuclear localization signal (NLS) motifs (three green lines located near the SH1 domain) and one nuclear export signal (NES) (single red line in FA BD) in its C terminus. Both paralogs have conserved XPxXP motifs to mediate protein–protein interactions (denoted as black vertical lines in both structures). P131/158L is a mutation that destroys SH3-mediated interactions and R171/198K is a mutation that destroys SH2-mediated interactions. L290/317R are kinase inactivating mutations. **B)** Inactive and active forms of the ABL kinases are regulated by dynamic intramolecular interactions that modulate ABL kinase activity. The SH3 domain binds to the linker sequence connecting the SH2 and the kinase (SH1) domains, and the SH2 domain interacts with the C-terminal lobe of the kinase domain forming an SH3–SH2 clamp structure locking the kinase in an inactive state. The dashed line represents ABL N-terminal sequences upstream of the SH3 domain that fold over and bind to the myristoyl group in a pocket of the C-lobe of the kinase domain. The myristoylated residue is present in in the N terminus of the ABL 1B isoforms and creates a hydrophobic pocket within the C-lobe of the kinase domain that stabilizes the auto-inhibited conformation. Activation of the ABL kinases by diverse stimuli disrupts the inhibitory intra-molecular interactions. Phosphorylation within the activation loop of (Y412 in ABL1; Y439 in ABL2) as well as within the SH2-kinase domain linker (Y245 in ABL1; Y272 in ABL2) stabilizes the active conformation. Binding of pharmacological inhibitors to the ATP-binding site (Nilotinib or Imatinib) or to the allosteric site (GNF5 or ABL001) disrupts these interactions and causes kinase inhibition by eliciting different conformations.

1.5 Role of ABL kinases in solid tumors

Large-scale sequencing projects have identified increased expression of the ABL kinases in different solid tumor types due to *ABL* amplification, somatic mutations, and/or increased mRNA expression (reviewed in (107)). These findings are consistent with clinical reports analyzing patient samples for genomic and/or gene expression changes in high-grade pancreatic, renal, colorectal, breast and gastric tumors (132-135). Studies examining Kaplan-Meier survival curves of lung, breast, colorectal, hepatocellular carcinoma patients of varying subtypes found that elevated ABL1 and/or ABL2 is associated with decreased metastasis-free survival and/or lower overall survival (99, 101, 106, 136, 137).

The consequences of elevated expression of ABL1 and ABL2 for tumor progression are cell context dependent. Single knockdown of either ABL1 or ABL2 in triple-negative breast cancer cells impaired anchorage independent growth, while expression of a constitutively active form of ABL1 in 4TI murine mammary tumors inhibited tumor growth (138, 139). Consistent with these findings, knockdown of ABL2 in triple-negative MDA-MB-231 breast cancer xenografts promoted tumor growth via increased cell proliferation (97). In contrast, depletion of ABL1 and ABL2 in MCF7 cells impairs the growth of MCF7 xenograft tumors (140). While the effects of ABL1 or ABL2 inhibition has mixed effects on primary breast tumor growth, genetic or pharmacologic inhibition of the kinases impairs breast cancer metastasis (97, 104, 106). Notably, ABL1 plays a critical role in an aggressive form of hereditary kidney cancer observed in patients with a germline mutation in the enzyme fumarate hydratase (FH) that leads to the development of hereditary leiomyomatosis and renal cell carcinoma (HLRCC) (141). In these cells, ABL1 signals through mTOR and HIF1α to upregulate aerobic glycolysis and neutralize proteotoxic stress by promoting nuclear accumulation of NRF2, a transcription factor that activates a cell detoxification program (Figure 2). Inactivation of ABL1 markedly inhibited the growth of HLRCC xenografts (141).

Preclinical mouse models have shown that genetic or pharmacologic inhibition of the kinases has a greater impact impairing cancer cell metastasis of solid tumors in comparison to primary tumor growth (97, 99-101, 104, 112-114). The predominant effects of the ABL kinases on metastatic phenotypes might be due to cumulative regulation of the epithelial to mesenchymal transition and other distinct steps of the metastatic cascade required for initiation, dissemination and colonization of distal sites (142-145).

1.5.1 Role of ABL kinases in solid tumor metastasis

Several reports have shown a requirement for ABL kinases in breast cancer metastasis using preclinical mouse models. Knockdown of ABL2 in breast cancer cells resulted in decreased spontaneous metastasis to the lungs following orthotopic implantation of breast tumors in the mammary fat pad (97). Using an intracardiac mouse model of metastasis, shRNA-mediated knockdown of both ABL1 and ABL2 in bone tropic triple-negative breast cancer cells decreased metastasis to the bone and increased overall survival (106). Importantly, this study demonstrated that ABL-dependent activation of the TAZ and STAT5 transcription factors was required for breast cancer metastasis to the bone (Figure 3). Further, treatment with ABL kinase pharmacologic inhibitors reduced breast cancer spontaneous metastasis to the lungs (104).

Following intracardiac injection of non-small cell lung cancer (NSCLC) cells in preclinical mouse models, it was found that the ABL kinases, specifically ABL2, drove metastasis of lung cancer cells to distal sites in the body including the brain (99-101). Genetic and pharmacologic inhibition suppressed metastasis and increased overall survival in mice. Global transcriptome analysis revealed that the ABL kinases are required for expression of pro-metastasis genes (99). Specifically, ABL kinases promote stability of the transcriptional coactivators TAZ and β-catenin by decreasing their interaction with the β-TrCP ubiquitin ligase (99). Both TAZ and β-catenin have been implicated in EMT. Active TAZ can promote tumorigenesis by increasing cell proliferation, metastatic colonization, chemoresistance, and EMT (146-148). In this regard, β-catenin is expressed at the invasive front of colorectal carcinomas and upregulates a pro-invasive gene expression profile during colorectal metastasis (149, 150). Interestingly, it was found that ABL2 and TAZ activate an autocrine signaling loop during lung adenocarcinoma metastasis to promote colonization of the brain parenchyma (101). The ABL2–TAZ signaling axis induces expression of multiple targets including the AXL RTK that engages with ABL2 protein kinase in bi-directional signaling (Figure 3). ABL2 targets distinct transcriptional regulatory networks that include the heat shock factor 1 (HSF1) in lung adenocarcinoma cells to drive brain colonization through increased lung cancer cell survival and outgrowth (Figure 3) (100). Further, lung cancer cells harboring shRNAs against the ABL kinases exhibited decreased extravasation from blood vessels into lung tissue in preclinical mouse models of metastasis (99). Recently, ABL kinases were shown to be activated by co-culture of lung adenocarcinoma cells with mesenchymal stem cells (MSCs) leading to ABL-mediated MMP-9 expression, secretion, activation of MMP-9 proteolytic activity and metastasis (112) (Figure 3). Both ABL1 and ABL2 kinases are required for metastasis of MSC-primed lung cancer cells to distal sites following intracardiac injection in mouse models.

ABL kinases target diverse protein signaling pathways to facilitate EMT and metastasis. In hepatocellular carcinomas, ABL1 was shown to be important for claudin1 expression (105, 117). Claudin1 promotes a malignant phenotype by inducing expression of the EMT transcription factors Slug and Zeb1 leading to repression of cell adhesion proteins and increased cell motility (105). ABL1 and ABL2 promote invasion and metastatic progression of melanomas in part by activating the transcription factors Ets1, Sp1, and NF-κB/p65 which induce expression of cathepsin ECM proteases (114, 116). In colorectal cancer, when the tumor suppressor gene *Aes* is knocked out NOTCH1 becomes activated and stimulates ABL1 activity (136). ABL1 then phosphorylates the Rac/RhoGef protein TRIO on Y2681 causing Rho activation and colorectal cancer cell invasion. Phosphorylation of Y2681 on TRIO is correlated with poor colorectal cancer patient prognosis and inhibition of ABL suppressed cancer cell invasion in mice (136). In non *Aes* mutant colorectal cancer, ABL1 can also increase NOTCH1 and MYC protein levels leading to enhanced tumor growth (151). Additionally, ABL1 can become activated following PDGF stimulation leading to phosphorylation of Y593 on the nuclear RNA helicase p68. Phosphor-p68 then promotes nuclear translocation of β-catenin and stimulation of EMT (152). These findings highlight the ability of the ABL kinases to promote metastasis by modulating a vast array of substrates in diverse signaling pathways necessary for cellular processes that contribute to EMT and subsequent steps in the metastasis cascade (highlighted in Figure 3).

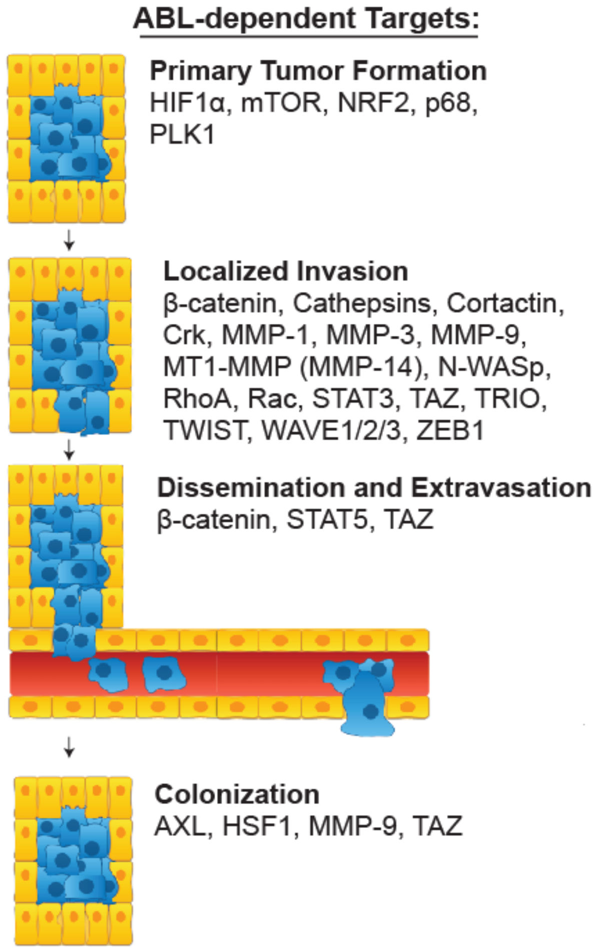

Figure 3: ABL-dependent targets promote EMT and metastasis. Activated ABL kinases and their downstream signaling targets promote tumor progression and metastasis by targeting distinct processes required for tumor growth, invasion, dissemination, extravasation and colonization of distal sites.

1.6 Role of ABL kinases in cancer cell metabolism

Studies examining the role of ABL kinases in tumor metabolism have shown that the kinases modulate glycolysis and mitochondria function. ABL kinases have been shown to modulate glycolysis in the context of BCR-ABL1 driven leukemia cells. Inducible expression of BCR-ABL1 in a hematopoietic cell line caused increased expression of GLUT1 and increased glucose transport (153). The effects were nullified following treatment with imatinib. Interestingly, treatment with sublethal doses of imatinib in BCR-ABL1 mutant chronic myelogenous leukemia (CML) causes a reduction in glycolytic activity and while increasing flux through the TCA cycle (154). However, upon treatment with lethal doses, both glycolysis and TCA cycle activity are shut down.

ABL kinases have also been shown to have differential effects on mitochondria function depending on the cell context. In mouse embryonic fibroblasts (MEFs) and a myeloid leukemia cell line, treatment with hydrogen peroxide to elevate intracellular ROS levels caused ABL1 to localize to the mitochondria (155). It was shown that in MEF cells, ABL1 localization at the mitochondria decreased mitochondrial membrane potential and caused cells to undergo cell death (155). Hematopoietic cells inducibly expressing BCR-ABL1 were treated with sorafenib (a pan inhibitor that targets the Raf serine/threonine kinases (Raf-1, wild-type B-Raf, and oncogenic B-Raf V600E), receptor tyrosine kinases (VEGFR-1, VEGFR-2, VEGFR-3, PDGFR-β, Flt-3, and c-Kit), and ABL) and underwent mitochondrial-mediated apoptosis suggesting a potential regulatory role of ABL kinases at the mitochondria (156). Further exploration in the context of HER2 amplified breast cancer cells found that ABL1 phosphorylates mitochondrial creatine kinase 1 (MtCK1), which stabilizes MtCK1 causing increased activity of the phosphocreatine energy shuttle and promoted cancer cell proliferation (157). Knockdown of MtCK1 reduced mitochondrial respiration and decreased cancer cell outgrowth. These results suggest ABL kinases influence cell metabolism in a cell context dependent manner.

1.7 Therapeutics targeting ABL kinases

Among the clinically available tyrosine kinase inhibitors (TKIs), some of the most successful to date target the ABL kinases, specifically in the context of BCR-ABL driven chronic myelogenous leukemia (CML) (Appendix Table 1). ABL kinases are also activated in many solid tumors, expanding the utility of ABL kinase inhibitors, and particularly the highly specific ABL allosteric inhibitors have shown efficacy in the treatment of metastatic lung cancer (99, 100). Importantly, the available ATP-competitive ABL kinase TKIs target multiple tyrosine kinases in addition to ABL1 and ABL2, whereas the ABL allosteric inhibitors are specific to the ABL kinases (Appendix Table 1). The ability of the ATP-competitive inhibitors to target other kinases, such as PDGFRA and KIT, has made these inhibitors efficacious in the treatment of selective solid tumors that require the activity of such kinases to promote tumor growth. However, in tumors where these mutations are not driving growth, the necessary concentration needed to effectively inhibit disease progression by non-selective ATP-competitive inhibitors may result in detrimental off-target effects due to the promiscuous nature of the ATP-site inhibitors. Therefore, using ABL inhibitors that are highly specific and mono-selective, such as the allosteric inhibitors and PROTACS, might be a more effective strategy for developing future therapies.

1.7.1 ATP-competitive ABL inhibitors

Classical ABL tyrosine kinase inhibitors can be stratified into classes based on their mechanism of action. ATP competitive inhibitors target the ATP binding pocket of the kinase domain and can be further subdivided into type 1 or type 2 based on whether they target the active or inactive conformation of the kinase domain. Imatinib (Gleevec) was the first TKI developed against BCR-ABL. It binds the ATP-binding site of ABL1 and inhibits both BCR-ABL1 and ABL1 resulting in inhibition of cell proliferation and apoptosis of leukemic cells (158-161). Treatment of early chronic phase CML patients with Imatinib as a first line therapy leads to durable remission and a stark improvement in 5 year overall and progression free survival (162). However, the relapse rate among patients with advanced or blast crisis phase CML is high due to the development of drug resistance mutations in the ABL kinase domain. This clinical need led to the development of several second and third generation TKIs targeting BCR-ABL including: Dasatinib, Nilotinib, Bosutinib, and Ponatinib (163) (Appendix Table 1). Dasatinib and Nilotinib have been FDA approved as first and second line therapy, and Ponatinib and Bosutinib have been approved as second line therapy for Ph+ leukemia patients with BCR-ABL mutations (163). Additionally, Axitinib, a vascular endothelial growth factor receptor (VEGFR) inhibitor has been shown to inhibit the drug resistant gate keeper mutant of BCR-ABL (164). Vandetanib, originally designed as a VEGFR2 inhibitor, has also been shown to be a potent inhibitor of several kinases including ABL and has been FDA approved for the treatment of medullary thyroid carcinoma (Appendix Table 1) (165, 166). Type 1 ATP competitive inhibitors including Dasatinib, Bosutinib, Vandetanib, and Axitinib target the active conformation of the kinase domain. Conversely, type 2 ATP competitive inhibitors including Imatinib and Nilotinib target the inactive conformation of the kinase domain (167, 168) (Appendix Table 1).

Clinical trials have effectively used the ATP-site inhibitors imatinib and nilotinib to treat melanoma patients harboring c-Kit mutations as these drugs can target the c-Kit receptor kinase in addition to ABL and other tyrosine kinases (169-171). However, clinical trials designed to use the ATP-site inhibitors in non-c-Kit mutant solid tumors because of their ability to target multiple tyrosine kinases, such as PDGFR, Kit, DDR1/2, or Src, were ineffective (167, 168, 172-176). The lack of efficacy could be due in part to toxicity elicited by effective tumor killing doses or activation of alternative cell survival pathways (167, 168, 176). These findings have been further substantiated by preclinical data showing that treatment with imatinib induces activation of the RAF-ERK pathway in cancer cells (99, 106, 177).

1.7.2 ABL allosteric inhibitors

Allosteric ABL inhibitors bind to regulatory regions that inhibit kinase activity. Unlike ATP competitive inhibitors, allosteric inhibitors are highly specific for ABL kinases and effectively target ABL1, ABL2, as well as the BCR-ABL1 fusion protein. The first allosteric ABL inhibitor to be described was GNF2, a compound that bound to the myristate binding cleft of ABL (178).To circumvent inherently limiting pharmacokinetic properties of GNF-2, GNF-5 a structural analog of GNF-2 was designed and shown to have similar inhibitory properties to GNF-2 (178). Treatment with GNF-5 effectively decreased tumor burden in mice harboring BCR-ABL1 leukemias and sensitized ATP-site inhibitor resistant leukemias to the ATP competitive TKIs (178). Recently, the ABL allosteric inhibitor ABL001 (Asciminib) which binds to the myristoyl binding site with a higher affinity than GNF-2/5 (179), has been evaluated in multicenter clinical trials in patients with CML and Ph+ ALL (NCT02081378, NCT03292783) (Appendix Table 1). More recently, Asciminib was used in a Multicenter Phase 3 Study in CML chronic phase patients that had been previously treated with two tyrosine kinase (180). Notably, ABL allosteric inhibitors have also been shown to be efficacious in preclinical mouse models of breast and lung cancer metastasis, as treatment with GNF5 or ABL001 decreased lung adenocarcinoma metastasis to the brain and breast cancer metastasis to the bone (99, 101, 106). Unexpectedly, recent work uncovered functional differences between ABL allosteric versus ATP-competitive inhibitors as the pro-metastatic ABL2-HSF1 complex was completely disrupted by GNF5 treatment, but was largely unaltered after treatment with the ATP-competitive inhibitor Nilotinib (100). These exciting findings support the notion that allosteric and ATP-competitive inhibitors have differential effects on the protein-interactome of the ABL kinases, which suggests that these drugs could have distinct therapeutic effects in cancer cells and patients harboring solid tumors.

1.7.3 Emerging strategies to target ABL kinases: PROTACs

While established ABL inhibitors have been instrumental in the treatment of CML and have emerging potentials in solid tumors, treatment with these inhibitors can result in drug resistance. Resistance mechanisms could be due to previously described mutational changes as well as residual scaffolding functions of ABL outside of its kinase activity (181, 182). Proteolysis Targeting Chimera (PROTAC) technology is an emerging therapeutic strategy that could be useful to impair ABL expression and function. PROTACs are bifunctional small molecules designed to target both the target protein as well as an E3 ubiquitin ligase to induce degradation of the target protein (183). Recent studies designing PROTACs that effectively degrade ABL1, ABL2 and BCR-ABL1 have been successful *in vitro* (184-186). ABL was partially degraded by targeting the kinase domain using either Bosutinib and a ligand that recruits E3 ligase Cereblon, or -Dasatinib fused to ligands for either Cereblon or VHL (186). However, because both Bosutinib and Dasatinib target multiple protein kinases other than ABL (Appendix Table 1), it is likely that the effects of these PROTACS are mediated by degradation of several kinases. A recent study showed enhanced sensitivity and complete degradation of ABL by targeting the myristoyl binding pocket of ABL and VHL-mediated degradation (185). While these early studies have only been conducted *in vitro*, they are promising for potential future *in vivo* preclinical and clinical studies.

2. ABL allosteric inhibitors synergize with statins to promote lung cancer cell apoptosis

Material from this chapter will be published in *Cell Reports*, 2021

2.1 Introduction

Metabolic reprogramming is a hallmark of cancer and contributes to tumor development (8). Oncogenic activation can increase expression and activity of metabolic enzymes and transporters to meet the bioenergetic and biosynthetic needs of the cancer cell thus creating metabolic vulnerabilities that might be exploited for emerging cancer therapies (14, 187-190). Among these dependencies is mitochondrial metabolism which generates energy, regulates redox homeostasis, and provides key metabolites for macromolecule synthesis (191). While results from clinical trials evaluating the anticancer capability of drugs targeting mitochondrial metabolic pathways have shown potential benefits, the utility of these drugs is limited by expression of transporters that facilitate import of these drugs into cancer cells, or toxicity associated with targeting mitochondrial metabolism not only in tumor cells but also in non-cancerous tissue (42).

The ABL family of non-receptor tyrosine kinases, ABL1 and ABL2, are activated downstream of diverse stimuli, including oncogenic drivers such as EGFR, HER2, and KRAS, and promote progression and metastasis of solid tumor types including lung and breast cancer (99, 106, 112, 113, 192). ABL1 and ABL2 promote cancer cell growth, survival, adhesion, and migration depending on the cellular context (107, 111). Recently, a role for ABL kinases in the regulation of mitochondria function was shown in HER2 amplified breast cancer cells as HER2 promoted ABL-mediated tyrosine phosphorylation of mitochondrial creatine kinase 1 (MtCK1) leading to increased cellular energy production through the mitochondrial phosphocreatine shuttle (157). These findings suggested that inhibition of ABL signaling may uncover additional metabolic vulnerabilities in tumor cells.

Lung cancer is the leading cause of mortality among cancers worldwide in part due to the lack of actionable targets and transient responses to current therapies (193). Here, we show that ABL kinases regulate mitochondrial function and integrity in lung adenocarcinoma cells harboring EGFR and KRAS mutations, and that inactivation of ABL kinases impairs oxidative mitochondrial metabolism. As ABL inhibition impairs mitochondrial oxidation, we sought to determine whether targeting metabolic pathways could enhance sensitivity to ABL allosteric inhibitors by performing a CRISPR/Cas9 loss-of-function screen targeting 2,322 metabolic enzymes and transporters. This screen identified HMG-CoA reductase (HMGCR), a rate-limiting enzyme of the mevalonate pathway and target of statin therapy, as a top-scoring sensitizer capable of potentiating cell death in the presence of sublethal doses of ABL allosteric inhibitors. Notably, we found that combination therapy of ABL kinase allosteric inhibitors with lipophilic statins impaired growth of clinically relevant therapy-resistant and brain metastatic lung cancer cells *in vitro* and *in vivo* mouse models. These results suggest new treatment avenues for lung cancer patients with advanced disease.

2.2 Results

2.2.1 ABL kinase allosteric inhibitors regulate mitochondria function in lung cancer cells

We investigated whether inhibition of the ABL kinases could perturb mitochondrial function in lung adenocarcinoma cells with oncogenic mutations in EGFR, either sensitive to EGFR tyrosine kinase inhibitors (TKIs) (PC9) or TKI-resistant (PC9 GR4), as well as KRAS mutant large cell lung carcinoma (LCC) H460 cells and KRAS mutant lung adenocarcinoma H358 cells. Lung cancer cells were analyzed for mitochondrial basal respiration, maximal respiration, and ATP production following treatment with ABL kinase inhibitors (Figures 4A-D). For these studies we used ABL allosteric inhibitors, GNF5 and ABL001 (Asciminib), which bind with high affinity to the unique myristate-binding pocket of the ABL kinases, as well as the second-generation ABL ATP-competitive inhibitor Nilotinib (194, 195).

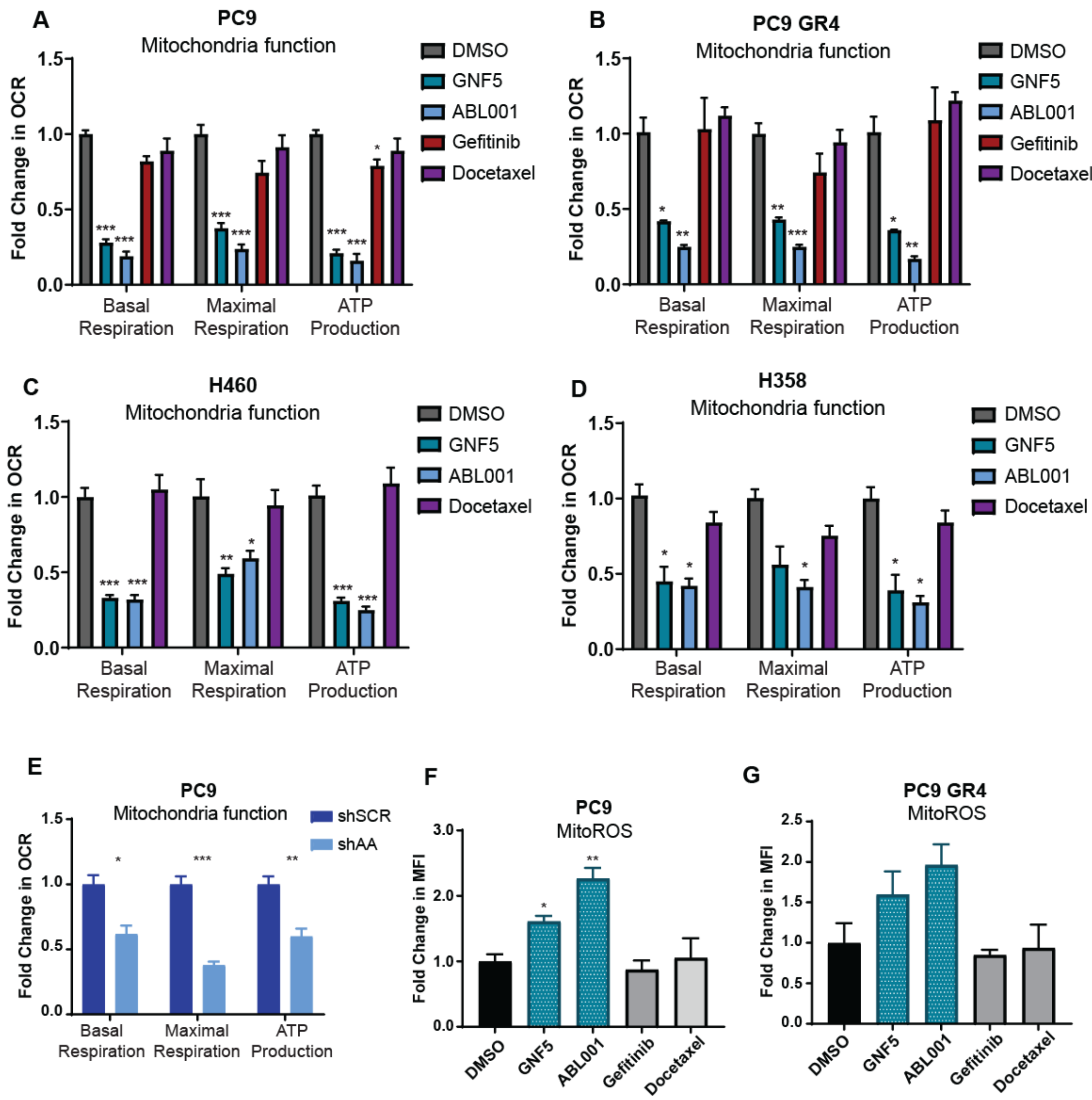

Figure 4. ABL kinase allosteric inhibitors regulate mitochondria function in lung cancer cells. (A-D) Seahorse XF Analyzer Mito Stress Test analysis of mitochondrial basal respiration, maximal respiration, and ATP production as measured by changes in oxygen consumption rate (OCR). Cells were treated with IC_{50} doses of each drug (see Appendix Table 2) for 24 hours. (E) Mitochondrial basal respiration, maximal respirati\on, and ATP production as measured by Seahorse XF Analyzer's Mito Stress Test for PC9 cells harboring shRNAs against ABL1/ABL2 (shAA) and non-targeting control (shSCR). (F-G) Mitochondrial ROS (MitoROS) release as measured by FACS analysis of median fluorescent intensity (MFI) using Mitosox probe. Cells were treated with IC_{50} doses for 24 hours. Statistical analysis was performed using one-way ANOVA and Tukey post hoc testing (n = 3). *$p<0.05$, **$p<0.01$, ***$p<0.001$, ****$p<0.0001$. Data are mean ± SEM.

Surprisingly, only the ABL allosteric inhibitors, but not Nilotinib, markedly impaired mitochondria basal respiration, maximal respiration, and ATP production at all time points evaluated (Figures 4A-D and 5A-E). The inability of Nilotinib to inhibit mitochondria function might be due to the lack of specificity of ABL ATP-competitive inhibitors as these drugs inhibit multiple enzymes other than ABL in solid tumors, and/or the inability of Nilotinib to disrupt interactions with specific ABL downstream targets, which we showed can be blocked by ABL allosteric inhibitors through binding to a distinct site in the ABL kinase domain (100). Moreover, treatment with ABL ATP-competitive inhibitors, but not allosteric inhibitors, induces activation of the RAF-ERK pathway in diverse cancer cell types (99, 106, 177). Notably, genetic knockdown of ABL1 and ABL2 (shAA) demonstrated that depletion of the ABL kinases similarly decreased mitochondrial respiration and ATP production in EGFR and KRAS mutant lung cancer cells (Figures 4E and 6A). Thus, depletion of ABL kinases phenocopied the ABL allosteric inhibitors by decreasing mitochondria function in lung cancer cells.

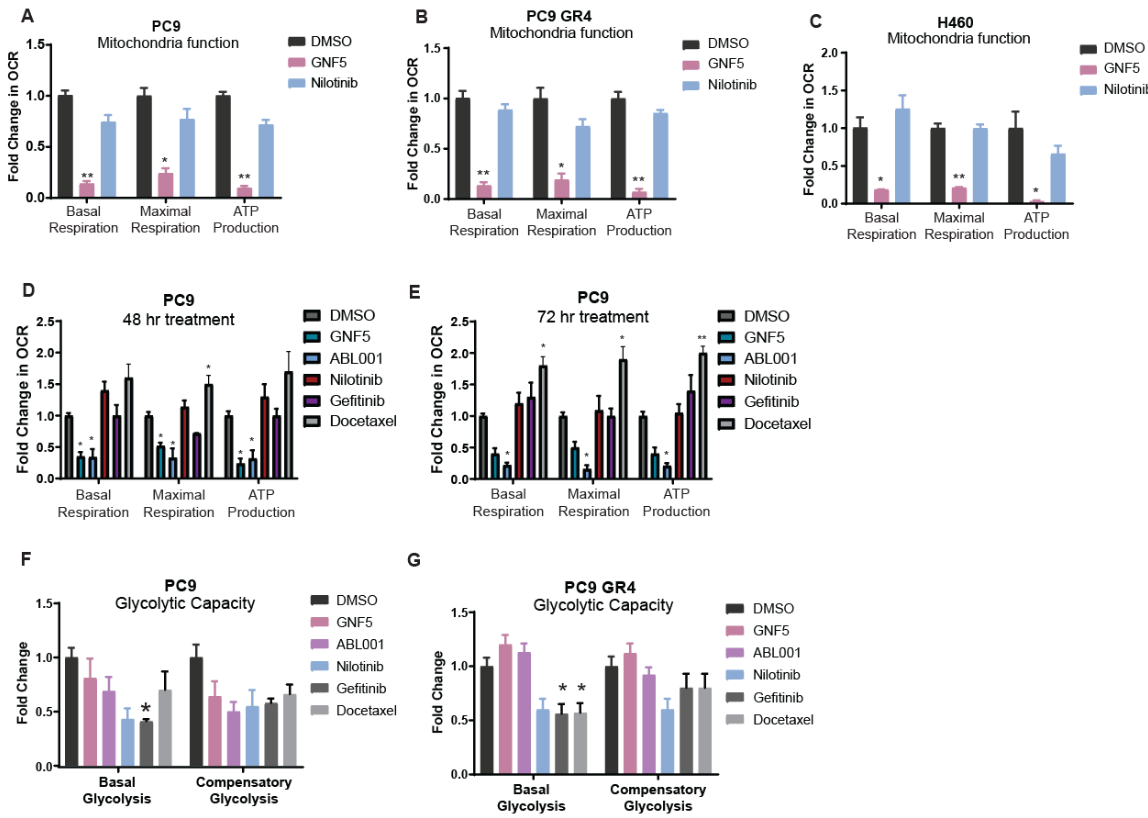

Figure 5. ABL allosteric inhibitors preferentially impair mitochondria function in lung cancer cells. (A-E) Seahorse XF Analyzer Mito Stress Test analysis of mitochondrial basal respiration, maximal respiration, and ATP production as measured by changes in oxygen consumption rate (OCR) in the indicated lung cancer cells. Cells were treated with IC_{50} drug doses for each drug in cell line. Cells were treated for either 24 hr (A-C), 48 (B), or 72 hours (C). (F-G) Seahorse XF Analyzer Glycolytic Rate analysis of basal and compensatory glycolysis in PC9 and PC9 GR4 cells. Cells were treated with IC_{50} doses for 24 hours. Statistical analysis was performed using one-way ANOVA and Tukey post hoc testing (n = 3). *p<0.05

Next we evaluated whether aberrant mitochondria function induced by treatment with ABL allosteric inhibitors was also observed following treatment with two current FDA-approved therapeutics for lung adenocarcinoma patients: gefitinib, an EGFR TKI, and docetaxel, a taxane chemotherapy (196). Lung cancer cells were treated with IC_{50} drug doses determined by dose-response assays (Appendix Table 2). Strikingly, mitochondrial function as measured by basal and maximal respiration, and ATP production, was greatly decreased following treatment with either GNF5 or ABL001 in lung cancer cells harboring EGFR or KRAS mutations (Figures 4A-D), but was not impaired upon treatment with gefinitib or docetaxel in EGFR mutant PC9 parental cells and gefitinib-resistant PC9 GR4 cells (Figures 4A, B and 5D, E). Additionally, treatment with docetaxel in KRAS mutant H460 and H358 lung cancer cells, did not significantly impair mitochondria function (Figure 4C, D). Notably, while the ABL001 and GNF5 allosteric inhibitors markedly decreased mitochondrial function as measured by decreased mitochondrial respiration and impaired ATP production at all the time points examined, treatment with gefitinib, nilotinib, and docetaxel failed to elicit these changes (Figure 4A-D and 5D, E). Further, we examined changes in basal and compensatory glycolysis in lung cancer cells following drug treatment. In contrast to nilotinib, gefitinib, and docetaxel which decreased basal and compensatory glycolysis in PC9 and PC9 GR4 cells, the ABL allosteric inhibitors did not inhibit glycolytic capacity in these cells (Figure 5F, G). Thus, ABL allosteric inhibitors promote lung cancer cell death in part by impairing mitochondria function and integrity.

To dissect the mechanism by which mitochondria function is impaired by ABL allosteric inhibitors, mitochondrial superoxide release was examined to identify changes in organelle integrity (197, 198). We observed that mitochondrial reactive oxygen species (MitoROS) levels were increased upon GNF5 or ABL001 treatment, but not following gefitinib or docetaxel treatment in EGFR mutant lung cancer cells sensitive or resistant to gefitinib therapy (Figure 4F, G). MitoROS levels were also increased in KRAS mutant H460 cells upon ABL allosteric inhibitor treatment, but not by docetaxel (Figure 6B). Thus, ABL allosteric inhibitors impair organelle integrity in lung cancer cells irrespective of oncogenic driver (Figures 4F,G and 6B). MitoROS levels were also increased following ABL1 and ABL2 knockdown in PC9 and H460 cells (Figure 6C, D). Analysis of mitochondria number following knockdown or pharmacologic inhibition of the ABL kinases did not show detectable changes in mitochondria numbers in PC9 and H460 cells indicating that the decrease in OCR is not due to changes in mitochondrial density but rather mitochondria function (Figure 6E- H). Examination of changes in mitochondrial morophology by immunoflorescence staining with Mitotracker revealed that ABL001 caused a marginal, non-significant increase in mitochondrial network morphology, while the other drugs did not affect mitchondria length and width (Figure 6I, J).

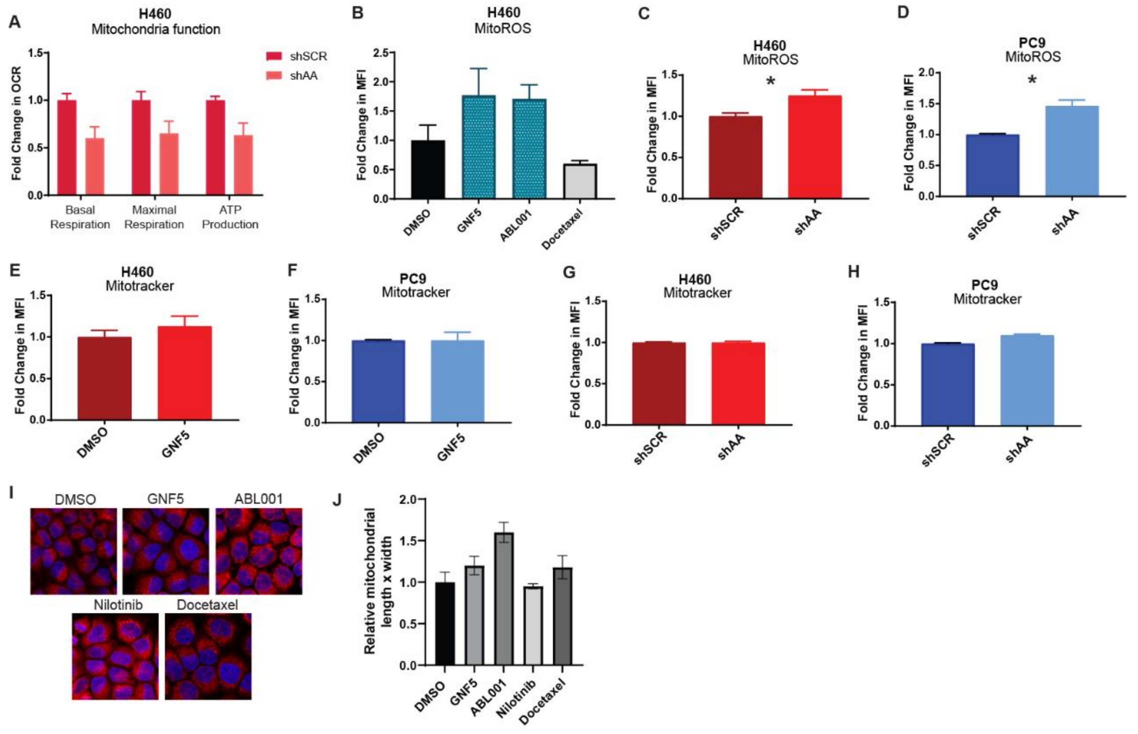

Figure 6: ABL inhibition impacts mitochondria function in lung cancer cells without altering mitochondria number. (A) Mitochondrial basal respiration, maximal respiration, and ATP production as measured by changes in oxygen consumption rate (OCR) from Seahorse XF Analyzer Mito Stress Test analysis for H460 cells harboring shRNAs against ABL1/ABL2 (shAA) and non-targeting control (shSCR). (B) FACS analysis of mitochondrial ROS (MitoROS) using mitosox probe in H460 cells treated with IC_{50} doses for each drug for 24 hours. n = 3 (C-D) MitoROS in H460 AA knockdown cells (C) or PC9 AA knockdown cells (D). (E-F) Mitotracker staining to analyze mitochondria number in H460 cells with 15 uM GNF5 (E) or PC9 cells treated with 10 uM GNF5 (F). n = 3 (G-H) Mitotracker staining of H460 AA knockdown cells (G) or PC9 AA knockdown cells (H). n = 3. Statistical analysis was calculated using unpaired two-tailed t test *$p<0.05$, Data are mean ± SEM. (I) Representative immunofluorescence images of H460 cells stained with Mitotracker and Hoescht 33342 following treatment with IC_{50} dose for each drug for 24 hours. (J) Image quantification for Fig. S2I showing mitochondrial length × width plotted for thousands of mitochondria from >10 cells across at least two independent experiments. Changes were not statistically significant.

2.2.2 Metabolically focused CRISPR/Cas9 loss-of-function screen identifies HMGCR inhibition with statin therapy as an apoptotic sensitizer in lung cancer cells

Because inhibition of ABL kinases impairs oxidative mitochondrial metabolism, we sought to determine whether targeting additional metabolic nodes enhanced sensitivity to ABL inhibition. Thus, we employed a CRISPR/Cas9 loss-of-function screen targeting 2,322 metabolic enzymes and transporters (199) in the absence and presence of sublethal doses of the ABL allosteric inhibitor GNF5 that corresponded to a 20% loss in cell viability following a 3-day dose response assay (Figure 7A). Library-transduced cells were puromycin selected and grown for 10 days prior to treatment. The cells were then exposed to either vehicle or GNF5 for two weeks after which DNA was extracted from cell samples and polymerase chain reaction (PCR) was used to amplify and index barcode short guide RNA (sgRNA) amplicons, and the composition of sgRNA pools was deconvoluted through deep sequencing. The screen was validated for known essential genes by comparing the final and initial sgRNA pools in the vehicle treated screen as previously described (199). Depletion metrics for each sgRNA were determined by normalizing the relative abundance of each construct following GNF5 treatment to the construct quantity present in vehicle treated cells. The three most depleted constructs per gene were averaged to produce a gene-level three score (TS) as previously detailed (199). TS scores were ranked allowing for identification of genes that were specifically depleted or enriched in the GNF5 treated cell population (Figure 7B; Appendix Table 3). We focused on the subset of depleted genes that fell below the inflection point of the curve to experimentally evaluate whether loss of the top 5% of deleted genes could potentiate the cell killing effects of ABL allosteric inhibition. Among these hits were metabolic enzymes and transporters that converged on metabolic nodes that regulate cholesterol synthesis and mobilization, as well as complexes of the electron transport chain. We focused on targets that could be pharmacologically inhibited with FDA-approved drugs, and identified HMG-CoA reductase (HMGCR*)*, the rate-limiting enzyme of the mevalonate pathway, as a top-scoring reactive sensitizer to cell death in the presence of low dose GNF5 (Figure 7B, C). We selected *HMGCR* for further study because it was in the top 1% of depleted genes and is the target of statin therapies commonly prescribed for patients with high cholesterol (200). Statins have a highly tolerable pharmacokinetic profile and availability making HMGCR an attractive target for combination therapy.

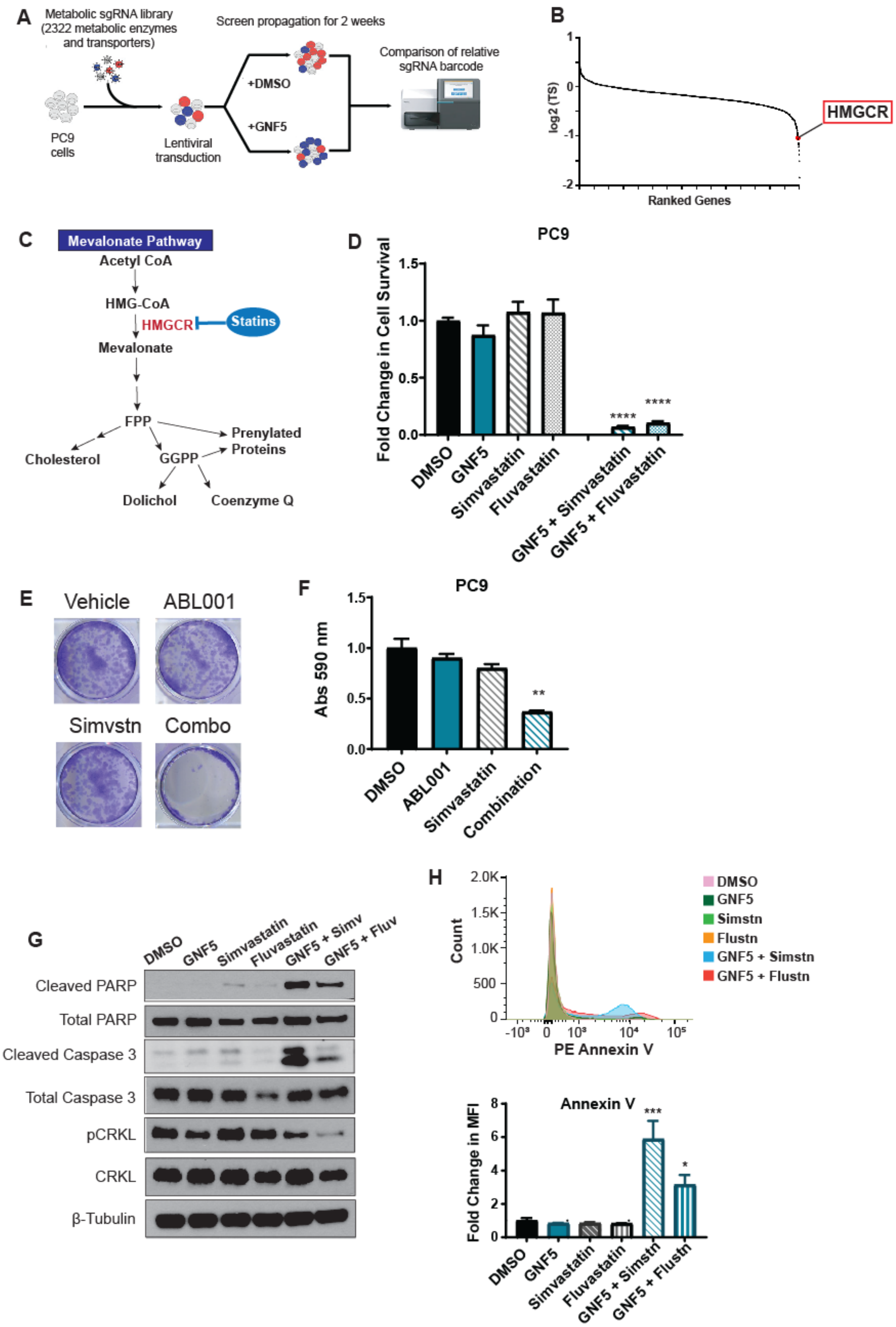
A
Metabolic sgRNA library (2322 metabolic enzymes and transporters)
Screen propagation for 2 weeks
Comparison of relative sgRNA barcode
+DMSO
+GNF5
PC9 cells
Lentiviral transduction
B
log2 (TS)
Ranked Genes
HMGCR
C
Mevalonate Pathway
Acetyl CoA
HMG-CoA
HMGCR
Statins
Mevalonate
FPP
Prenylated Proteins
Cholesterol
GGPP
Dolichol
Coenzyme Q
D
PC9
Fold Change in Cell Survival
DMSO
GNF5
Simvastatin
Fluvastatin
GNF5 + Simvastatin
GNF5 + Fluvastatin
E
Vehicle
ABL001
Simvstn
Combo
F
PC9
Abs 590 nm
DMSO
ABL001
Simvastatin
Combination
G
DMSO
GNF5
Simvastatin
Fluvastatin
GNF5 + Simv
GNF5 + Fluv
Cleaved PARP
Total PARP
Cleaved Caspase 3
Total Caspase 3
pCRKL
CRKL
β-Tubulin
H
Count
PE Annexin V
DMSO
GNF5
Simstn
Flustn
GNF5 + Simstn
GNF5 + Flustn
Annexin V
Fold Change in MFI
DMSO
GNF5
Simvastatin
Fluvastatin
GNF5 + Simstn
GNF5 + Flustn

Figure 7: Metabolically focused CRISPR/Cas9 loss-of-function screen identifies HMGCR as an apoptotic sensitizer in the presence of ABL allosteric inhibitors. (A) Diagram of CRISPR/Cas9 loss-of-function screening strategy adapted from [29]. (B) Gene-level representation of GNF5 sensitization phenotype. Genes were ranked by their log2-transformed three score (TS) (GNF5-treated/DMSO-treated). Apoptotically reactive genes are denoted by the red box and HMGCR TS is highlighted. (C) Schematic of the mevalonate pathway indicating statin inhibition of HMGCR. (D) Validation of pharmacologic sensitization of statin therapeutics to GNF5-mediated cell death using 72 hr growth inhibition assays. Shown are sublethal doses of GNF5 (5 μM), simvastatin (1 μM), and fluvastatin (0.5 μM) derived from 72 hr dose-response curves in the presence and absence of each drug. (E) Representative images from colony formation assays of PC9 cells treated with ABL001 (1 μM), simvastatin (100 nM) alone and in combination for 1 week. (F) Quantification of absorbance reading for colony formation assays from Fig. 2E (n=2). (G) Immunoblots of cleaved PARP, cleaved caspase-3, and β-tubulin in PC9 cells treated for 24 hr with GNF5 (5 μM), simvastatin (1 μM), and fluvastatin (0.5 μM) alone and in combination. (H) FACS of total events and relative change in Annexin V+ PC9 cells treated for 24 hr with GNF5 (5 μM), simvastatin (1 μM), and fluvastatin (0.5 μM) alone and in combination. Graph (bottom) shows fold change in Annexin V staining. Statistical analysis was performed using one-way ANOVA and Tukey post hoc testing (n = 3). *p<0.05, **p<0.01, ***p<0.001, ****p<0.0001. Data are mean ± SEM.
Acknowledgement: CRISPR/Cas9 library was obtained from Kevin Lin, deep sequencing analysis was performed by the Duke Center for Genomic and Computational Biology, and Jiaxing Lin performed the bioinformatics analysis of the sgRNA abundance from deep sequencing (Figure 7B).

To validate the results of the screen, PC9 cells were treated with sublethal doses of GNF5 and two statins, simvastatin and fluvastatin. Following 72hr of combination treatment, over 90% of cells underwent cell death (Figure 7D). Similar results were seen when cells were cultured in colony formation assays (Figure 7E, F; Figure 8A, B). To validate the on-target effect of statins, shRNAs against HMGCR were transduced into PC9 lung cancer cells, and these cells were then treated with GNF5 (Figure 8C, D). HMGCR was partially knocked down allowing for the cells to remain viable albeit with reduced pathway activity. HMGCR-knockdown exhibited markedly decreased cell survival compared to control lung cancer cells following treatment with GNF5 (Figure 8C, D), which corresponds with the pharmacologic data. Further, immunoblotting revealed dramatic induction of the apoptotic mediators cleaved poly (ADP-ribose) polymerase (PARP) and cleaved caspase-3 following 24hr of combination treatment with GNF5 and statins, which was consistent with identification of apoptotic cells by flow cytometry of annexin V-stained lung cancer cells co-treated with GNF5 and statins (Figure 8G, H). These data reveal a novel treatment paradigm whereby HMGCR inhibition combined with ABL allosteric inhibition sensitizes cells towards apoptotic cell death.

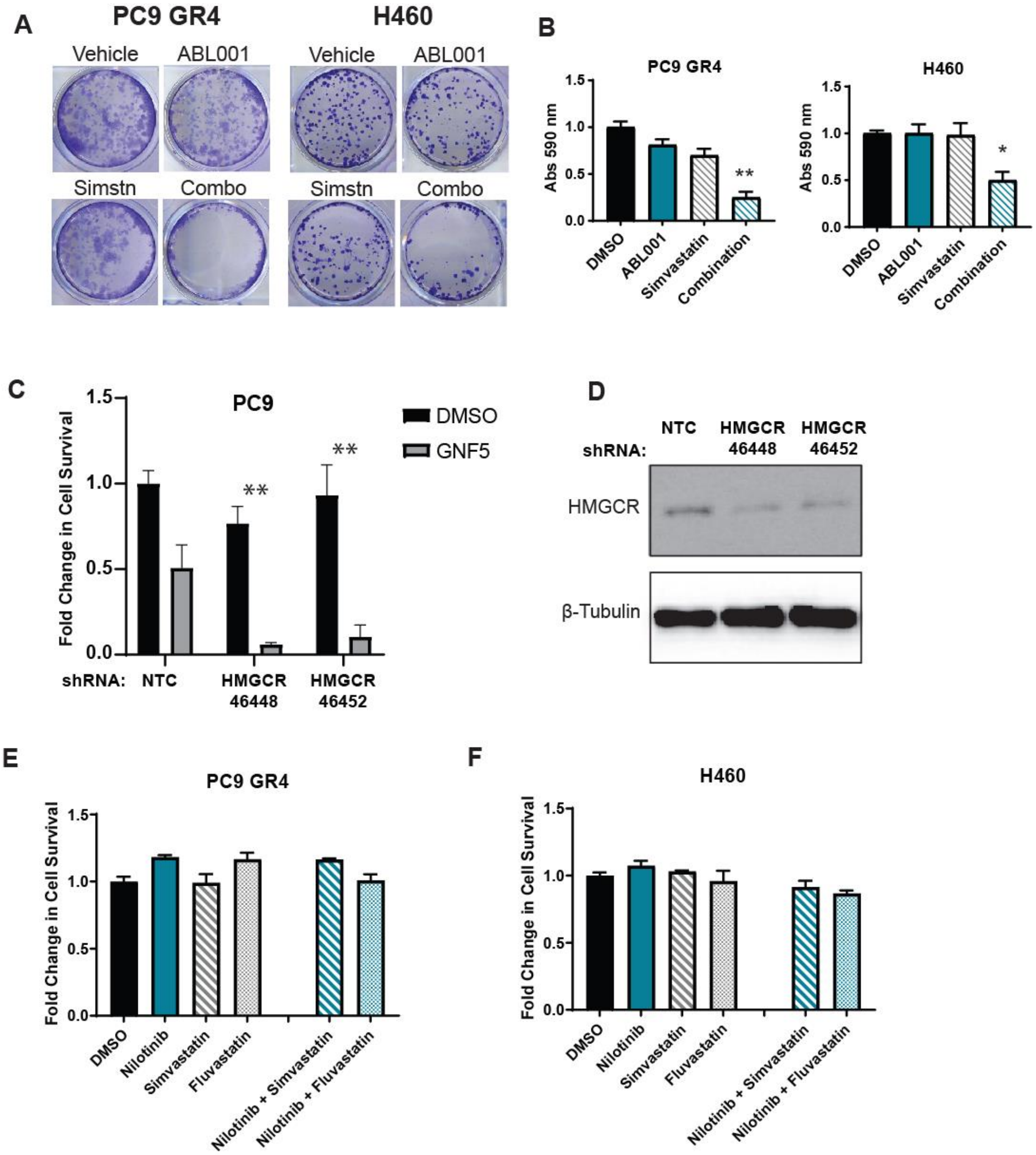

Figure 8: HMGCR inactivation sensitizes lung cancer cells to cell death in the presence of ABL allosteric inhibitor but not ATP-competitive inhibitor. (A) Representative images from colony formation assays of PC9 GR4 and H460 cells treated with ABL001 (1 μM), simvastatin (100 nM), and combination of ABL001 and simvastatin for 1 week. (B) Quantification of absorbance reading for colony formation assays from Fig. S3A (n=2). (C) PC9 cells harboring two distinct shRNAs (#46448 and #46452) against HMGCR or non-targeted control (NTC) were treated with GNF5 for 72hr to assess cell

viability. (D) Immunoblotting for HMGCR and β-Tubulin shows knockdown of HMGCR protein with both shRNAs #46448 and #46452. (E-F) Cell viability assays were used to examine sensitization of statin therapeutics to the ABL ATP-site inhibitor Nilotinib after 72 hr of co-treatment in the indicated lung cancer cells. Sublethal doses of Nilotinib (PC9 GR4, 5 uM; H460, 7.5 uM), simvastatin (PC9 GR4, 1 uM; H460 3 uM), and fluvastatin (PC9 GR4, 0.5 uM; H460 2 uM), were used and cell viability assays were performed after 72 hr with indicated drugs. Statistical analysis was performed using one-way ANOVA and Tukey post hoc testing ($n = 3$). *$p<0.05$, ** $p<0.01$

2.2.3 ABL allosteric inhibitors preferentially synergize with statins to induce lung cancer cell death

To assess whether ABL allosteric inhibitors preferentially synergize with statins in comparison to EGFR inhibitors and chemotherapeutic drugs, lung cancer cells were treated at equivalent sublethal doses below the IC_{50} value of each drug as determined with dose response assays for each cell line. Notably, only the ABL allosteric inhibitors exhibited enhanced cell killing effects upon combination with either simvastatin or fluvastatin in EGFR mutant cells sensitive to EGFR TKIs (PC9), resistant to gefitinib (PC9 GR4), or harboring metastatic tropism to the brain (PC9 BrM3) (Figure 9A-C). Similar findings were observed in KRAS mutant H460 and H358 cancer cell lines (Figure 9D, E). The combination of ABL allosteric inhibitors with statins was found to be synergistic across cell lines as assessed by the Bliss formula for synergy (201), where a score of 1 indicates true synergy (Figure 9F).

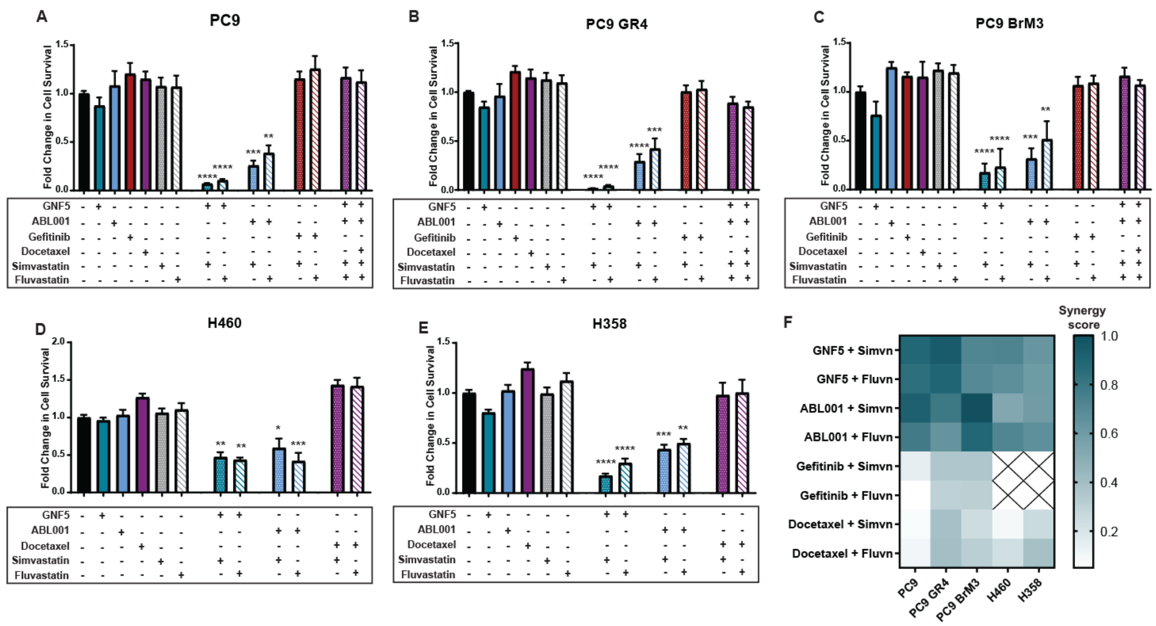

Figure 9: ABL allosteric inhibitors preferentially synergize with statins to induce lung cancer cell death. (A-E) Comparison of pharmacologic sensitization of statin therapeutics to ABL allosteric inhibitors versus FDA-approved therapies using 72 hr growth inhibition assays. Shown are sublethal doses of GNF5 (PC9, PC9 GR4, PC9 BrM3 5 μM; H460, H358 7.5 μM), ABL001 (PC9, PC9 GR4, PC9 BrM3 5 μM; H460, H358 7.5 μM), Gefitinib (PC9, PC9 BrM3 7.5 nM; PC9 GR4 100 nM), Docetaxel (PC9, PC9 GR4, PC9 BrM3, H358 0.5 nM; H460 0.25 nM), Simvastatin (PC9, PC9 GR4, PC9 BrM3 1 μM; H460, H358 3 μM), and Fluvastatin (PC9, PC9 GR4, PC9 BrM3 0.5 μM; H460, H358 2 μM), derived from 72 hr dose-response curves in the presence and absence of each drug. (F) Heat map representing the synergy score for each drug interaction as calculated by the Bliss formula for synergy. A score of 1.0 indicates true synergy. Statistical analysis was performed using one-way ANOVA and Tukey post hoc testing (n = 3). *p<0.05, **p<0.01, ***p<0.001, ****p<0.0001. Data are mean ± SEM.

Next, we sought to evaluate whether sensitization to statin treatment was specific to the ABL allosteric inhibitors or could also be induced by ABL ATP-site inhibitors. Co-treatment of PC9 GR4 and H460 cells with sublethal doses of Nilotinib and either simvastatin or fluvastatin did not promote additive or synergistic decreases in cell viability (Figure 8E, F). These findings highlight the differential effects induced by ABL allosteric versus ATP-competitive inhibitors, and support the notion that ABL allosteric inhibitors preferentially sensitize lung cancer cells to cell death by combination treatment with lipophilic statins.

There are conflicting *in vitro* reports indicating additive cell killing effects of chemotherapy with high-dose statin therapeutics (202, 203). Thus, we treated lung cancer cells with IC_{50} doses of GNF5, ABL001, gefitinib, and docetaxel to determine whether treatment at higher than sublethal doses could enhance the cell killing effects of these drugs. Again, we found that only ABL allosteric inhibitors could synergize with simvastatin and promote cleavage of PARP and caspase-3 in PC9 cells (Figure 10A-C). In this regard, clinical trial data have shown that statins in combination with various chemotherapies had either marginal or no effect on progression-free survival or overall survival in lung cancer patients (204-206). Together, these results show that in contrast to gefitinib and docetaxel, ABL allosteric inhibitors are preferentially capable of sensitizing lung cancer cells to statins and dramatically inhibit cancer cell survival.

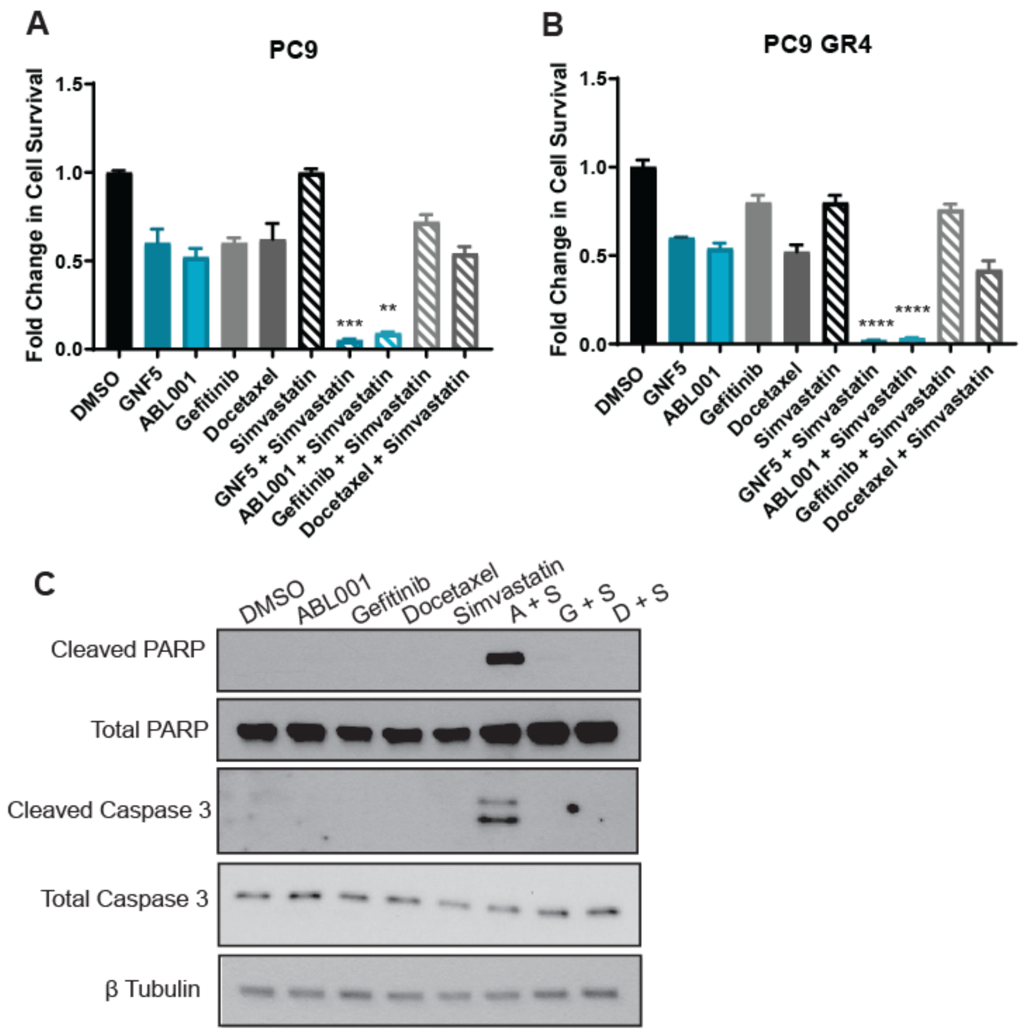

Figure 10: IC$_{50}$ doses for ABL allosteric inhibitors, Gefitinib, or Docetaxel, with low dose statins demonstrate preferential synergy with ABL allosteric inhibitors. (A-B) Cell viability assays to evaluate sensitization of statin therapeutics to ABL allosteric inhibitors versus FDA-approved therapies at IC$_{50}$ doses using 72 hr growth inhibition assays. Simvastatin was used at subtherapeutic doses (PC9, PC9 GR4 1 uM). (C) Corresponding western blot analysis of cleaved PARP, total PARP, cleaved caspase 3, total caspase, and β-Tubulin in PC9 cells treated with IC$_{50}$ doses of ABL001, Gefitinib, and Docetaxel combined with subtherapeutic doses of simvastatin.

2.2.4 Mevalonate, but not cholesterol, rescues cell survival in lung cancer cells co-treated with statins and ABL allosteric inhibitors

The mevalonate (MVA) pathway catalyzes the conversion of acetyl-CoA to HMG-CoA which is then converted by HMGCR into mevalonate (Figure 2C). Mevalonate is required for the generation of cholesterol and isoprenoids among other end products. Rescue experiments were performed to identify if MVA or the downstream metabolite cholesterol could reverse the cell killing effect induced by low dose simvastatin treatment in cells co-treated with sublethal doses of ABL allosteric inhibitors. Interestingly, only MVA, but not cholesterol, could rescue cell survival in PC9 GR4 and H460 lung cancer cells (Figure 11A, C). Consistent with these findings, addition of MVA, but not cholesterol, prevented cleavage of PARP and caspase-3 suggesting that sensitization of lung cancer cells to apoptosis induced by ABL allosteric inhibitors in combination with statin therapy is independent of cholesterol (Figure 11B, D).

The apoptotic cascade is mediated by interplay among BCL-2 family proteins comprised of pro-apoptotic and anti-apoptotic proteins (207). Following combination treatment with ABL allosteric inhibitors and statins, we observed that gene expression of the pro-survival factors BCL-2 and BCL-X_L was downregulated, while expression of pro-apoptotic PUMA was increased (Figure 11E). Supplementation with MVA, but not cholesterol, restored gene expression back to baseline (Figure 11E). Changes in BCL-2 family member expression can elicit pore formation in the mitochondria, resulting in mitochondria outer membrane permeabilization (MOMP), leading to cytochrome c release (208). Subcellular fractionation revealed release of cytochrome c from the mitochondrial membrane fraction into the cytosol in response to co-treatment with ABL001 and Simvastatin, which was reversed following the addition of MVA (Figure 11F). Further, treatment with IC_{50} values of ABL inhibitors rescued cell survival in the presence of BAX knockdown indicating that high doses of ABL inhibitors alter BCL2 expression and promotes mitochondrial mediated cell death (Figure 11G). These data show that ABL001 and Simvastatin combination therapy alters gene expression of BCL-2 family members leading to permeabilization of the mitochondria, release of cytochrome c into the cytosol, and cleavage of caspase 3, and that these processes can be reversed by the addition of MVA.

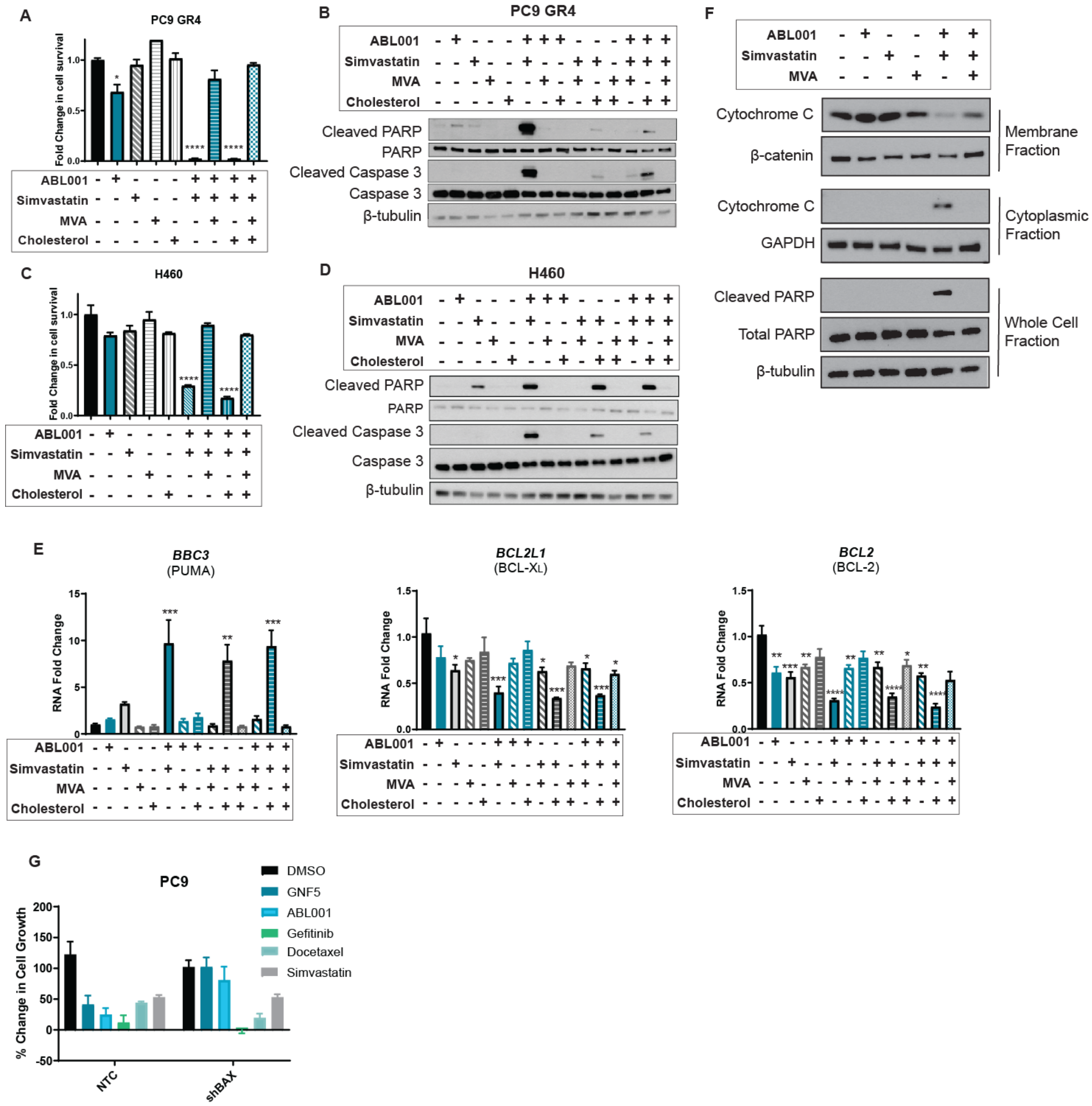

Figure 11: Mevalonate, but not cholesterol, rescues cell survival in lung cancer cells co-treated with statins and ABL allosteric inhibitors. (A) Cell viability of PC9 GR4 cells treated with the combination of 5 μM ABL001 and 1 μM simvastatin supplemented with 500 μM mevalonate (MVA) or 25 μM cholesterol for 72 hours. Statistical analysis was performed using one-way ANOVA and Tukey post hoc testing (n = 3). (B) Immunoblots of cleaved PARP, cleaved caspase 3, and B-tubulin in PC9 cells treated for 24 hr with 5 μM ABL001 and 1 μM simvastatin supplemented with 500 μM MVA or 25 μM

cholesterol. (C) Cell viability of H460 cells treated with the combination of 7.5 μM ABL001 and 3 μM simvastatin supplemented with 500 μM MVA or 25 μM cholesterol for 72 hours. Statistical analysis was performed using one-way ANOVA and Tukey post hoc testing (n = 3). (D) Immunoblots of cleaved PARP, cleaved caspase 3, and β-tubulin in H460 cells treated for 24 hr with 7.5 μM ABL001 and 3 μM simvastatin supplemented with 500 μM MVA or 25 μM cholesterol. (E) qRT-PCR of indicated mRNAs in PC9 GR4 cells treated with 5 μM ABL001 and 1 μM simvastatin supplemented with 500 μM MVA or 25 μM cholesterol for 24 hours. Statistical analysis was performed using one-way ANOVA and Fisher post hoc testing (n = 3). (F) Immunoblots of cytochrome c, cleaved PARP, β-catenin, GAPDH, and β-Tubulin. PC9 GR4 cells were treated with of 5 μM ABL001 and 1 μM simvastatin supplemented with 500 μM MVA for 24 hr, collected, and fractionated. Cytoplasmic, membrane, and whole cell fractions are shown for drug treatments. (G) Bax shRNA mediated knockdown in PC9 cells rescued cell survival following IC50 treatment of the indicated drugs. *p<0.05, **p<0.01, ***p<0.001, ****p<0.0001. Data are mean ± SEM.

2.2.5 Apoptotic sensitization to statin therapy by ABL allosteric inhibitors requires inhibition of protein prenylation

Mevalonate is the precursor to farnesyl diphosphate (FPP), which can either be converted to geranylgeranyl diphosphate (GGPP) or cyclized to produce squalene for cholesterol production (209). Both FPP and GGPP are metabolites in the isoprenoid pathway required for protein prenylation, a posttranslational enzymatic modification that adds a prenylated motif to CAAX proteins, such as the RAP1A GTPase (210). These modifications regulate protein localization to different cellular compartments, facilitate specific protein–protein interactions and modulate protein stability. Since the downstream sterol metabolite cholesterol did not rescue cell survival, we investigated whether metabolites in the isoprenoid pathway were critical for sensitization to statin therapeutics. We found that addition of GGPP preferentially rescued cell viability compared to FPP in PC9 GR4, PC9, and H460 cells co-treated with ABL001 and simvastatin (Figures 12A and 13A, B). Immunoblotting was performed to assess whether protein prenylation was altered following simvastatin treatment (Figure 12B). Simvastatin treatment increased levels of unprenylated RAP1A protein indicating inhibition of the geranylgeranylation pathway and induced a mobility shift in HDJ2 signifying inhibition of the farnesylation pathway, both of which were reversed by the addition of the indicated prenylation metabolites (Figure 12B) (211, 212). We next tested whether inhibition of either geranylgeranyl transferase (GGT) or farnesyl transferase (FT) could impact cell survival in a manner similar to simvastatin treatment. Survival of PC9 GR4, PC9, and H460 cells co-treated with ABL001 and the GGT-1 inhibitor (GGTI-298) was significantly impaired, but cell survival was only slightly decreased following addition of the FT inhibitor (FTI-277) in the presence of ABL001. Further, the non-additivity observed for statin treatment and GGT and FT inhibition suggested that the synergizing effects of statins or GGTI-298 + FTI-277 in the presence of ABL allosteric inhibitor operate through the same pathway (Figures 12C and 13C, D). Immunoblotting confirmed that each inhibitor specifically suppressed its target pathway (Figure 12D). Collectively, these data reveal that inhibition of protein geranylgeranylation is sufficient to sensitize cells to ABL allosteric inhibitors leading to enhanced intrinsic apoptosis.

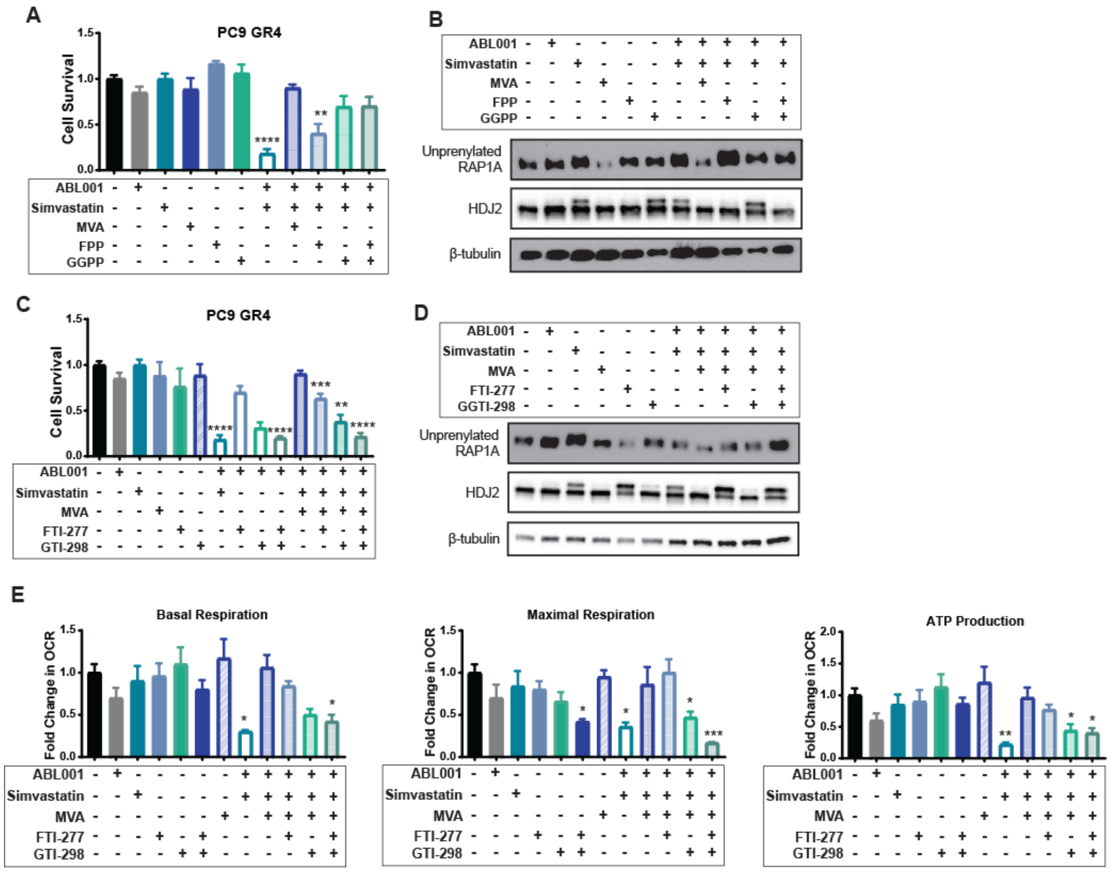

Figure 12: Apoptotic sensitization to statin therapy by ABL allosteric inhibitors requires inhibition of protein prenylation. (A) Cell viability of PC9 GR4 cells treated singly or with the combination of 5 μM ABL001 and 1 μM simvastatin supplemented with 500 μM MVA, 10 μM FPP, or 10 μM GGPP for 72 hours. (B) Immunoblots of unprenylated RAP1A, HDJ-2, and β-tubulin in PC9 GR4 cells treated for 24 hr with 5 μM ABL001 and 1 μM simvastatin supplemented with 500 μM MVA, 10 μM FPP (farnesylation metabolite), or 10 μM GGPP (geranylgeranylation metabolite). Simvastatin caused a mobility shift of HDJ-2 (slower, migrating unprenylated form) and induced the appearance of unprenylated RAP1A. Prenylation alterations were rescued with the indicated metabolites for each pathway. (C) Cell viability of PC9 GR4 cells treated with 5 μM ABL001 and 1 μM simvastatin, 500 μM MVA, 5 μM GGTI-298 (GGT inhibitor), 12.5 μM FTI-277 (FT inhibitor) for 72 hr (n=3). (D) Immunoblots of unprenylated RAP1A, HDJ-2, and β-tubulin in PC9 GR4 cells treated for 24 hr with 5 μM ABL001 and 1 μM simvastatin supplemented with 500 μM MVA, 5 μM GGTI-298, and 12.5 μM FTI-277. Statistical analysis was performed using one-way ANOVA and Tukey post hoc testing (n = 3). (E) Mitochondrial basal respiration, maximal respiration, and ATP production as measured by Seahorse XF Analyzer's Mito Stress Test for PC9 GR4 cells treated singly or with indicated combinations of 2.5 μM ABL001, 1 μM simvastatin, 500 μM MVA, 5 μM GGTI-

298 (GGT inhibitor), or 12.5 μM FTI-277 for 24 hr (n=2). **$p<0.01$, ***$p<0.001$, ****$p<0.0001$. Data are mean ± SEM.

Since we observed that oxidative metabolism was impaired following treatment with IC_{50} doses of the ABL allosteric inhibitors and that combination therapy induced MOMP, we next investigated whether combination treatment with ABL allosteric inhibitor and statin affected mitochondrial metabolism and whether these effects might be due to changes in the protein prenylation pathway. To this end, we examined changes in mitochondrial respiration in cells co-treated with low doses of ABL001 and Simvastatin and found that basal and maximal respiration as well as ATP production were decreased (Figure 12E). Notably, addition of MVA restored mitochondrial respiration back to baseline, and while treatment with FTI-277 had minimal effect, treatment with GGTI-298 negated the MVA rescue and caused mitochondrial respiration levels to drop to a similar degree as to those observed following ABL001 and simvastatin treatment (Figure 12E). These data indicate that inhibition of the mevalonate pathway in combination with ABL kinase inhibition promotes cell death by impairing mitochondrial function.

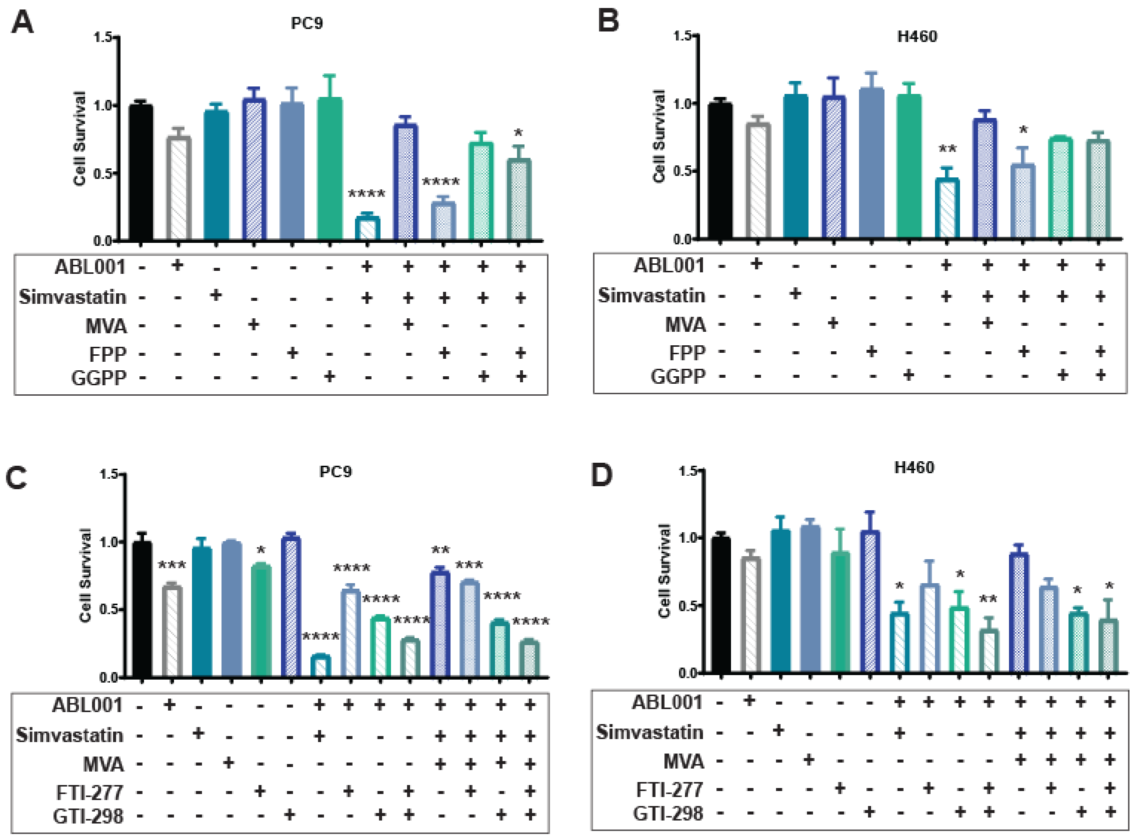

Figure 13: Inhibition of protein prenylation sensitizes lung cancer cells to ABL allosteric inhibitor. (A) Cell viability of PC9 cells treated with the combination of 5 uM ABL001 and 1 uM simvastatin supplemented with 500 uM MVA, FPP, or GGPP for 72 hours. (B) Cell viability of H460 cells treated with the combination of 7.5 uM ABL001 and 3 uM simvastatin supplemented with 500 uM MVA, FPP, or GGPP for 72 hours. (C) Cell viability of PC9 GR4 cells treated 5 uM ABL001 and 1 uM simvastatin, 500 uM MVA, 5 uM GGTI-298, 12.5 uM FTI-277 for 72 hr. (D) Cell viability of H460 cells treated with the combination of 7.5 uM ABL001, 3 uM simvastatin, 500 uM MVA, 3 uM GGTI-298, 3 uM FTI-277 for 72 hr. Statistical analysis was performed using one-way ANOVA and Tukey post hoc testing (n = 3). **p<0.01, ***p<0.001, ****p<0.0001. Data are mean ± SEM.

2.2.6 Combination therapy of ABL001 and simvastatin impairs tumor growth and increases survival in mouse models of lung cancer brain metastasis and gefitinib resistance

Despite recent clinical successes with next-generation EGFR TKIs such as Osimertinib, relapses often occur among patients harboring EGFR mutant NSCLC. Moreover, patients harboring KRAS driver mutations have few tractable therapeutic options available (213, 214). Further, the ability of anti-cancer drugs to efficiently penetrate the blood-brain barrier (BBB) and reach therapeutic doses for lung cancer patients harboring brain metastases is limited. Thus, we chose to evaluate whether statins could synergize with ABL inhibitors *in vivo* to treat cancer cells seeded at distal sites following intracardiac injection in clinically relevant mouse models of brain metastasis and therapy-resistance. We employed ABL001 as it has been shown to cross the BBB in preclinical mouse models and is currently in clinical trials for therapy-resistant patients with BCR-ABL+ chronic myeloid leukemia (192, 215). Importantly, administration of ABL001 by oral gavage is well tolerated and does not induce weight loss in mice (195). Pharmacokinetic data has shown that lipophilic statins can cross the BBB more readily than hydrophilic statins (216). In this regard, studies testing the ability of radiolabeled simvastatin to cross the BBB identified simvastatin-derived radioactivity in the rat brain following oral administration (217). Thus, we employed clinically relevant low doses of simvastatin, and treated mice with 10 mg/kd qd simvastatin, which is equivalent to doses used in humans (218-220)

To determine whether combination treatment could impair brain metastatic outgrowth, we used brain-metastatic PC9-BrM3 cells derived through serial rounds of intracardiac injection in athymic nude mice (192). Previous studies have shown that following injection into the arterial circulation, brain-metastatic lung cancer cells extravasate into the brain parenchyma by day 6 post-injection (221, 222). Thus, to evaluate the effectiveness of combination ABL001 and statin treatment on metastatic colonization, we performed bioluminescent imaging (BLI) on day 6 post-intracardiac injection to stratify mice into treatment groups and began drug treatments on day 7 (Figure 14A). Mice were divided into four treatment groups: vehicle, ABL001, simvastatin, or combination of ABL001 and simvastatin. We found that overall survival was significantly increased in mice harboring PC9-BrM3 brain metastases following combination treatment in comparison to vehicle, ABL001, or simvastatin alone (Figure 14B). Similar results were observed in mice harboring gefitinib resistant PC9 cells (PC9 GR4) as ABL001 and simvastatin combination therapy extended overall survival (Figure 14C). Quantification of brain flux at day 27 revealed decreased disease burden in mice treated with both ABL001 and simvastatin compared to vehicle or single drug treatment groups (Figure 14D,E). Immunofluorescence analysis of brain metastases for proliferation and apoptotic markers revealed decreased expression of the proliferative marker Ki67 and increased expression of the cell death marker cleaved caspase-3 (Figure 14F-H).

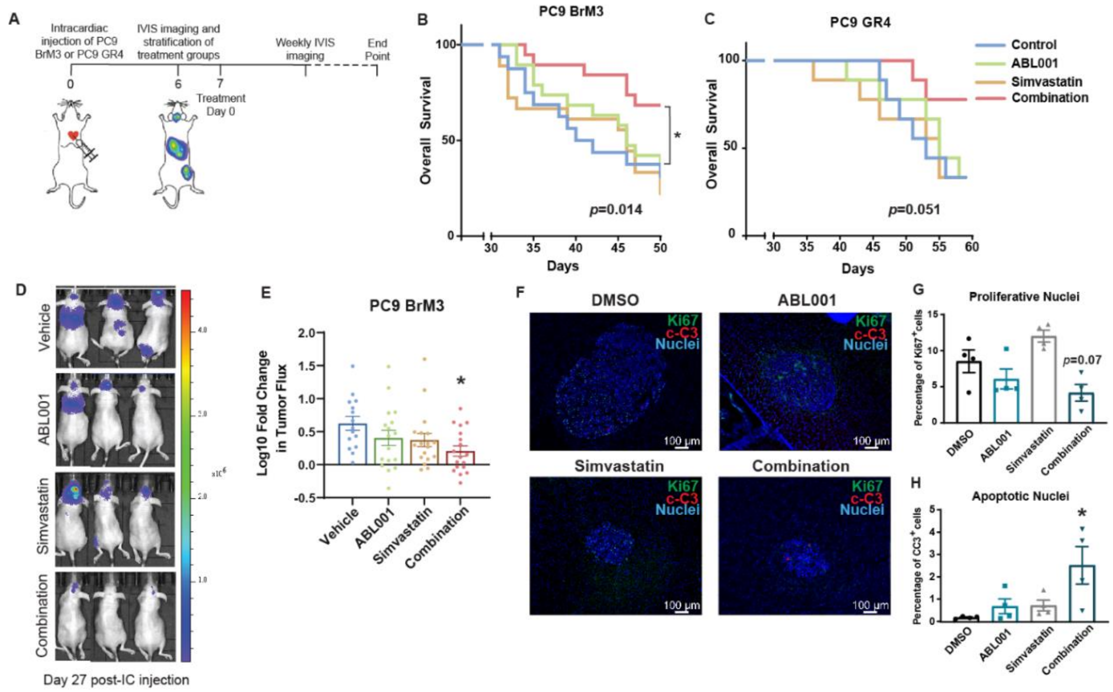

Figure 14: Combination therapy of ABL001 and simvastatin increases survival in mouse models of lung cancer brain metastasis and gefitinib resistance. (A) Schematic showing experimental overview. PC9 BrM3 or PC9 GR4 labeled with luciferase-tomato (pFULT) were intracardially injected into mice on Day 0. IVIS imaging of metastatic burden was performed on Day 6 followed by equivalent stratification of mice into treatment groups based on tumor flux. Oral gavage treatment of drugs began on Day 7 followed by weekly IVIS imaging until experimental end point (Day 50). Statistical analysis of overall survival was calculated using log rank (MantelCox) test and interactions below an adjusted $p<0.017$ were deemed significant accounting for 3 pairwise comparisons. (B) Overall survival of mice injected intracardially with PC9 BrM3-pFULT cells treated with DMSO (n=16), ABL001 (n=19), simvastatin (n=17), and combination of ABL001 and simvastatin (n=19). (C) Overall survival of mice injected intracardially with PC9 GR4-pFULT cells treated with DMSO (n=9), ABL001 (n=9), simvastatin (n=9), and combination (n=9). (D) Representative images (day 27 post-injection) of mice intracardially injected with PC9 BrM3-pFULT cells. (E) Quantitative analysis (day 30 post-injection) of whole-body metastatic index in mice injected intracardially with PC9 BrM3 cells and treated with DMSO (n=16), ABL001 (n=19), simvastatin (n=17), and combination (n=19). (F) Immunofluorescence staining of brain tumors from PC9 BrM3 mice on Day 35 stained with Ki67 (green), cleaved caspase 3 (c-C3) (red), and Hoescht 33342 (nuclei) (blue). (G-H) Quantification of percent positive proliferative (G) and apoptotic (H) nuclei in tumor sections. Statistical analysis was

performed using one-way ANOVA with Dunnet post hoc testing (n = 3) *$p<0.05$. Data are mean $\pm$ SEM. *Acknowledgement: Jacob Hoj intracardially injected mice with tumor cells.*

Notably, the effect of combination drug treatment on primary tumor growth was minimal in comparison to vehicle or single treatment groups for PC9 GR4 cells injected subcutaneously into the flank (Figure 15A, B). This finding is consistent with previous reports showing that the inhibitory effects of ABL inactivation on primary tumor growth are cell context-dependent, and that genetic and pharmacologic inhibition of the ABL kinases decreased spontaneous metastasis but not primary tumor growth (97, 104). Together, these data reveal that combination treatment with both ABL001 and simvastatin impairs metastatic outgrowth of lung cancer cells by promoting tumor cell death.

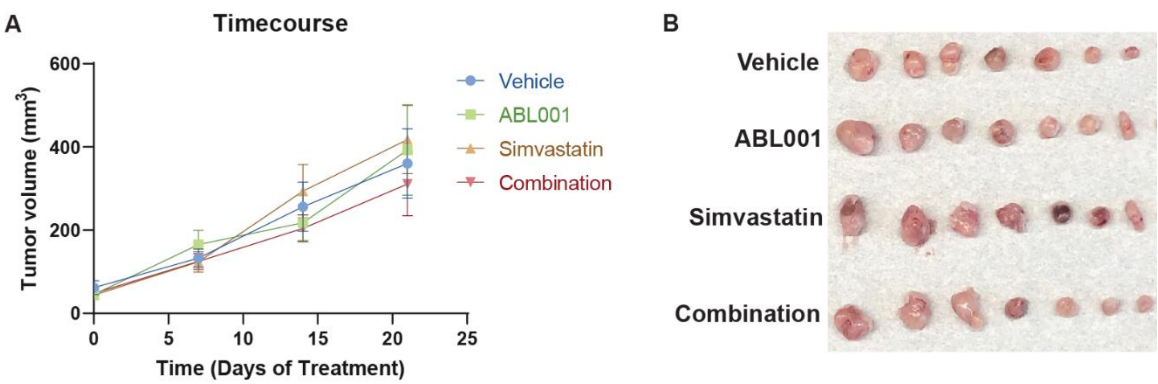

Figure 15: Combination therapy of ABL001 and simvastatin does not affect primary tumor growth. (A) Mice were subcutaneously injected with PC9 GR4 cells and stratified into four treatment groups once tumors reached 50 mm^3 and indicated drug treatment began on Day 1. Mice were treated for a total of 3 weeks and tumor volume was measured weekly. (B) Image of final tumors harvested from mice showing no appreciable change in tumor size of ABL001 + simvastatin combination treatment in comparison to vehicle or single treatment groups. *Acknowledgement: Jacob Hoj subcutaneously injected mice with tumor cells.*

2.3 Discussion

Metabolic reprogramming in tumors is an adaptation that allows cancer cells to meet enhanced bioenergetic needs, but metabolic dysregulation also generates vulnerabilities in cancer cells that can be exploited for the development of treatment strategies. Among these vulnerabilities is mitochondrial oxidative metabolism as cancer cells are reliant on functional mitochondria for malignant transformation and growth (42). Here we show that in comparison to current FDA-approved therapeutics, gefitinib and docetaxel, ABL allosteric inhibitors markedly decrease mitochondria function in lung cancer cells without affecting glycolysis. A CRISPR/Cas9 loss-of-function screen targeting metabolic enzymes revealed that HMGCR inactivation synergizes with ABL allosteric inhibitors at sublethal doses to induce lung cancer cell apoptosis, thereby revealing dual inactivation of the mevalonate pathway and ABL kinases as a strategy to augment apoptotic cell death and enhance therapeutic efficacy. Patients with lung cancer have the highest leading cancer-related mortality worldwide in part due to the lack of durable responses to current therapies resulting in metastatic and therapy-resistant disease progression (193). By targeting unique metabolic vulnerabilities of lung cancer cells treated with ABL kinase inhibitors, we uncovered novel combination treatment strategies using available ABL allosteric inhibitors with FDA-approved statins for treatment of therapy-resistant and brain metastatic lung cancer cells in preclinical mouse models.

Dysregulation of the mevalonate pathway has been implicated in the progression of solid tumors including glioblastoma, breast, and liver cancer (223-226). Cancer cells exploit distinct bioactive end-products generated by the mevalonate pathway, including cholesterol and isoprenoid intermediates, to promote tumor progression and therapy resistance. For example, glioblastomas rely on exogenous cholesterol for survival and cholesterol depletion induces glioblastoma cell death (225). In contrast, we found that the synergistic interaction between ABL allosteric inhibitors and statins appears to be mediated by inhibition of protein prenylation and is independent of decreased cholesterol. Specifically, metabolic rescue of the geranylgeranylation pathway, but not cholesterol, was capable of rescuing cell survival in lung cancer cells co-treated with ABL001 and statins to an extent equivalent to mevalonate. Protein geranylgeranylation is required for processes such as protein and vesicular trafficking, and cell proliferation (227). Multiple geranylgeranylated proteins might be targeted by statins in ABL-depleted lung cancer cells. A recent report showed that lipophilic statins prevent membrane association of Rab11b, a small GTPase that regulates endosomal recycling, and decreases breast cancer brain metastasis in mice (228). Among numerous substrates of the geranylgeranylation pathway are RAS-related GTPases, including members of the RAS and RHO–RAC families (227), which can function to regulate lung cancer cell survival *in vitro* and metastasis in mice. Future studies are needed to assess whether decreased protein geranylgeranylation of specific targets mediates the striking decrease in lung cancer cell survival *in vitro* and in *in vivo* mouse models of metastasis following combination therapy with ABL001 and statins.

ABL kinases can target multiple substrates in cancer cells to promote cytoskeletal alterations, organelle trafficking, cell growth and cell survival (107, 111). Here we show that ABL inactivation impairs mitochondria function and organelle integrity following pharmacologic inhibition or genetic depletion, which are not induced by treatment with gefitinib or docetaxel. These findings suggest that sensitization to statin therapy might be mediated through mitochondrial priming triggered by ABL kinase inhibition. Statins have also been shown to inhibit synthesis of coenzyme Q and ubiquinol–cytochrome c reductase, critical components of the electron transport chain (ETC), through impeding mevalonate production (229-232). Previous reports showed that statins can enhance mitochondrial priming and sensitize cancer cells to mitochondrial-mediated apoptosis (233). For example, inhibition of the pro-survival factor BCL-2 sensitized leukemia cells to statin therapeutics promoting apoptosis (233). Future studies are needed to assess whether ABL kinase inhibition impairs mitochondria by altering the activity of the ETC. In this regard, Src family tyrosine kinases have been shown to phosphorylate subunits of the ETC resulting in subsequent changes in ETC complex activity, and inhibition of Src kinases results in decreases in complex I activity and decreased mitochondrial respiration (234, 235). ABL1 has been shown to be activated downstream of oncogenic Src (236). Thus, combination treatment of ABL allosteric inhibitors and statins might impair one or more complexes of the ETC, thereby augmenting mitochondrial-mediated apoptosis.

Previous reports have identified the potential of statins to function as anticancer agents; however, clinical trials using various chemotherapies in combination with statins have had either marginal or no effect on distant metastasis-free survival or overall survival in lung cancer patients with advanced disease (204-206). Retrospective analyses of various lung cancer patient cohorts have reported mixed findings on the impact of statin therapeutics on cancer related mortality for patients taking statins at the onset of chemotherapy treatment (90, 237-239). Our findings are consistent with clinical reports showing that statins added to first-line standard of care chemotherapy do not impact lung adenocarcinoma tumors (205, 206) and suggest the potential use of ABL allosteric inhibitors in combination with statins for the treatment of lung cancer patients with advanced metastatic disease with enhanced ABL signaling.

Whereas inactivation of ABL kinases impairs breast and lung cancer metastasis in mouse models (99, 106, 112, 192), clinical trials to treat breast and lung cancer patients with ABL ATP-site inhibitors have been ineffective in part due to targeting of multiple kinases other than ABL, possibly leading to paradoxical activation of cell survival pathways (172-175, 240). Moreover, upon inhibiting the ABL kinases, the ATP competitive inhibitors cause the ABL kinase SH3-SH2 cassette to remain in an open conformation while the allosteric inhibitors induce a closed conformation (241). In the open conformation, the SH3-SH2 domains can bind to downstream targets, and these domains are not available upon binding to the ABL allosteric inhibitors. Notably, our recent work revealed that ABL allosteric inhibitors, but not ABL ATP-competitive inhibitors, disrupt the interaction between ABL2 and the HSF1 transcription factor (100). This finding suggests that protein-protein interactions dependent on distinct ABL protein conformations are specifically disrupted by the binding of the allosteric inhibitors to a unique site in the ABL kinase domain. Consistent with these findings, our work shows that the ABL allosteric inhibitors, which bind to the myristoyl-binding pocket in the C-lobe of the ABL kinase domain and are highly selective inhibitors of the ABL kinases, are capable of impairing mitochondria function in a manner similar to genetic inhibition of the ABL kinases, whereas the ATP-competitive inhibitors fail to impair mitochondrial function (195). Thus, our findings support the potential use of ABL allosteric site inhibitors in combination with statins as a treatment strategy for lung cancer patients with advanced metastatic disease, including those patients with difficult to treat brain metastases or EGFR TKI resistance.

3. ABL kinases regulate SLC7A11 expression and system xCT function

3.1 Introduction

Patients harboring primary or secondary malignant brain tumors often present with neurologic symptoms such as headache, cognitive impairment, seizures, and focal deficits, all having negative consequences on quality of life and survival (242). Surgery, stereotactic radiosurgery (SRS), and whole brain radiation therapy (WBRT) have been historically used to treat patients with brain tumors (243, 244). However, surgery is limited to patient cohorts whose tumors are surgically accessible and do not exceed a certain number or are within an easily resectable size (245). Even if these conditions are met, disease recurrence occurs in approximately 50% of patients (246). Radiation may be used on patients who do not meet the criteria for surgery, but unfortunately it is rarely curative and can have harsh side effects.

Chemotherapies have been explored as treatment for patients with brain tumors, but many have failed due to low blood-brain barrier (BBB) penetration causing inability to accumulate at effective therapeutic doses (247). BBB-penetrable targeted therapies have had greater relative success in the clinic, such as the EGFR-targeted inhibitor Osimertinib (248, 249). However, drug resistance to these therapies still arises causing drug discovery efforts to focus on tumor brain-specific growth and survival.

One of the mechanisms by which tumors grow and survive in the brain parenchyma is through enhanced extracellular glutamate release (250). Glutamate released by gliomas has been suggested to enhance tumor growth through neuronal cell glutamate excitotoxicity (251). By killing the surrounding neurons, tumor cells have more space to grow out. However, this causes patients to experience deleterious side effects such as strokes, seizures, or epilepsy (252, 253). It is believed that the release of peritumoral glutamate is due to upregulation of System xCT, particularly its catalytic subunit SLC7A11 (254). SLC7A11 is responsible for glutamate release while its system xCT counterpart SLC3A2 transports cystine into the cell for glutathione-mediated detoxification. This phenomenon can be observed in the context of gliomas where SLC7A11 is upregulated in malignant human gliomas and patients with these tumors have greater neuronal cell death in the surrounding parenchyma due to neuronal glutamate excitotoxicity (254). Further, glioma patients that lack SLC7A11 expression live on average nine months longer than those with high-level SLC7A11 expression.

One FDA-approved drug exists to inhibit SLC7A11, and it is called sulfasalazine. However, this is an imperfect drug as its half-life in the body is 80 mins due to the breakdown of the majority of the drug by gut bacteria (252). It is currently the only approved SLC7A11 inhibitor, but its short half-life does not make it a good option for use as an anticancer treatment. Thus, other pharmaceuticals need to be explored to inhibit SLC7A11.

ABL kinase inhibitors have been shown to cross the BBB and elicit therapeutic responses in mouse models of brain metastasis and neurodegenerative disorders (255-

260). Through unbiased RNA sequencing, SLC7A11 was identified as a top statistically significant downregulated target in ABL-inhibited cells. The work described herein identifies a new role for ABL kinases in regulating SLC7A11 expression, and a novel discovery that inhibition of ABL kinases and/or SLC7A11 (1) downregulates glutamate export in a cell, (2) prevents or reduces neuronal cell death through decreasing system xCT activity, and (3) serves as a potential treatment for CNS disorders in a subject.

3.2 Results

3.2.1 ABL kinases regulate SLC7A11 RNA and protein expression

We performed global transcriptome analysis on PC9 EGFR mutant lung cancer cells treated with the ABL allosteric inhibitor GNF5 for 72 hours to find the top differentially up or downregulated targets (Figure 16A). We ranked the top 25 statistically significant targets regardless of increased or decreased RNA expression (Figure 16B). We found that SLC7A11 was a top downregulated target upon ABL kinase inhibition. In addition to SLC7A11, we also noted that DMBT1, ZNF37BP, and SPAG1 were among the top downregulated targets. DMBT1 is thought to be a tumor suppressing glycoprotein, but its function in tumors is largely unknown. ZNF37BP and SPAG1 have not been associated with tumor progression as ZNF37BP is a pseudogene and SPAG1 is associated with spermatogenesis. Because of the lack of association of these targets to tumor progression, we chose not to focus on them and instead study SLC7A11.

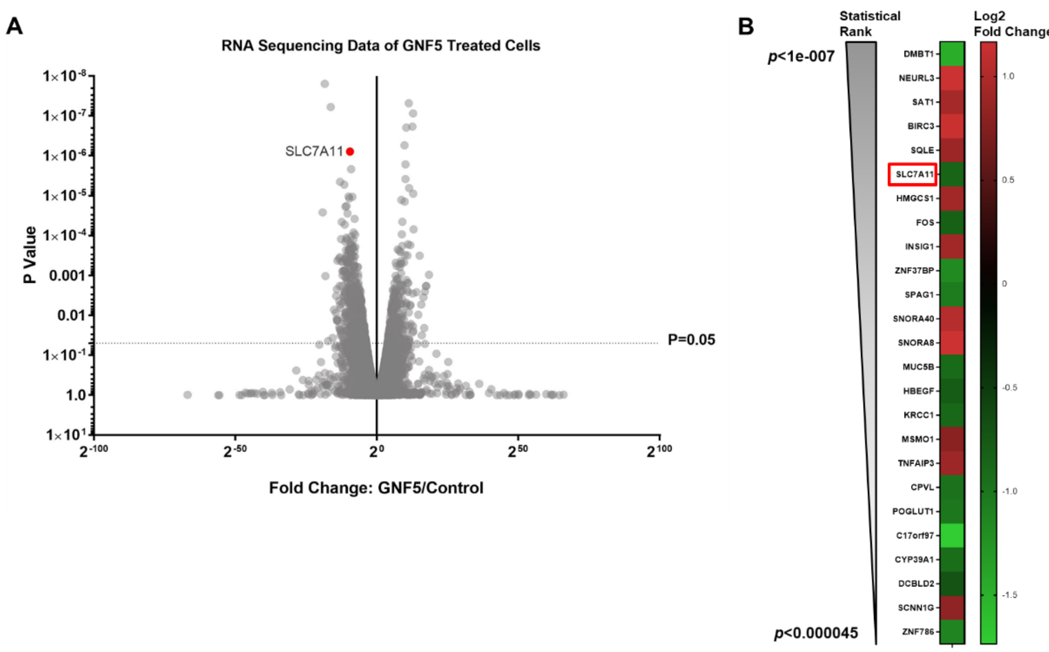

Figure 16: Gene expression is altered by allosteric inhibition of the ABL kinases: identification of SLC7A11 as a downregulated transcript. A) Results from RNA sequencing analysis of PC9 cells treated with vehicle or GNF5 for 72 hours. B) Top 25 statistically significant targets from RNA sequencing analysis. *Acknowledgement: Samples for RNA sequencing were collected by Jing Jin Gu.*

To understand the clinical significance of SLC7A11 in lung cancer, we examined Kaplan-Meier curves for overall survival of lung cancer patients expressing high levels of SLC7A11 or ABL2 mRNA. We found that elevated expression of ABL2 or SLC7A11 was correlated with poor patient prognosis (Figure 17A). Thus, we performed quantitative PCR analysis to analyze the relative abundance SLC7A11 mRNA following either ABL kinase genetic or pharmacologic inhibition. In both cases, knockdown or allosteric inhibition decreased *SLC7A11* gene expression by ~50%, confirming the results of the RNA sequencing analysis (Figure 17B,C). To understand the level to which ABL kinases regulate SLC7A11 expression, we examined protein expression of SLC7A11 following ABL1/ABL2 shRNA-mediated knockdown and saw that SLC7A11 protein expression was decreased to an even greater extent than the reduction in mRNA levels (Figure 17D). These data suggest that inactivation of ABL kinases decreases SLC7A11 via transcriptional and post-transcriptional mechanisms.

Further, since the kinases can have overlapping and divergent functions, we wanted to see which paralog of ABL regulated SLC7A11 or if both could genetically modulate the protein. Thus, we used shRNAs against either ABL1 or ABL2, and found that only upon knock down of both kinases did SLC7A11 protein levels decrease (Figure 17E). This suggests that both ABL kinases are required for full SLC7A11 expression.

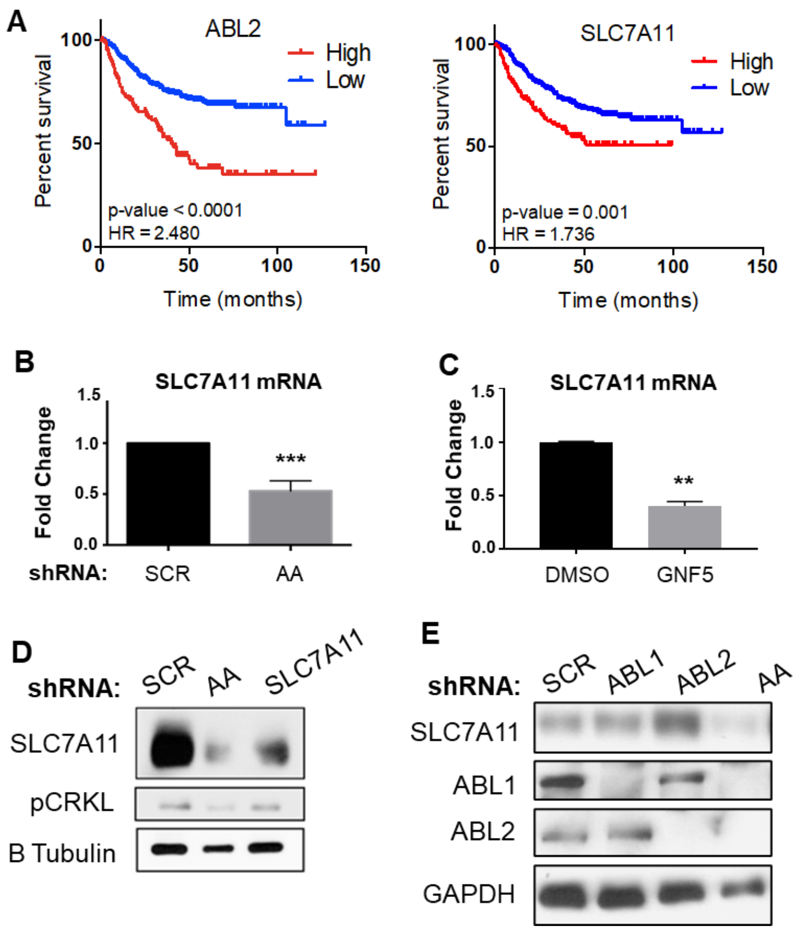

Figure 17. ABL2 and SLC7A11 are associated with poor overall survival in lung cancer patients and ABL kinase inactivation decreases SLC7A11 expression. A) Kaplan-Meier curve analysis of overall survival of lung cancer patients expressing high mRNA levels ABL2 or SLC7A11 correlates with a decrease in survival. B) RT-PCR analysis of SLC7A11 mRNA expression in PC9 cells transduced with shRNAs against ABL1/ABL2 (shAA) or SCR control (shSCR). C) RT-PCR analysis of SLC7A11 mRNA expression in PC9 cells treated for 72 hours with 10 uM GNF5. D) SLC7A11 protein analysis in PC9 cells expressing shRNAs against SCR, AA or SLC7A11 (TRC clone #43124). E) SLC7A11 protein analysis in PC9 cells expressing shRNAs against SCR, ABL1, ABL2, AA. **p<0.01, ***p<0.005

3.2.2 ABL kinases regulate SLC7A11 expression is conserved across breast, lung, and glioma cell lines

Since elevated expression of SLC7A11 has been linked to outgrowth of malignant gliomas, we wanted to determine how baseline SLC7A11 expression varies across metastatic variants of breast, lung, and glioma cell lines. We analyzed a panel of triple-negative breast cancer cell lines with different metastatic capabilities, glioma cell lines with variable mutations, and lung cancer cells with EGFR and KRAS mutations. We hypothesized that SLC7A11 levels would be highest in the glioma cell lines since these cells have been linked to elevated levels of system xCT expression; however, we were surprised to find that SLC7A11 was highest in breast and lung cancer cells with greater metastatic capability (Figure 18). Elevated expression of SLC7A11 in breast, lung, and glioma cell lines is correlated with decreased metastasis-free and overall patient survival, which corresponds to the findings in Figure 18 where SLC7A11 expression is highest in the cancer cell lines with greater metastatic capability (254, 261, 262).

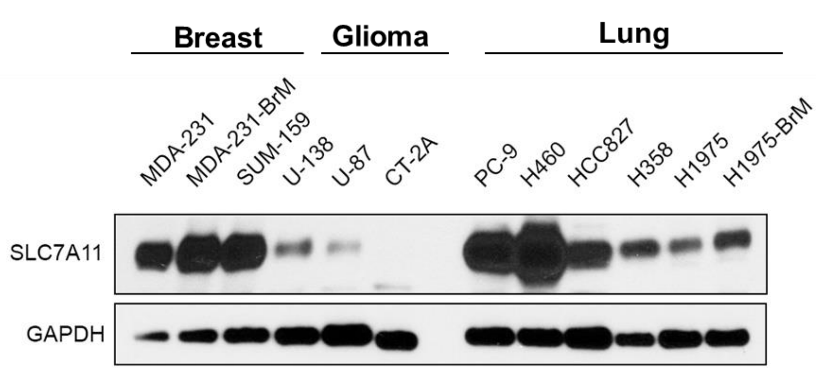

Figure 18. Expression of SLC7A11 protein levels across breast, glioma, and lung cell lines. Expression of SLC7A11 is highest in metastatic breast and lung cancer cell lines.

BrM is an abbreviation for brain metastatic. *Acknowledgement: Felix Steinruecke ran the lysates on western blot.*

Next, we wanted to evaluate whether ABL mediated regulation of SLC7A11 was conserved across cell lines. We transduced lung, breast, and glioma cell lines with shRNAs against ABL1/ABL2 and probed for SLC7A11. In all cell lines tested, SLC7A11 protein levels were decreased upon ABL kinase genetic inhibition (Figure 19A-C). These results imply that ABL kinases can promote SLC7A11 protein stability regardless of mutational status or tumor subtype.

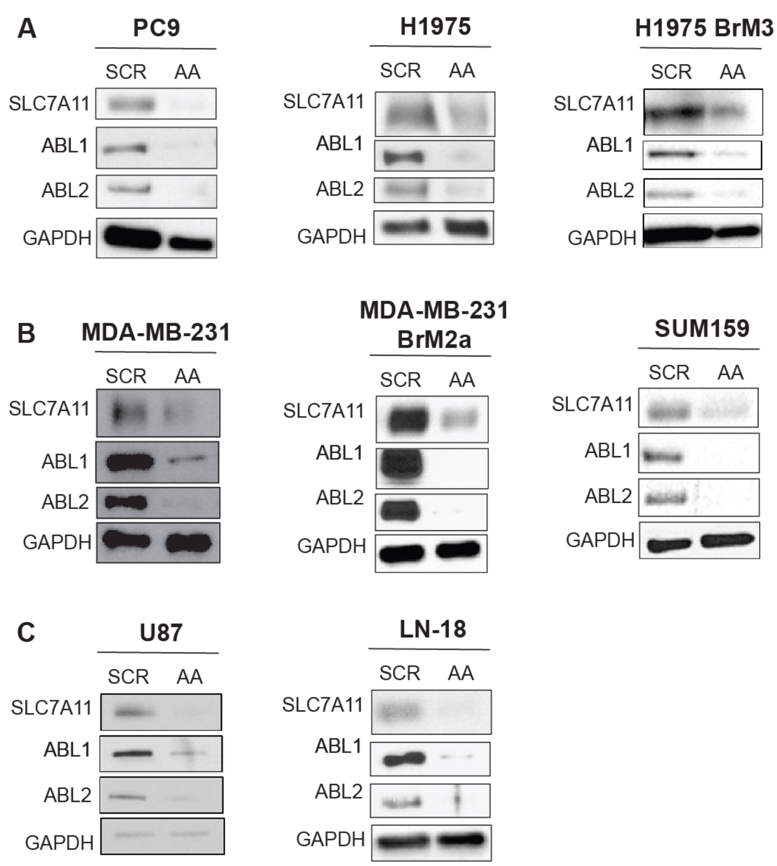

Figure 19: Knockdown of ABL kinases decreases SLC7A11 protein expression across cell lines. A-C) Transduction of shRNAs against ABL1/ABL2 (AA) in lung (A), breast (B), and glioma (C) cell lines showed decreased SLC7A11 protein expression.

To ascertain whether these results held true following pharmacologic inhibition, we exposed breast and glioma cells to the ABL allosteric inhibitors GNF5 and ABL001. After 3-day treatment, SLC7A11 protein levels were decreased in the MDA-MB-231 and SUM159 triple-negative breast cancer cell lines and the U138 glioma cell line (Figure 20A-C). These results are exciting as inhibition of SLC7A11 has been shown to impair tumor outgrowth and metastatic progression in preclinical mouse models (261, 263). Further, ABL kinase signaling has a greater impact on driving the metastatic cascade versus enabling primary tumor growth, thus it is possible that SLC7A11 could be a downstream mediator of ABL kinase signaling during metastatic outgrowth (97, 104).

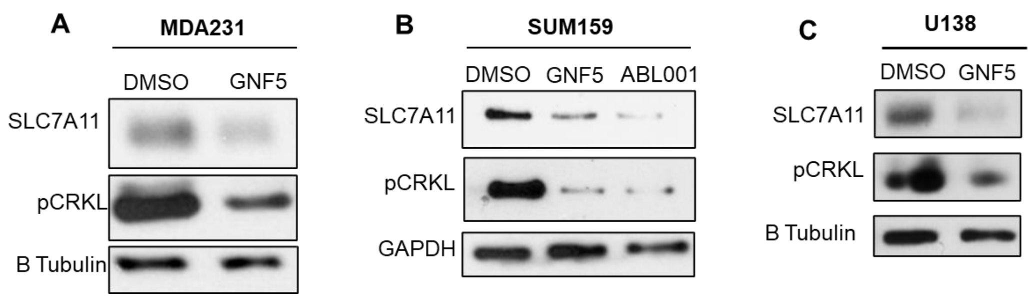

Figure 20: Pharmacologic inhibition of ABL kinases decreases SLC7A11 protein expression. A-C) Treatment of triple-negative breast cancer (A-B) or glioma cells (C) with the ABL kinase allosteric inhibitors GNF5 or ABL001 for 72 hours decreased SLC7A11 protein expression.

3.2.3 ABL kinase inhibition functionally impairs system xCT

SLC7A11 functions as part of system xCT to import cystine for cell detoxification and simultaneously export glutamate to enable transporter activity (Figure 21A). System xCT activity surges as metastatic potential multiplies causing exogenous glutamate levels to increase, which in the context of the brain can be detrimental to neurons and cause glutamate excitotoxicity. To understand if ABL kinases regulate system xCT activity, functional assays were employed to measure changes in exogenous glutamate and intracellular glutathione.

Knockdown of ABL1/2 in lung and breast cancer cells exhibited markedly decreased intracellular GSH levels, which were reduced to levels similar to those of SLC7A11 knockdown cells (Figure 21B, C). Further, we observed decreased extracellular glutamate in both ABL knockdown and SLC7A11 knockdown cells indicating impaired System xCT function (Figure 21 D, E). These data suggest that ABL allosteric inhibitors could be employed to inhibit SLC7A11 function leading to decrease tumor cell survival and might also be effective in preventing neuronal cell death in mice bearing brain metastases in part through decreased glutamate release.

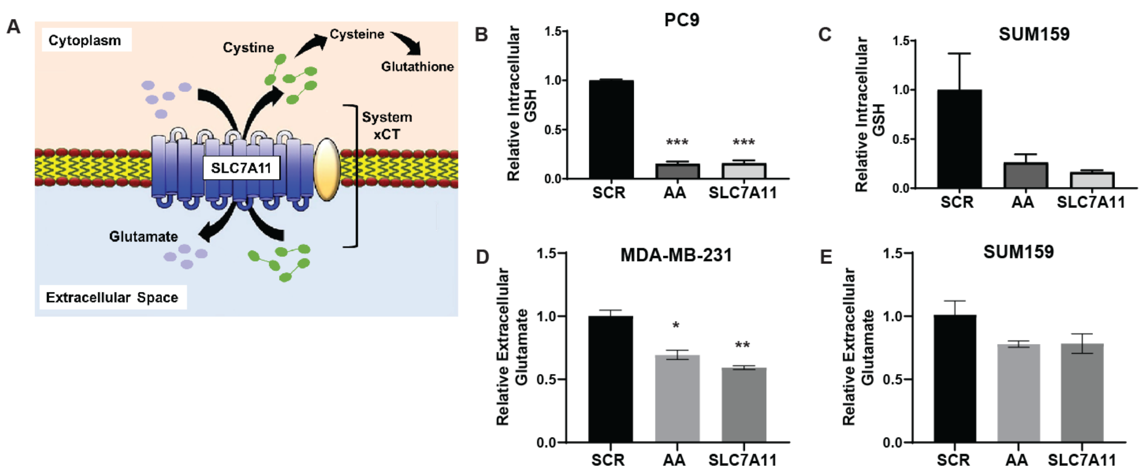

Figure 21: Genetic inhibition of ABL or SLC7A11 decreases functional capacity of System xCT. A) Model of SLC7A11 function as part of the System xCT showing export of glutamate and import of cystine. B-C) Lung (B) or breast cancer cells (C) harboring shRNAs against ABL1/ABL2 (AA) or SLC7A11 (TRC clone #43124) have decreased intracellular glutathione (GSH) levels. D-E) Breast cancer cells have decreased glutamate

export following ABL1/ABL2 or SLC7A11 shRNA-mediated knockdown.To test whether ABL kinase inhibition reduces glutamate export neuronal cell excitotoxicity, we exposed rat cortical neurons to conditioned media from tumor cells harboring shRNA mediated ABL1/ABL2 knockdown, treated with the SLC7A11 inhibitor sulfasalazine (SAS), or media containing exogenous glutamate (Figure 22A). We examined the impact of ABL-mediated regulation of SLC7A11 on neuronal cell viability and found that conditioned media from lung cancer cells or addition of glutamate induced cytotoxicity of rat cortical neurons whereas this effect was abrogated by ABL knockdown in lung cancer cells or upon treatment with SAS (Figure 22 B-C). These results suggest that ABL kinase inhibition has a protective effect on the surrounding tumor microenvironment and prevents neuronal cell death.

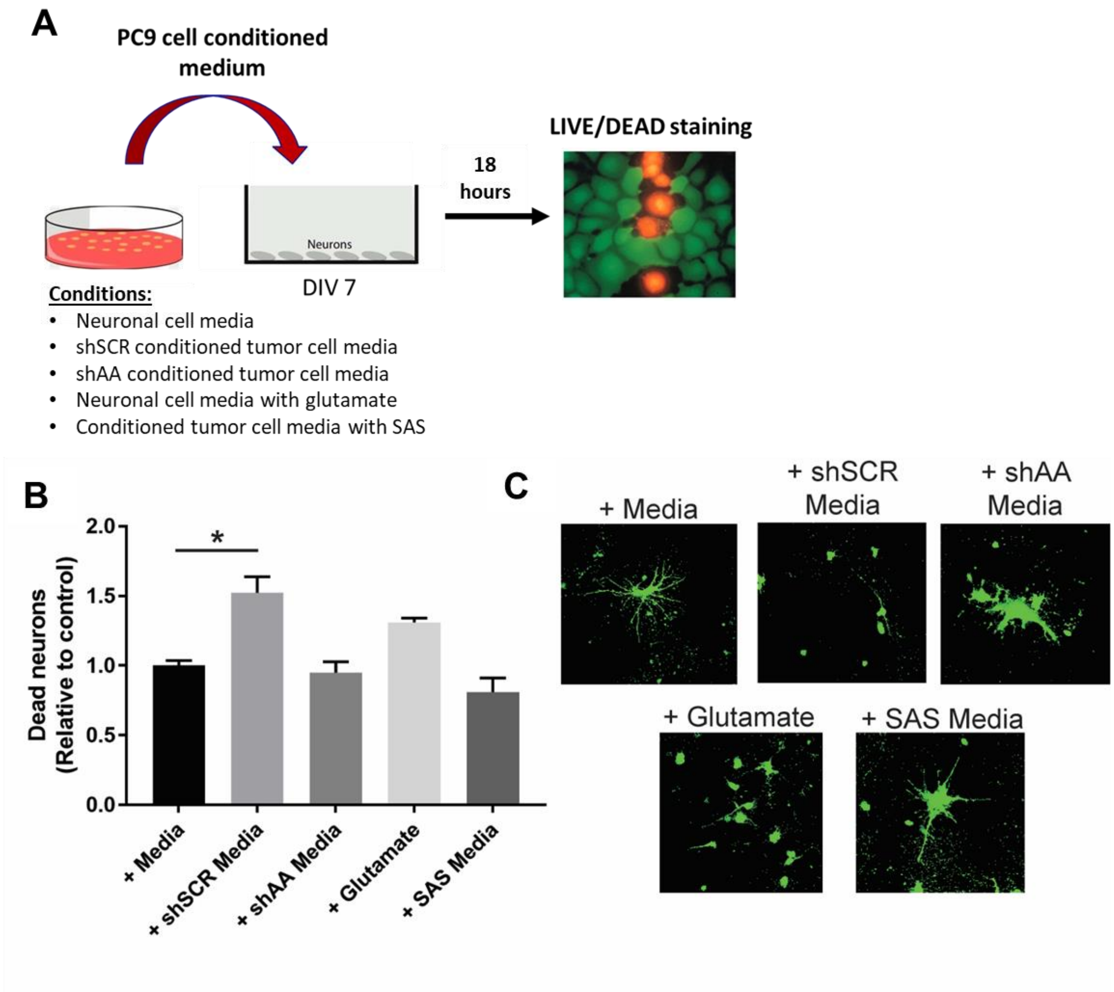

Figure 22: Conditioned media from ABL-deficient lung cancer cells fails to elicit tumor-induced neuronal cytotoxicity. A) Schematic showing experimental overview. B) Neurons cultured in PC9 shSCR conditioned media or exposed to exogenous glutamate had a higher dead cell count in comparison to neurons cultured in PC9 shAA conditioned media, PC9 + SAS conditioned media, or fresh media. C) Neurons cultured in conditioned media from PC9 shSCR cells or glutamate conditioned medium show fewer protrusion compared to neurons cultured in ABL-depleted PC9 shAA conditioned media, PC9 + SAS conditioned media, or fresh media. *p<0.05 N=2 biological replicates. *Acknowledgement: Rat cortical neurons were obtained from Cagla Eroglu's lab.*

3.2.4 Treatment with ferroptosis inhibitors does not rescue ABL kinase allosteric inhibitor mediated cell death

Pharmacologic inhibition of SLC7A11 function has been linked to a form of cell death called ferroptosis (264). Ferroptosis is an iron-dependent form of cell death caused by the accumulation of lipid peroxides in the cell membrane (265, 266). System xCT-mediated cystine import enables production of glutathione which enables cell detoxification processes. Glutathione does this in part by activating GPX4, a lipid peroxidase that converts toxic lipid hydroperoxides into non-toxic lipid alcohols (267). When this process is obstructed by either a system xCT inhibitor or direct GPX4 inhibition, ROS levels increase in the cell causing lipid peroxides to form which can accumulate in cell membranes causing them to become unstable and trigger cell death.

To understand if ABL-mediated inhibition of system xCT caused cells to undergo ferroptosis, we treated triple-negative breast cancer cells with ferroptosis inhibitors in the presence of ABL001 at a concentration that decreased cell survival and SLC7A11 protein levels (Figure 23A,B). Ferrostatin-1 (Fer-1) and liproxstatin-1 (Liproxstn) slow the accumulation of lipid hydroperoxides by inhibiting lipoxygenases and acting as radical-trapping antioxidants downstream of GPX4 (268). Deferoxamine (DFO) is an iron chelator that prevents ROS accumulation by removing excess iron, which has been shown to potentiate ferroptosis (264). Addition of these compounds did not rescue cell survival in the presence of ABL001 (Figure 23A,B). Interestingly, neither did treatment with the ROS scavenger N-acetylcysteine suggesting that the mechanism by which cancer cells are undergoing cell death following ABL inhibition is not dependent upon the accumulation of free radicals(**Figure 23C**). However, further studies will need to be performed to truly understand how much decreased SLC7A11 protein expression contributes to cell death following ABL inhibition.

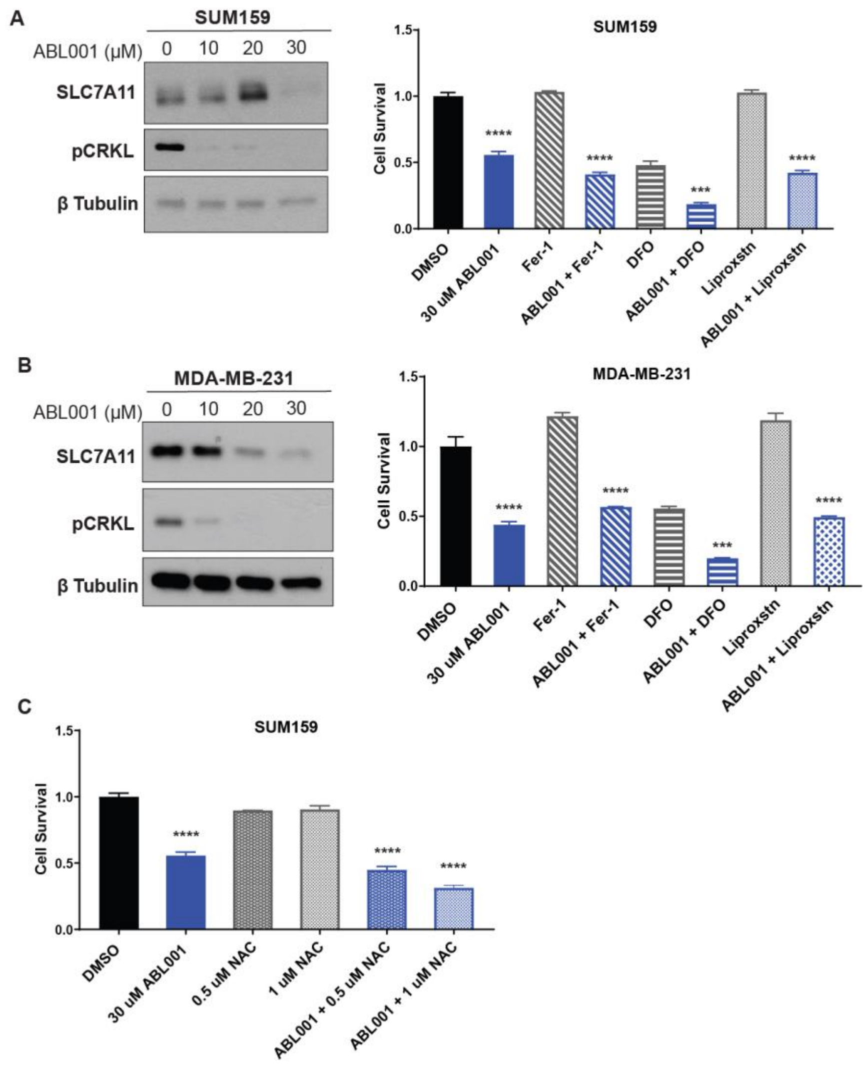

Figure 23: Treatment with ferroptosis inhibitors did not rescue ABL001-mediated cell death. SUM159 (A) or MDA-MB-231 (B) cells treated with a concentration of ABL001 that depletes SLC7A11 levels were not responsive rescue experiments with ferroptosis

inhibitors. C) Exposure of SUM159 to N-acetylcysteine, a ROS scavenger, also did not rescue cell viability. ***p<0.005, ****p<0.001

3.2.5 Mechanistic understanding of ABL-mediated regulation of SLC7A11

ABL kinases regulate expression of SLC7A11 at both the transcriptional and post-transcriptional levels. Reports in the literature have described multiple pathways regulating SLC7A11 expression and many of these signaling mediators are also ABL kinase targets (Figure 24).

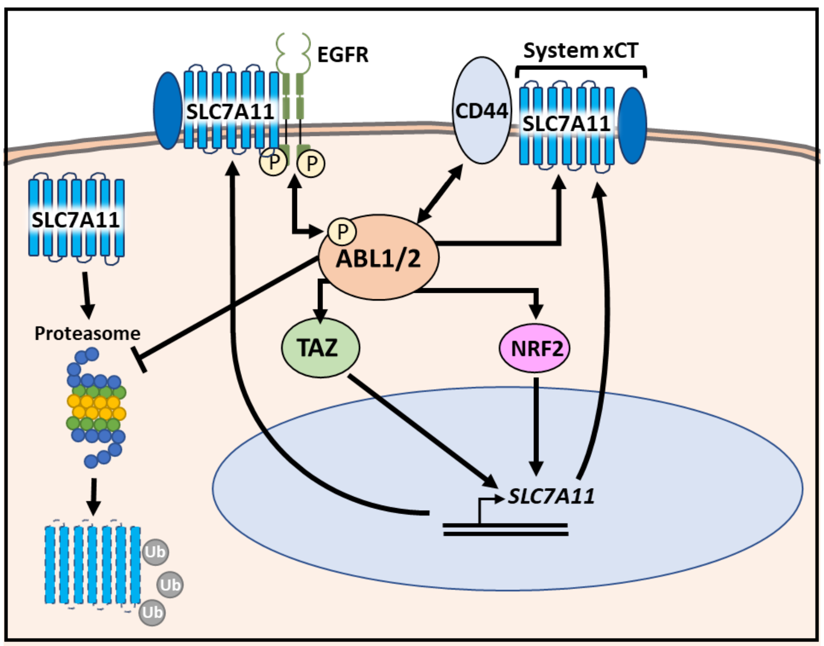

Figure 24: Model of possible mechanisms of ABL kinase regulation of SLC7A11.

In breast cancer cells, the antioxidant transcription factor NRF2 promotes *SCL7A11* gene expression, and we have reported that ABL kinases regulate nuclear accumulation of NRF2 and promote expression of NRF2 target genes in renal cancer cells (141, 269). NRF2 expression is triggered by oxidative stress, thus we exposed cells to low doses of hydrogen peroxide (H2O2) and examined changes in NRF2 expression following ABL inhibition. NRF2 and SLC7A11 levels were decreased upon GNF5 treatment in cells not exposed to H2O2 (Figure 25). Following H2O2 exposure, NRF2 levels were increased in vehicle treated cells while GNF5 suppressed increases in NRF2 and SLC7A11 protein. This suggests that ABL kinases do modulate NRF2 expression and that an ABL-NRF2-SLC7A11 signaling axis potentially exists in breast cancer cells.

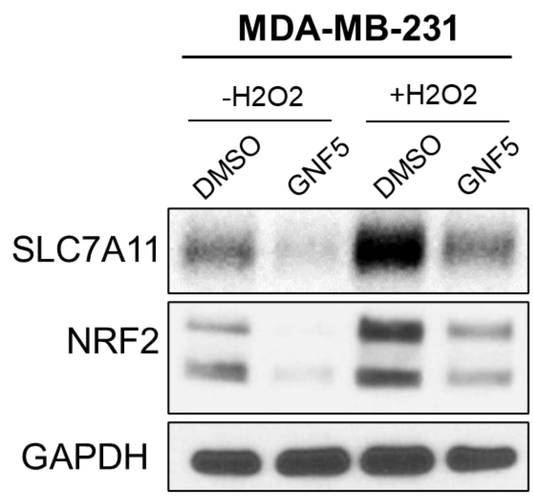

Figure 25: Elevated levels of NRF2 as mediated by treatment with hydrogen peroxide (H2O2) partially rescues NRF2 levels following GNF5 treatment. Breast cancer cells were treated with GNF5 or vehicle in the presence or absence of H2O2 and SLC7A11 and NRF2 protein levels were examined.

Further, we have previously described that ABL2 enhances protein stability of TAZ, a Hippo pathway transcriptional coactivator, by decreasing its interaction with the β-TrCP E3 ubiquitin ligase and subsequent protein degradation (99, 192). The ABL2-TAZ signaling axis promotes brain metastasis in mouse models of non-small cell lung cancer. Interestingly, TAZ has also been shown to be modulated by cell density whereupon periods of low cell density, TAZ will translocate into the nucleus and increase susceptibility to ferroptosis (270). We wanted to investigate potential regulation of the ABL2-TAZ pathway on SLC7A11 protein stability. Thus, we expressed a mutant form of TAZ that is constitutively activated (TAZ4SA: alanine substituted for S66, S89, S311, and 314) in SUM159 cells lacking functional ABL kinases. TAZ4SA rescued SLC7A11 protein following ABL1/2 knockdown and restored system xCT function as quantified by intracellular glutathione levels (Figure 26 A-C). Analysis of the *SLC7A11* promoter did not reveal the presence of TAZ/TEAD binding sites indicating that the regulatory effects of TAZ on SLC7A11 could be non-transcriptionally related.

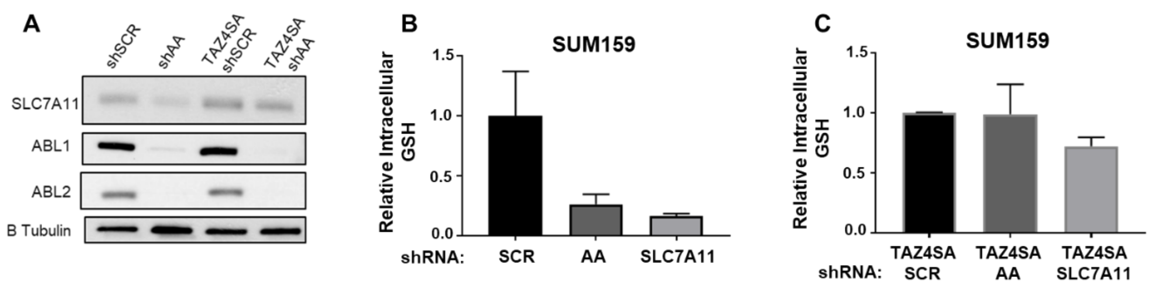

Figure 26: Constitutive TAZ expression rescues SLC7A11 protein and system xCT function in ABL depleted cells. SUM159 triple-negative breast cancer cells expressing activated TAZ (TAZ4SA) were transduced with either SCR or AA shRNAs. SLC7A11 protein levels (A) and intracellular glutathione (GSH) levels were assayed (B,C).

Additionally, SLC7A11 protein stabilization is mediated in part by the binding of SLC7A11 to the CD44 cell surface receptor in cancer cells (271). In this regard, we recently found that knockdown of ABL kinases in lung cancer cells downregulates CD44 protein expression. Further, EGFR was reported to interact with SLC7A11 through its intracellular domain, thereby promoting cell surface expression of the xCT transporter

(272). We reported that ABL kinases regulate EGFR endocytosis and active ABL impairs EGFR internalization (273). Further examination will need to be done to evaluate whether ABL kinase inhibition impairs SLC7A11 expression and/or stabilization in a manner dependent on EGFR or CD44 cell surface expression.

3.3 Discussion

Overexpression of SLC7A11 in cancer cells enhances their survival by producing glutathione to neutralize ROS and detoxify cancer cells as well as chemotherapeutic compounds (274). Further, SLC7A11 enables cancer growth in the brain by killing surrounding neurons allowing for tumor outgrowth. Thus, treatment with ABL allosteric inhibitors is expected to decrease brain metastatic outgrowth and colonization and ameliorate tumor-induced neurotoxicity through reduced system xCT activity. It is possible that the effect of decreased SLC7A11 expression on tumor outgrowth has less to do with the impact changes in glutamate production has on the microenvironment and more so related to decreased intracellular glutathione production. In this regard, a recent report on breast cancer brain metastasis described a role for paracrine glutamate secretion from glutamatergic synapses in promoting metastatic colonization of breast cancer cells in mouse models (275). However, further work will need to be conducted to understand how SLC7A11 depletion in parental cancer cells as well as SLC7A11 overexpression in ABL deplete cancer cells effects cell survival, metastasis, and tumor outgrowth.

4. Conclusions

The overarching aim of this body of work was to identify metabolic vulnerabilities in solid tumors that could be exploited following treatment with ABL kinase inhibitors. By uncovering unique changes in cancer cell metabolism following treatment with ABL kinase inhibitors, we defined a novel combination therapy using available ABL allosteric inhibitors with FDA-approved statins for treatment of therapy-resistant and brain metastatic lung cancer cells in preclinical mouse models. Additionally, we also discovered a novel ABL-mediated regulatory mechanism of SLC7A11 RNA and protein expression. Given that metabolic rewiring is among the mechanisms cancer cells utilize to evade cytotoxic therapies and survive in metastatic environments, our findings expose targetable vulnerabilities that can be exploited as new treatment options for patients with refractory or metastatic tumors.

In the first story, we identified a synergistic interaction between ABL kinase allosteric inhibitors and statin therapeutics that can increase overall survival in mouse models of therapy resistance and brain metastasis. Importantly, statins are FDA-approved therapeutics taken by patients with hypercholesterolemia and the ABL allosteric inhibitor ABL001 is currently in phase III clinical trials making our findings clinically relevant and suggest that these inhibitors might be effective treatment options for patients who have failed first-line therapeutics. Further, these findings are of clinical importance as we show a strong dichotomy between current FDA-approved therapeutics, gefitinib and docetaxel, and ABL allosteric inhibitors in synergizing with statins. While simvastatin has been linked to a marginal decrease in breast cancer recurrence, our findings are consistent with clinical reports showing that statins added to first-line standard of care chemotherapy do not extend survival in lung adenocarcinoma patients (205, 206).

A possible explanation for why the ABL allosteric inhibitors synergize well with statins is potentially due to their ability to markedly decrease mitochondria function in lung cancer cells without affecting glycolysis. This alteration causes the mitochondria to become primed towards cell death and, as shown in Figure 12, low doses of ABL001 and simvastatin in combination decreased mitochondria function. This finding suggests that mitochondrial sensitization to ABL001 enhances the organelle's response to statin therapy, however further work is needed to address this, such as also testing to see if gefitinib or docetaxel in combination with simvastatin could impair organelle function.

Statins have also been shown to enhance mitochondrial priming. Statin-mediated inhibition of the MVA pathway impairs synthesis of coenzyme Q and ubiquinol–cytochrome c reductase, critical components of the ETC (229-232). Previous reports showed that statins can enhance mitochondrial priming and sensitize cancer cells to mitochondrial-mediated apoptosis, such as in the case of leukemia cells with oncogenic BCL-2 mutations (233). It is possible that the ABL kinases could also be impacting stability of complexes within the ETC, but future studies are needed to address this question. This point is described in more detail in the Future Directions section.

Additionally, we found that the synergistic interaction between ABL allosteric inhibitors and statins appears to be mediated by inhibition of protein prenylation and is independent of decreased cholesterol (Figure 27). Specifically, metabolic rescue of the geranylgeranylation pathway was capable of rescuing cell survival in lung cancer cells co-treated with ABL allosteric inhibitors and statins to an extent equivalent to mevalonate. Protein geranylgeranylation is required for a vast array of cellular processes such as protein and vesicular trafficking, and cell proliferation (227). Multiple geranylgeranylated proteins might be targeted by combination therapy and future studies are needed to assess whether decreased protein geranylgeranylation of specific targets mediates the striking decrease in lung cancer cell survival.

Notably, our work outlines a dichotomous function of ABL allosteric versus ATP-site inhibitors on regulating mitochondria function. This difference is most likely due to the different conformation the kinases undergo upon inhibitor binding. The ATP-site competitive inhibitors force the kinases into an open conformation while the allosteric inhibitors induce a closed conformation (241). The open conformation leaves SH3-SH2 domains available to interact with downstream protein targets while the closed conformation prevents these protein-protein interactions. This phenomenon was described in a recent publication from our lab that showed that ABL allosteric inhibitors, but not ABL ATP-competitive inhibitors, disrupt the interaction between ABL2 and the HSF1 transcription factor (100). This finding suggests that protein-protein interactions dependent on distinct ABL protein conformations are specifically disrupted by the binding of the allosteric inhibitors to the myristoyl domain in the C-lobe in the kinase domain of the ABL kinases. In a similar manner, only the ABL allosteric inhibitors are capable of impairing mitochondria function in a manner equivalent to genetic inhibition of the ABL kinases, whereas the ATP-competitive inhibitors fail to impair mitochondrial function.

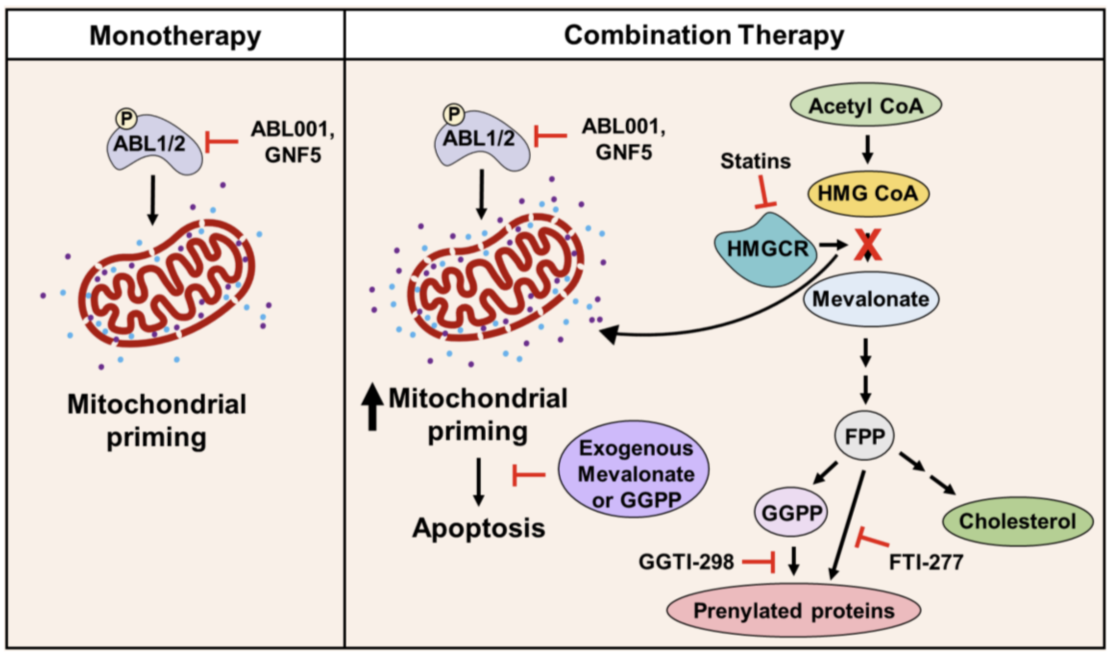

Figure 27. Summary of ABL allosteric inhibitor and statin therapeutics combination therapy. Model diagram summarizing the signaling pathways modulated by combination therapy.

We made the unexpected discovery that ABL kinases regulate mitochondria function, but we also wanted to know what other metabolic targets may be regulated by ABL. In this regard, we performed unbiased RNA sequencing analysis and found that

ABL inhibition altered expression of a multitude of proteins with one of the most statistically significant downregulated targets being SLC7A11. We found that both pharmacologic and genetic inhibition decreases SLC7A11 mRNA and protein expression across breast, lung, and glioma cancer cell types. These findings are novel as overexpression of SLC7A11 enhances cancer cell survival by producing glutathione to neutralize ROS and to detoxify cancer cells from chemotherapeutic compounds. Simultaneously, SLC7A11 exports glutamate into the tumor microenvironment, which can become cytotoxic to surrounding cells allowing for tumor expansion. Breast, lung, and glioma patients with overexpression of SLC7A11 have decreased overall survival making these findings clinically relevant as treatment with ABL allosteric inhibitors may help extend patient lifespan. Further, decreased glutamate secretion from cancer cells following ABL inhibition should dampen the cognitive side effects caused by primary and secondary brain tumors, such as seizures and epileptic episodes.

4.2 Current limitations

A consideration of these studies that should be acknowledged is the impact of statins and ABL allosteric inhibitors combination treatment on CYP3A4 activity. A subset of statins, such as simvastatin, are metabolized by CYP3A4, whereas other statins, such as fluvastatin, are non-CYP3A4 substrates (276). Adverse side effects can be caused by administration of statin CYP3A4 substrates in a multidrug treatment regimen if combined with CYP3A4 inhibitors leading to adverse accumulation of statin levels in the body (276, 277). The impact of ABL allosteric inhibitors on CYP3A4 activity has not been tested, but to combat potential off-target effects in our model we chose to treat mice at low doses of simvastatin and ABL001 and monitored mice for changes in body weight, activity, eating habits, or digestive changes. Of note, we did not observe alterations in any parameter due to pharmacologic treatment, but further understanding of potential drug interactions should be considered prior to prolonged treatment or clinical trial study with advisement to lower drug dosage or switch to fluvastatin if side effects do occur.

Further, another limitation of these studies were the mouse models used to study metastasis. The athymic nude mice used in these studies lack a thymus and full immunogenic profile. Thus, how the treatment strategy outlined in our studies could interact with the immune system in promoting or impairing tumor metastasis is limited. To our knowledge, there are no good models to brain metastasis or therapy resistance in a syngeneic or genetic mouse model. However, in the future, pilot studies should be performed in an immunocompetent genetic or syngeneic mouse line to understand the impact the immune system may have on treatment response.

4.3 Future Directions

This body of work identified metabolic vulnerabilities in cancer cells following treatment with ABL kinase inhibitors, but a few key areas of research were left unaddressed. The first question is how the ABL kinases are regulating mitochondrial function and structural integrity. ABL kinases have been classified to target multiple substrates in cancer cells and a recent report uncovered ABL kinases tyrosine phosphorylate mitochondrial creatine kinase 1 (MtCK1) leading to increased cellular energy production through the mitochondrial phosphocreatine shuttle in HER2 amplified breast cancer cells (157). The authors showed that ABL kinases phosphorylate MtCK1 at Y153 and expression of a Y to F mutant (MtCK1 Y153F) caused an approximate 30% decrease in ATP production and mitochondria function. Our findings show that in lung cancer cells treatment with ABL allosteric inhibitors can cause a striking 50-80% decrease in mitochondria function suggesting that the kinases could be regulating multiple substrates in addition to MtCK1.

One possible mechanism could be that the kinases are regulating one or more complexes of the ETC. Src family tyrosine kinases have been shown to phosphorylate subunits of the ETC resulting in subsequent changes in ETC complex activity, and inhibition of Src kinases results in decreased complex I activity and mitochondrial respiration (234, 235). ABL1 has been shown to be activated downstream of oncogenic Src (236). Among the top genes that scored from the CRISPR screen, proteins that assemble complexes of the ETC were identified (Figure 28A).

Thus, we treated lung cancer cells with inhibitors for complexes I-IV of the ETC. We treated cells with IC20 doses of the ETC compounds, similar to the treatment strategy used with the statin therapeutics, but discovered that treatment with sublethal doses of ETC inhibitors in combination with ABL001 did not affect cell viability (Figure 28B). To confirm that the inhibitors were in fact impairing ETC function, we performed Mitostress tests and saw depletions in mitochondrial basal respiration (Figure 28C).

A

ETC Target	ETC Complex
NDUFA11	1
NDUFA12	1
NDUFB10	1
NDUFC1	1
NDUFS6	1
NDUFB3	1
NDUFB8	1
UQCRC2	2
COX17	4
COX15	4
ATP5A1	5
ATP5B	5
ATP5D	5

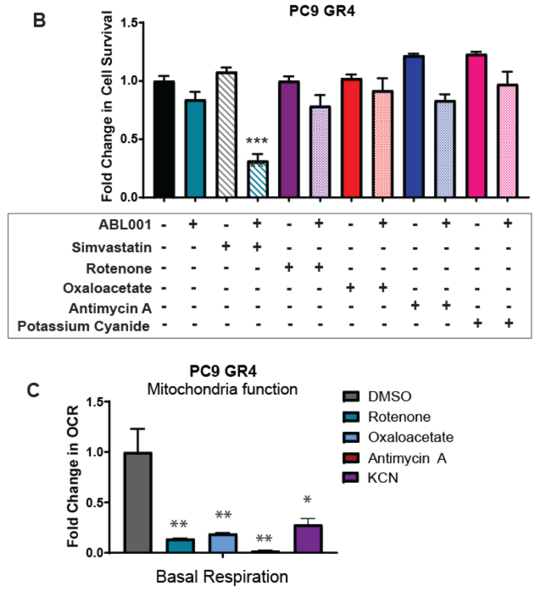

Figure 28. ABL001 in combination treatment with inhibitors of complexes I-IV of the electron transport chain did not affect cell viability. **A**) ETC targets identified from the CRISPR screen. **B**) Cell viability analysis for inhibitors of complexes I-IV of the electron transport chain in combination with ABL001 for 72 hr (n=2). **C**) Results from Seahorse Mitostress tests analyses showing that doses used in cell viability studies impaired ETC function but did not impact cell survival (n=2).

These results suggest that ABL allosteric inhibitors could be impairing mitochondrial function in part through altering ETC complex activity causing depletion of oxygen consumption rate and ATP production. Ongoing work is being performed to address this question, and to identify if and how ABL kinases are modulating mitochondrial proteins. One project currently underway by other members of the lab that has shed some light on this matter was a mass spectrometry analysis probing for changes in ABL2 binding partners following treatment with allosteric versus ATP-competitive inhibitors. ABL2 was captured using pull-down assays from lysates of lung and breast cancer cells treated with either ABL001 or Nilotinib.

Interestingly, the top depletion hit that was modified by ABL001, but not Nilotinib, was NDUFA7, a member of complex I. Complex I is critical for processing NADH to generate hydrogen ions to fuel the hydrogen pump and create an electrostatic pull to bring electrons through the ETC. The flux of oxygen ions through the ETC is related to the concentration of potential electron donors. If these bioenergetics are impaired, the redox balance within the mitochondria shifts causing a build-up of reactive oxygen species (278). As shown in Figure 4F,G, treatment with GNF5 and ABL001 caused increases in mitochondrial ROS. Thus, it is possible that the kinases could be stabilizing complex I activity, but future studies need to be performed to characterize the impact of the interaction between ABL2 and NDUFA7.

Another possible reason as to why statins and ABL allosteric inhibitors synergize together is that the MVA pathway is necessary for ubiquinol production. Ubiquinol has been shown to be necessary for tumor growth *in vivo* as it serves as an electron donator to the pyrimidine pathway (279). Depletion of ubiquinol decreased tumor growth and ETC function. Since the ABL allosteric inhibitors also impair ETC activity and transfer of electrons through the mitochondrial membrane, together both inhibitors could be depleting ETC activity from different angles.

Another key outstanding question relates to which protein prenylation targets are being modulated by ABL allosteric inhibitors and statin therapy. There are many proteins that have been shown to be modulated by protein prenylation with the most canonical protein family being RAS, which requires prenylation modifications to induce malignant transformation (280). RAS proteins favor farnesylation modifications but can also undergo geranylation if farnesylation transferases are inhibited (281). Proteins that favor geranylation include Rho GTPases, such as Cdc42, Rac, and RhoC (281).

Our findings show that following treatment with ABL001 and a geranylation inhibitor, mitochondrial function is impaired, and cells undergo apoptosis (Figure 12). To date, PubMed searches to uncover proteins that regulate mitochondrial activity following geranylation modification do not report targets of interest. Thus, a potential future experiment to uncover which proteins mediate this phenotype would involve a high-throughput profiling approach using alkyne-tagged prenyl probes coupled to a capture reagent, a technique known as 'click' chemistry (282). The alkyne moiety will structurally resemble the natural geranylgeraniol product allowing for high-fidelity incorporation of the probe into cellular geranylation targets by geranyltransferase. Proteins containing the probe will be affinity captured using a column and mass spectrometry will be performed to identify prenylated proteins. Through mass spectrometry analysis, protein targets can be characterized and explored further to see which modulate mitochondria function.

Regarding the SLC7A11 project, several outstanding questions remain: (1) what is the effect of inducible knockdown of *SLC7A11* on primary and metastatic tumor growth across a panel of cancer cell lines, (2) will mice harboring brain metastases either pharmacologically treated with an ABL allosteric inhibitor, or harboring shRNAs against ABL1/ABL2, have decreased SLC7A11 expression, metastatic outgrowth, and neuronal cell death, (3) will overexpression of *SLC7A11* from a heterologous promoter in ABL1/ABL2-knockdown lung cancer cells rescue metastatic activity, (4) what are the transcriptional and post-transcriptional mechanisms by which the ABL kinases regulate SLC7A11 expression.

To address questions 1-3, cancer cells should be injected intracardially and intracranially to measure metastatic and primary tumor growth. Specifically, intracranial injections will be beneficial as SLC7A11 expression is known to effect neuronal cell death thus measuring the number of neurons in the tumor microenvironment can serve as a surrogate measure for tumor-derived glutamate secretion due to glutamate neuronal cell excitotoxicity. Brain slices from tumor bearing mice will be analyzed and immunofluorescence staining with NeuN+, a neuronal antibody, followed by co-staining with TUNEL will assay the number of apoptotic nuclei. Further, changes in neuronal hyper-excitability and seizures can be performed through video monitoring and use of an electroencephalogram (283). Additionally, for questions 1 and 3, whole body flux following intracardiac injection should be examined as well.

To evaluate the transcriptional and post-transcriptional mechanisms by which the ABL kinases control SLC7A11 expression, analysis of transcription factor regulation of *SLC7A11* expression by NRF2, TAZ, or other transcription factors/coactivators can be examined. Additionally, post-transcriptional regulation through EGFR or CD44 as well as proteasomal degradation can be examined. shRNA mediated knockdown for transcriptional or post-transcriptional regulators can be employed to see which phenocopy ABL kinase inhibition. A caveat to this approach is that ABL can modulate SLC7A11 expression at multiple levels thus by knocking down one target of interest may not fully recapitulate the phenotype of ABL kinase knockdown. Further, overexpression plasmids for each protein can also be used to see which might restore protein stability in ABL deplete cells.

Appendix A: Table 1. ABL kinase inhibitors

Name	Alternative Name	Inhibitor Type	Targets	References	Clinical Trials in Solid Tumors	Regulatory Status
Imatinib	Gleevec/STI57	ATP-site, Type II	ABL1, ABL2, BCR-ABL1, CSF1R, DDR1, DDR2, KIT, NQO2, PDGFR1	**(284)**	**Yes** **Non-small cell lung cancer:** NCT01011075; NCT00408460 **Breast Cancer:** NCT00193180; NCT00338728; NCT00087152 **Gastrointestinal tumors:** NCT01151852; NCT00867113 **Melanoma:** NCT00424515; NCT00470470	FDA approved for CML, Ph+ ALL, MDS/MPD, ASM, HES/CEL, DFSP, GIST
Dasatinib	Sprycel/ BMS-354825	ATP-competitive, Type I	ABL1, ABL2, BCR-ABL1, BLK, BTK, CSK, CSR1R, DDR1, DDR2,	**(284-286)**	**Yes** **Non-small cell lung cancer:** NCT00858403; NCT00826449; NCT01999985	FDA approved for CML, Ph+ ALL

			EGFR, ERBB2, FGR, FRK, FYN, GAK, GCK, HCK, ILK, KIT, LCK, LIMK1, LIMK2, LYN, MAP2K, MAP3K, MAP4K, PDGFR, RIPK2, SLK, SRC, SYK, TEC, TYK2, YES1,		**Breast Cancer:** NCT00817531,NCT00924352, NCT00767520, NCT00410813 **Gastrointestinal tumors:** NCT00568750; NCT01643278;NCT00504153 **Melanoma:** NCT00597038;NCT00436605	
Nilotinib	/AMN107	ATP-site, Type II	ABL1, ABL2, BCR-ABL1, CSF1R, DDR1, DDR2, KIT, NQO2, PDGFR	**(284)**	**Yes** **Breast Cancer:** NCT04205903 **Gastrointestinal tumors:** NCT00976612 ; NCT00471328 **Melanoma:** NCT0139512	FDA approved for CML

					1; NCT00788775; NCT01099514	
Bosutinib	Bosulif/SKI-606	ATP-competitive, Type I	ABL1, ABL2, BCR-ABL1, CAMK2G, CDK2, HCK, LYN, MAPKK1, MAPKK2, MAPKKK2, SRC	**(287-289)**	**Yes Non-small cell lung cancer:** NCT03023319 **Breast Cancer:** NCT00793546; NCT00319254; NCT00880009; NCT03854903; NCT00959946; NCT00759837 **Advanced Solid Tumors:** NCT03297606; NCT01001936	FDA approved for CML, Ph+ CML
Ponatinib	Iclusing/AP24534	ATP-site, Type II	ABL1, ABL2, BCR-ABL1, BLK, CSFR1, DDR1, DDR2, EPHRs, FGFR1,	**(290-293)**	**Yes Non-small cell lung cancer:** NCT01761747; NCT03704688; NCT01935336;	FDA approved for CML, Ph+ ALL

			FGFR2, FGR, FLT3, FRK, FYN, HCK, LCK, LYN, RET, SRC, TEK, TIE2, TRKA, TRKB, TRKC, PDGFR, VEGFR1, VEGFR2, VEGFR3, YES1		NCT01813734; NCT01813734; **Breast Cancer:** NCT03878524; NCT04591431 **Gastrointestinal tumors:** NCT01874665	
Axitinib	Inlyta/AG013736	ATP-competitive, Type I	BCR-ABL1 (T315I), KIT, PDGFR, VEGFR1, VEGFR2, VEGFR3	**(294)**	**Yes Non-small cell lung cancer:** NCT03472560; NCT00094094; NCT00094094 **Breast Cancer:** NCT00076024; **Gastrointestinal tumors:** NCT00700258	FDA approved for Renal Cell Carcinoma

					Renal Cell Carcinoma: NCT02493751; NCT00678392; NCT00920816; NCT02579811	
Vandetanib	Caprelsa/ZD-6474	ATP-competitive, Type I	ABL1, EGFR, RET, VEGFR	**(295)**	**Yes** **Non-small cell lung cancer:** NCT01586624; NCT00753714; NCT01823068 **Breast Cancer:** NCT01934335; NCT00481845; NCT00494481 **Gastrointestinal tumors:** NCT02015065 **Thyroid Cancer:** NCT01876784; NCT01496313;	FDA approved for Advanced Medullary Thyroid Cancer

GNF2, GNF5		Allosteric	ABL1, ABL2, BCR-ABL1	**(178)**	**No**	Not FDA approved
ABL001	Asciminib	Allosteric	ABL1, ABL2, BCR-ABL1	**(179)**	**Yes- Advanced solid tumors:** NCT04492033; NCT03292783	Phase III Clinical Trials in CML
DAS-6-2-2-6-CRBN		PROTAC	BCR-ABL1	**(186)**	**No**	Preclinical Studies Only
BOS-6-2-2–6-CRBN		PROTAC	BCR-ABL1	**(186)**	**No**	Preclinical Studies Only
GMB-475		PROTAC	BCR-ABL1	**(185)**	**No**	Preclinical Studies only

Appendix B: Table 2. IC_{50} calculations for cell lines

Cell Line	Drug	Calculated IC50
PC9	GNF5	10 mM
	ABL001	7.5 mM
	Gefitinib	15 nM
	Docetaxel	1 nM
	Nilotinib	2 mM
	Simvastatin	4 mM
	Fluvastatin	2 mM
	FTI-277	50 mM
	GGTI-298	20 mM
PC9 GR4	GNF5	10 mM
	ABL001	7.5 mM
	Gefitinib	200 nM
	Docetaxel	1 nM
	Nilotinib	2 mM
	Simvastatin	4 mM
	Fluvastatin	2 mM
	FTI-277	50 mM
	GGTI-298	20 mM
H460	GNF5	15 mM
	ABL001	15 mM
	Docetaxel	0.5 nM
	Nilotinib	2 mM
	Simvastatin	12 mM
	Fluvastatin	4 mM
	FTI-277	15 mM
	GGTI-298	15 mM
H358	GNF5	15 mM
	ABL001	15 mM
	Docetaxel	1 nM
	Simvastatin	12 mM
	Fluvastatin	4 mM
PC9 BrM3	GNF5	10 mM
	ABL001	7.5 mM
	Gefitinib	15 nM
	Docetaxel	1 nM
	Simvastatin	4 mM
	Fluvastatin	2 mM

Appendix C: Table 3. Top CRISPR targets

Ranked list of top genes with negative TS values.

Rank	Gene	TS Score
1	NPC1	-1.84352
2	PNPLA6	-1.50963
3	ADSL	-1.30126
4	DEGS1	-1.29665
5	GATM	-1.21614
6	NDUFA11	-1.18712
7	SF3A1	-1.18088
8	PI4KB	-1.1646
9	ATIC	-1.15819
10	RRM2	-1.13772
11	GNPTAB	-1.07218
12	TXNRD1	-1.06214
13	HMGCR	-1.03835
14	THEM4	-1.02617
15	RPS8	-1.00065
16	SMC3	-0.9992

17	NR5A1	-0.9767
18	CYB5D2	-0.93303
19	SDR42E1	-0.89395
20	U2AF1	-0.8927
21	PAICS	-0.8788
22	BRD8	-0.87308
23	SDHC	-0.85023
24	SLC22A8	-0.84398
25	PGD	-0.8284
26	TYMS	-0.81976
27	PPP2CA	-0.80331
28	HNF4G	-0.80308
29	SLC11A2	-0.79828
30	MTMR6	-0.79513
31	SF3B3	-0.79188
32	PPP6C	-0.79169
33	TRPM7	-0.78332
34	ME2	-0.76729
35	ATP6V1D	-0.76334

36	NR4A3	-0.76038
37	GRIN2D	-0.74322
38	SOD1	-0.73139
39	HSD17B10	-0.72504
40	CTDSPL2	-0.72345
41	KCNS3	-0.71274
42	ADSS	-0.70165
43	CA8	-0.69377
44	PGM5	-0.69266
45	ATP5B	-0.68843
46	SF3B5	-0.68287
47	SLC2A1	-0.67894
48	GOT1	-0.67637
49	ATP6V1A	-0.67425
50	SDHA	-0.67347
51	ATP5A1	-0.67188
52	GFPT1	-0.67188
53	CRYZ	-0.67118
54	ATP2B1	-0.6689

55	ATP6V1C1	-0.66354
56	TSTA3	-0.66158
57	AKR1A1	-0.66089
58	COX17	-0.65998
59	ACBD5	-0.6591
60	FUT8	-0.65846
61	USP39	-0.65534
62	NPC2	-0.65316
63	TAP1	-0.65218
64	ARG1	-0.65155
65	RPL37	-0.64123
66	ELOVL1	-0.641
67	KCNH7	-0.63862
68	DLG1	-0.63414
69	LIPA	-0.63039
70	SLC24A4	-0.62865
71	RPA2	-0.62652
72	PRDX2	-0.6252
73	COX15	-0.62464

74	NAGLU	-0.62091
75	SLC27A2	-0.61923
76	ALDH1L2	-0.61917
77	PDE1B	-0.61497
78	TRPV5	-0.61253
79	UQCRC2	-0.61236
80	DUSP10	-0.61078
81	DUSP27	-0.61028
82	HCN2	-0.60553
83	SLC6A7	-0.60229
84	ATP6V1B2	-0.60104
85	AHCY	-0.59912
86	CYP4F2	-0.59303
87	TPK1	-0.58798
88	ACE2	-0.58658
89	PKD2	-0.58013
90	CYP4F22	-0.57831
91	SLC26A2	-0.57731
92	CDC25B	-0.57694

93	ATP5D	-0.57218
94	CHRND	-0.56864
95	CERS1	-0.5675
96	LIPE	-0.5632
97	CAD	-0.56241
98	PNLIPRP3	-0.56103
99	PIP5K1A	-0.56091
100	TRPC1	-0.55949

Appendix D: Lipid droplet and fatty acid depletion data

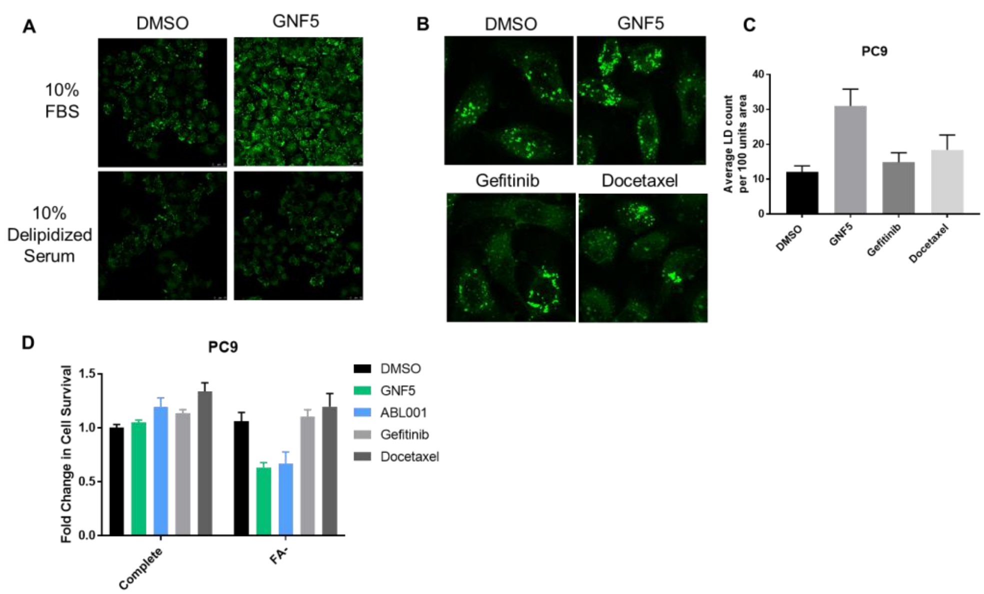

A) PC9 cells cultured in complete media with 10% FBS or 10% delipidized serum were treated with GNF5 for 3 hours. Cells were washed in PBS and then stained with BODIPY following instruction manual. Following staining, cells were washed with PBS and PFA fixed for image analysis. Treatment with GNF5 increased intracellular lipid droplet accumulation in the presence of 10% FBS whereas cells cultured in lipid deplete media had no lipid accumulation indicating lipid store were entering from the external environment.

B) Treatment with GNF5, Gefitinib, and Docetaxel indicated that only GNF5 caused lipid accumulation.

C) Quantification of lipid droplet count per 100 units of area shows cells treated with GNF5 had a greater lipid droplet accumulation.

D) Culturing PC9 cells in lipid deplete medium in the presence of inhibitors evoked cell death only following treatment with ABL allosteric inhibitors.

Appendix E: Table 4. List of Primers

Primer (Application)	**Source**	**Oligo Sequence**
GAPDH-F (RT-qPCR)	Sigma	TGTGGGCATCAATGGATTTGG
GAPDH-R (RT-qPCR)	Sigma	ACACCATGTATTCCGGGTCAAT
BBC3-F (RT-qPCR)	Sigma	GACCTCAACGCACAGTACGAG
BBC3-R (RT-qPCR)	Sigma	AGGAGTCCCATGATGAGATTGT

BCL2L1-F (RT-qPCR)	Sigma	GAGCTGGTGGTTGACTTTC TC
BCL2L1-R (RT-qPCR)	Sigma	TCCATCTCCGATTCAGTCC CT
BCL2-F (RT-qPCR)	Sigma	GGTGGGGTCATGTGTGTGG
BCL2-R (RT-qPCR)	Sigma	CGGTTCAGGTACTCAGTCA TCC

All primers were purchased through Sigma, and applications for each primer set are listed in parentheses.

Appendix F: Table 5. List of Antibodies and Source Information

ABL1 (8E9)	Millipore Sigma	MAB1130; RRID:AB_2220996
ABL2 (6D5)	Abnova	H00000027-M03; RRID:AB_828506
Cleaved PARP	Cell Signaling	Cat# 5625, RRID: AB_10699459
Total PARP	Cell Signaling	Cat# 9532, RRID: AB_659884
beta-Actin (8H10D10)	Cell Signaling	3700S; RRID:AB_2242334
Phospho-CrkL (Tyr207)	Cell Signaling	3181L; RRID:AB_331068
Cleaved Caspase-3	Cell Signaling	Cat # 9661, RRID: AB_2341188

Caspase-3	Cell Signaling	Cat# 9668, RRID:AB_2069870
Cytochrome C	Cell Signaling	Cat# 11940, RRID:AB_2637071
beta-Catenin	Cell Signaling	Cat# 8480, RRID:AB_11127855
Ki67	Cell Signaling	Cat# 9449, RRID:AB_2797703
HMGCR	Millipore	Cat# ABS229, RRID:AB_11203328
CRKL (C-20)	Santa Cruz	sc-319; RRID:AB_631320
beta-Tubulin (D2N5G)	Cell Signaling	15115S; RRID:AB_2798712
GAPDH (6C5)	Santa Cruz	sc-32233; RRID:AB_627679
Lamin B1 (D9V6H)	Cell Signaling	13435S; RRID:AB_2737428
RAP1	Santa Cruz	Cat# sc-398755, RRID:AB_2884025
HDJ2	Thermo Fisher	Cat# MA5-12748, RRID:AB_10982482
TdTomato	Kerafest	Cat# EST203, RRID:AB_2732803
SLC7A11	Cell Signaling	RRID:AB_2800296
Goat anti-Mouse IgG (H+L) Cross-Adsorbed Secondary Antibody, Alexa Fluor 488	Thermo Fisher	Cat# A-11001, RRID:AB_2534069
Goat anti-Rabbit IgG (H+L) Highly Cross-Adsorbed Secondary Antibody, Alexa Fluor 633	Thermo Fisher	Cat# A-21070, RRID:AB_2535731
Goat anti-Rat IgG (H+L) Cross-Adsorbed Secondary Antibody, Alexa Fluor 568	Thermo Fisher	Cat# A-11077, RRID:AB_141874
Peroxidase AffiniPure Goat Anti-Mouse IgG (H+L)	Jackson Immunoresearch	115-035-003; RRID:AB_10015289
Peroxidase AffiniPure Goat Anti-Rabbit IgG (H+L)	Jackson Immunoresearch	115-035-144
Anti-polyHistidine	Sigma	H1029; RRID:AB_260015

Normal Mouse IgG	Santa Cruz	sc-2025; RRID:AB_737182
Rabbit Anti-Mouse IgG (Light Chain Specific) (D3V2A)	Cell Signaling	58802S; RRID:AB_2799549
Goat Anti-Rat IgG, HRP-linked	Cell Signaling	7077S; RRID:AB_10694715

Appendix G: Materials and Methods

G.1: Cell lines and Cell Culture

PC9 parental cells were a gift from Dr. Joan Massagué (Memorial Sloan-Kettering Cancer Center, New York, NY, USA) (296). PC9-GR4 (gefitinib-resistant) cells were a gift from Dr. Passi Jänne (Dana-Farber Cancer Institute, Boston, MA, USA) (297). Large cell carcinoma (LCC) H460 cells were provided by Dr. Fernando Lecanda (University of Navarra, Pamplona, Spain) (298). PC9-BrM3, HCC4006-BrM, and H1975-BrM3 cell lines were derived in the Pendergast laboratory by serial intracardiac injection as previously described (192). Human NSCLC cell lines H358, HCC4006, HCC827 and H1975 were purchased from ATCC. MDA-MB-231 parental, 1833, BrM2A and 4175 cell lines were a gift from Dr. Joan Massagué (Memorial Sloan-Kettering Cancer Center, New York, NY, USA). Parental and derivative cell line pairs were subjected to short tandem repeat (STR) profiling through the Duke University DNA Analysis Facility Human cell line authentication (CLA) service to confirm their authenticity. Lung cancer cells were maintained in RPMI 1640 (Life Technologies) supplemented with 10% tetracycline-screened fetal bovine serum (FBS, Hyclone), 10 mM HEPES, 1 mM sodium pyruvate, and 0.2% glucose. H293T cells used for transfection and virus production were purchased from ATCC and were maintained in DMEM (Life Technologies) with 10% FBS (Corning). All cultures were maintained at 37°C in humidified air containing 5% CO2.

For experiments assessing effects of pharmacologic inhibitors in vitro (GNF-5, ABL001, Gefitinib, Docetaxel, Simvastatin, Fluvastatin, FTI-277, GGTI-298), drugs were dissolved in DMSO and the final concentration of DMSO in culture media did not exceed 0.1% v/v. Cholesterol was solubilized in 40% (2-hydroxypropyl)- β-cyclodextrin at room temperature, sterile filtered (0.45μM) and stored at -20 °C. MVA was resolved with 0.1M NaOH, followed by neutralizing with 0.1M HCL/1M HEPES. The ABL allosteric inhibitors GNF-5 and ABL001 were synthesized by the Duke University Small Molecule Synthesis Facility and validated by LC-MS and 1H-NMR, as well as cell-based assays. The following drugs used for in vitro analysis were purchased from: Cayman: Simvastatin (10010344); Sigma: Gefitinib (SML1657), Fluvastatin (SML0038), Mevalonolactone (M4667), Cholesterol (C3045), Geranylgeranyl pyrophosphate (G6025), Farensyl pyrophosphate (F6892); Tocris: FTI-277 (2407) and GGTI-298 (2430); LC Laboratories: Docetaxel (D-1000).

G.2: Intracardiac injections

All animal experiments were conducted in accordance with protocols approved by the Duke University Division of Laboratory Animal Resources Institutional Animal

Care and Use Committee (IACUC). Cells were stably transduced with pFU-luciferase-Tomato (pFuLT) DNA prior to injection to allow for bioluminescent imaging (BLI) in vivo. We used 8-12-week-old age-matched female athymic nu/nu mice for all studies (Jackson Laboratory). Mice were anesthetized with 5% isoflurane prior to injections. For all studies, 4x105 lung cancer cells suspended in 100 μL PBS were injected into the left cardiac ventricle with a 30-gauge needle. Animals were monitored until full recovery from anesthesia and were subsequently imaged weekly to both confirm proper anatomical injection and to monitor for progression of disease burden using an IVIS XR bioluminescent imager. The ABL allosteric inhibitor ABL001 (Asciminib) was used for in vivo inhibition of the ABL kinases in tumor-bearing mice and was prepared as a suspension in sterile 0.5% methylcellulose/0.5% Tween-80 as described previously (Wylie et al., 2017). Mice were treated with either vehicle control or 100 mg/kg/qd ABL001 via oral gavage once per day. ABL001 was synthesized by the Duke University Small Molecule Synthesis Facility and validated by LC-MS and 1H-NMR. Simvastatin was purchased from Toronto Research Chemicals (cat. S485000) and dissolved in aqueous 2% dimethylsulfoxide (DMSO), 30% polyethylene glycol 400 (PEG 400), and 5% Tween 80. Mice were treated with either vehicle control or 10 mg/kg/qd simvastatin. To account for potential interactions between the two drugs and solvents, mice were treated each morning with either simvastatin or vehicle control, and two hours later with either ABL001 or vehicle control via oral gavage. The presence of brain metastases was confirmed through in vivo BLI followed by isolation of brains for OCT or paraffin sectioning. Living Image software was used for analysis of BLI data.

G.3: Subcutaneous Flank Xenografts

Mice were injected subcutaneously with 1e6 PC9 GR4 cells resuspended in growth factor reduced Matrigel matrix in the back right flank. Mice were stratified into treatment groups once the tumors reached an average of 50 mm3. The animals were drug treated for a total of 3 weeks and tumor volume was measured weekly by a caliper. At the end of the study, mice were euthanized, and tumors were extracted for image collection.

G.4: Seahorse measurements

Basal and maximal oxygen consumption rate and ATP production were measured using a Mito Stress test Kit and a Glycolytic Rate Kit was used to measure basal and compensatory glycolysis. Both kits used a XF96 Extracellular Flux Analyzer (Seahorse Bioscience) to measure changes according to manufacturer's instructions. Cells were plated in XF96 plates at 10,000 cells per well on Day 0. Cells were treated on Day 1 with IC50 doses of GNF5, ABL001, gefitinib, docetaxel, and vehicle control. For rescue experiments, cells were treated with 2.5 μM ABL001, 1 μM simvastatin, 500 μM MVA, 5 μM GGTI-298, 12.5 μM FTI-277. On the day of the Seahorse run, media was aspirated and replaced with XF Assay Medium (Seahorse Bioscience) supplemented with 10 mM glucose, 1 mM pyruvate, and 2 mM glutamine supplemented with corresponding drug or vehicle. The plate was incubated in a non-CO_2 incubator at 37oC for 1hr to equilibrate. OCR measurements, taken every 6min, were collected at baseline and after the sequential addition of oligomycin 1 μM (final concentration), FCCP 0.5 μM, and rotenone 0.75 μM + antimycin A 1.5 μM. Data was normalized to total nuclei count per well.

G.5: Mitosox staining

MitoSOX was purchased from Thermofisher (cat. M36008). 100,000 cells were plated in six-well plates and treated with vehicle or IC50 doses of indicated drugs for 24hr. Cells were stained with 5 μM MitoSOX resuspended in serum-free RPMI containing associated drug concentration in the dark for 10 mins in a 37oC 5% CO_2 incubator. Cells were washed once with PBS and trypsinized followed by another wash in PBS and resuspended in 500 μL of PBS. The samples were analyzed using flow cytometer BD FACS Canto II. Gating strategy was defined using untreated/unstained cells. Analysis of flow cytometry data was performed with FlowJo v10.

G.7: MitoTracker staining

MitoTracker Red CMXRos was purchased from Thermofisher (cat. M7512). 100,000 cells were plated in six-well plates and treated with vehicle or IC50 doses of GNF5. Cells were stained with 100 nM MitoTracker resuspended in serum-free RPMI containing associated drug concentration in the dark for 30 mins in a 37oC 5% CO_2 incubator. Cells were washed once with PBS and trypsinized followed by another wash in PBS and resuspended in 500 μL of PBS. The samples were analyzed using flow cytometer BD FACS Canto II. Gating strategy was defined using untreated/unstained cells. Analysis of flow cytometry data was performed with FlowJo v10.

G.8: Pooled CRISPR screen

PC9 cells were seeded into 12, six-well plates at 0.25e6 cells/well. A separate plate was also prepared for no puromycin and puromycin controls of non-transduced cells. Cells were transduced at a MOI of 0.2. 24 hours after viral transduction, cells were replated into puromycin-containing media. A sample was collected at 48 hours of puromycin exposure to confirm library coverage in the transduced population. Transduced cells were expanded in puromycin for a total of 10 days prior to drug introduction, at which point the transduced cell population was split into vehicle (DMSO) and GNF5 treatment conditions and maintained for up to two weeks. Cells were treated with 2 μM GNF5 which corresponded to 20-30% loss in cell viability following a 3-day dose response assay. Cells were counted, replated, and drug replenished every day. At any given point during the screen, each replicate was represented by a minimum of 12E6 cells, sufficient to provide 1000x coverage of the library (~1000 cells per unique sgRNA). Samples of 25E6 cells were collected upon screen initiation, termination, and at weekly intervals. Following completion of the screens, DNA was extracted (DNeasy Blood & Tissue Kit, QIAGEN) and prepared for sequencing as previously described (299)

G.9: CRISPR screen analysis

Deep sequencing was performed on an Illumina Nextseq platform (75 bp, paired-ended) to identify differences in library composition. All sequencing was performed by the Duke University genome sequencing facility. Barcoded reads were mapped to the guide RNA library using bcSeq (Lin et al., 2018) to obtain the counts for each guide RNA. Determinations of genetic essentiality and drug sensitization/resistance were made by evaluating differential guide compositions between the initial population and subsequent drug-treated and vehicle-treated cells populations. Briefly, the fractional representation (FR) for the guide reads within a sample was normalized to the total reads attributed to that sample. A direct comparison between two samples was represented by the quotient of the respective FRs in the log2 scale, which we term the depletion metric (DM). The guide-level DMs for each gene were then collapsed to gene-level scores by taking the average of the top three most depleted constructs resulting in a biased analysis focused on depleted genes. Genes represented by fewer than 5 guides per condition were excluded from analysis. In the 2,322-gene library, 7 genes (representing 0.3% of the total library) were excluded. Genetic essentiality was calculated by considering the depletion/enrichment of the vehicle treated (DSMO) population over time (DMSO final / DSMO initial). Drug sensitization/resistance was calculated by considering the depletion/enrichment of the drug-treated population relative to the vehicle-treated population (Drug final / DMSO final). All depletion/enrichment effects are reported as log2 ratios. All analyses were conducted using the R statistical environment (https://www.r-project.org/) along with extension packages from the comprehensive R archive network (CRAN; https://cran.r-project.org/) and the Bioconductor project (Gentleman et al., 2004). The analyses were carried out with adherence to the principles of reproducible analysis using the knitr package (Xie, 2016) for generation of dynamic reports and gitlab for source code management. The code for replicating the statistical analysis was made accessible through a public source code repository: https://gitlab.oit.duke.edu/dcibioinformatics/pubs/pendergast-crispr-barcode.

Because many metabolic genes are known to be essential to cellular viability (Hart et al., 2015), determining the effect of cell-essential genetic loss on apoptosis is difficult. To this point, a subset of essential metabolic genes will have lost representation in our screen before the 10-day puromycin selection period is over; our screen does not capture the effect of these genes (which represent a trivial fraction of our library) on apoptosis. The remaining cell-essential genes are captured by the screen. Since our analysis normalizes the effect of gene knockout + drug treatment to gene knockout alone, the interpretation of these genes does not require additional correction, except that they necessarily suffer from reduced resolution.

G.10: Immunoblotting procedures

Cells were lysed in RIPA buffer (50 mM Tris-HCl pH 7.4, 150 mM NaCl, 1 mM EDTA, 1% Triton X-100, 1% sodium deoxycholate and 0.1% SDS) containing protease-phosphatase inhibitor cocktail (Cell Signaling). Cell suspensions were rotated at 4C for 15 minutes followed by microcentrifugation to remove cell debris, and protein concentration was quantified using the DC Protein Assay (BioRad). Equal amounts of protein were separated by SDS/PAGE and transferred onto nitrocellulose membranes using the Transblot Turbo Transfer system (Bio-Rad). Membranes were incubated with primary antibody overnight at 4oC, followed by 3 washes in 1xTBST and incubation with corresponding secondary antibody for 1 hr at room temperature. Blots were developed using SuperSignal West PLUS Chemiluminescent Substrate developing solution (Invitrogen) and imaged using either film or a ChemiDoc XRS+ imager (Bio-Rad). The following antibodies used for immunoblot analysis were purchased from: Cell Signaling: Phospho-CrkL (Tyr207) (3181L), beta-Tubulin (D2N5G) (15115S), cleaved PARP (5625), total PARP (9542), cleaved caspase 3 (9661), total caspase 3 (9668), cytochrome C (11940), beta-Catenin (8480); Thermofisher: HDJ2 (MA5-12748); Millipore Sigma: ABL1 (8E9) (MAB1130), ABL2 (6D5) (H00000027-M03); Santa Cruz: RAP1 (sc-398755), CRKL (C-20) (sc-319), GAPDH (6C5) (sc-32233); Jackson Immunoresearch: Peroxidase AffiniPure Goat Anti-Mouse IgG (H+L) (115-035-003), Peroxidase AffiniPure Goat Anti-Rabbit IgG (H+L) (115-035-144).

G.11: Real-time quantitative PCR

RNA was isolated from subconfluent monolayers of cancer cells using the RNeasy RNA isolation kit (QIAGEN), and cDNA synthesis was performed using oligo(dT) primers and M-MLV reverse transcriptase (Invitrogen). RT-qPCR was performed in triplicate wells using iTaq Universal SYBR Green Supermix (Bio-Rad). Primers used in this study were purchased from Sigma Aldrich. Analysis of real-time data was collected using a Bio-Rad CFX384 machine and CFX Maestro software. Expression levels of each gene were normalized to GAPDH control housekeeping genes using the ddCT algorithm. Primers sequences used: BBC3 Fwd (GACCTCAACGCACAGTACGAG), BBC3 Rev (AGGAGTCCCATGATGAGATTGT), Bcl2 Fwd (GGTGGGGTCATGTGTGTGG), Bcl2 Rev (CGGTTCAGGTACTCAGTCATCC), Bcl2L1 Fwd (GAGCTGGTGGTTGACTTTCTC), Bcl2L1 Rev (TCCATCTCCGATTCAGTCCCT).

G.12: DNA plasmids

Sequences for shRNAs targeting the ABL kinases were as follows: scrambled shRNA (GGTGTATGGGCTACTATAGAA); ABL1 shRNA (GGTGTATGAGCTGCTAGAGAA); ABL2 shRNA (CCTTATCTCACCCACTCTGAA). Stable non-inducible shRNAs against non-target control (NTC), HMGCR, and SLC7A11 in the pLKO.1 vector were from the Sigma Mission TRC1 Lentiviral shRNA library and were obtained through the Duke Functional Genomics Shared Resource Facility. The pLVX-Tet-On vector and pLVX-TP-3F-TAZ4SA (S66A, S89A, S117A and S311A) plasmids were provided by Dr. Xaralabos Varelas (Boston University, Boston, MA, USA). Sequences and Sigma clone identifiers for each of these shRNAs were as follows: HMGCR shRNA 46448 (CCGGGCAGTGATAAAGGAGGCATTTCTCGAGAAATGCCTCCTTTATCACTGCTTTTTG), HMGCR shRNA 46452 (CCGGCCTGCTGCTATAAATTGGATACTCGAGTATCCAATTTATAGCAGCAGGTTTTTG), SLC7A11 shRNA 43124 (CCGGGCACCCTTTGACAATGATAATCTCGAGATTATCATTGTCAAAGGGTGCTTTTTG).

G.13: Viral transduction protocol

Lentiviral shRNAs against the ABL kinases (ABL1, ABL2 and AA double knockdown), HMGCR, and SLC7A11 were packaged in 3rd generation lentiviral packaging vectors (pMDL, pCMV-VSV-G, pRSV-REV). Briefly, 293T cells were transfected with packaging DNAs and corresponding DNAs using FuGENE6 reagent (Promega). Culture supernatants containing virus were harvested and filtered 24 hours and 48 hours after transfection and were added to NSCLC cell cultures in the presence of 8 μg/ml polybrene (Sigma-Aldrich). Cells were spinfected with virus at 2200 RPM for 1 hr at 37oC. Stably-transduced cells expressing shRNAs cloned in the pLKO.1 backbone were selected with puromycin (1 μg/ml) for two days.

G.14: Immunofluorescence and confocal microscopy

Brains were perfused and fixed with 4% paraformaldehyde in PBS prior to extraction. Upon extraction, brains were rotated overnight (O/N) in 4% paraformaldehyde in PBS at 4oC followed by subsequent washes in PBS the following day. For OCT embedding, brains underwent sucrose protection in 15% sucrose in water at 4oC O/N rotation following by O/N rotation in 30% sucrose in water at 4oC before OCT embedding at -80oC. OCT sections were 10 μm thick. For paraffin embedding, brains were placed into 70% ethanol prior to paraffin embedding. Paraffin embedding was performed at the Duke University Immunohistopathology Core Facility sections were cut at 5 μm thick. OCT sections were thawed at room temperature for 15 minutes followed by acetone fixation. Paraffin sections were deparaffinized, rehydrated, and heat inactivated (BioCare Medical Decloaking Chamber). Both deparaffinized and OCT sections were then washed in PBS and blocked in 3% goat serum in PBS with 0.05% Tween-20 for one hour. Sections were incubated with primary antibodies in blocking solution overnight at 4°C in a humidified chamber at concentrations indicated below. Sections were then washed with PBS followed by incubation with the appropriate secondary antibody in blocking solution for one hour at room temperature. Sections were then washed with PBS, incubated with the nuclear stain, Hoechst33342, and washed again with PBS before mounting using aqueous mounting media (Dako-S3025). Antibodies for immunofluorescence and IHC experiments included: cleaved caspase 3

(Cell Signaling 9661) at 1:100 dilution, Ki67 (Cell Signaling 9449) at 1:200 dilution, tdTomato (Kerafast EST203) at 1:100 dilution. All images were captured on an Axio Imager D10 (Carl Zeiss) with a 20×/0.75 EC Plan-Neofluar objective lens.

Mitochondrial morphology analysis was performed by plating 75,000 H460 cells on glass coverslips in 12-well plates. Cells were treated with IC50 doses of each drug the following day. After 24 hours, the cells were stained with 100 nM MitoTracker Red CMXRos (Thermofisher cat. M7512) for 30 min, fixed (formaldehyde), permeabilized (Triton-X), stained with Hoescht 33342 and mounted. The slides were imaged using a Zeiss 880 inverted confocal Airyscan microscope with 63x oil objective. For all representative images in the manuscript, experiments were conducted at least twice, and had no repeatability issues. Mitochondrial morphology was determined using the tubeness and vesselness algorithms in Fiji. Mitochondrial fragmentation vs. connectivity was determined by plotting length × width of several thousand mitochondrial from at least 10 cells across at least two independent experiments.

G.15: Cell viability assay

Cells were seeded in white-walled clear bottom 96-well plates in triplicate at 3,000 cells per well. Each condition was run in triplicate wells each from three independent experiments and measured using CellTiter-Glo reagent (Promega). Plates were read on a Tecan Infinite M1000 Microplate Reader and results were analyzed in GraphPad.

G.16: Annexin V staining

Annexin V staining was performed to determine the percentage of cells undergoing apoptosis. 100,000 cells were plated in six-well plates and treated with vehicle, 10 μM GNF5, 1 μM Simvastatin, 0.5 μM Fluvastatin or the combination for 24hr. Upon collection, cells were trypsinized, washed twice with PBS, resuspended in 100 μL 1X Annexin V binding buffer (BD Biosciences) containing 5 μL Annexin V stain conjugated to APC (allophycocyanin) (BD Biosciences). Phosphatidylserine externalization was measured using APC-conjugated Annexin. Following a 15min incubation at RT, the samples were analyzed using flow cytometer BD FACS Canto II. Gating strategy was defined using untreated/unstained cells. Analysis of flow cytometry data was performed with FlowJo v10.

G.17: Colony formation assay

Cells were seeded in 12-well plates in duplicate at 1,000 cells per well for PC9 and PC9 GR4 cell lines and 250 cells per well for H460 cells (n=2). Cells were treated with 1 μM ABL001, 100 nM Simvastatin, or combination for 1 week. Cells were then fixed with methanol and stained with crystal violet. Images were taken using an Epson scanner. 1 mL of 10% acetic acid was added per well and a plate reader was used to measure absorbance at 590 nm.

G.18: Intracellular glutathione assay

0.5e6 cells harboring shRNAs against target genes were plated in 6-well dishes on Day 0 and harvested on Day 1. Cells were resuspended in PBS and a 15 uL aliquot was taken to count cells in automated cell counter. Glutathione levels were then measured followed the instructions in BioVision's Colorimetric Glutathione Kit (Cat. K261). Results were normalized to cell counts.

G.19: Extracellular glutamate assay

3,000 cells harboring shRNAs against target genes were plated in 96-well white walled dishes. Cells were plated in triplicate for technical replicate. 1 uL of media was taken from the cells and diluted with 45 uL of PBS. Extracellular glutamate levels were assayed following Promega's Glutamate Glo kit (Cat. J7021). The cells from which the media was taken were used for Cell Titer Glo analysis to normalize glutamate counts.

G.20: Neuronal cell culture

Rat cortical neurons, panned to remove astrocytes, were cultured 7 days *in vitro* (DIV7) to allow for neurons to polarize. On DIV7, half of the media was removed and replaced with either fresh media, 5 uM glutamate, or tumor conditioned media from PC9 cells harboring shRNAs against ABL1/ABL2 (shAA) or control shRNA (shSCR), or PC9 cells cultured with sulfasalazine (SAS), an xCT inhibitor. PC9 cells were cultured in matching neurobasal media. Neurons were cultured for 18 hours in tumor conditioned medium and then stained with a Live/Dead kit from Molecular Probes, and dead cells were counted using ImageJ software.

G.21: H2O2 treatments

75,000 cells were plated in 6-well dishes. Cells were treated with 200 uM H_2O_2 for 6 hours. Cells were washed with PBS and lysates were harvested for western blot analysis.

Appendix H: Statistical Analysis

Statistical analyses were performed using GraphPad Prism 7 and GraphPad Prism 9 software. Mouse numbers per group were determined through statistical power calculations where 10 mice per group allows for 90% power, at the unadjusted 0.05 two-sided level, to detect inter-group differences of 50% and assuming intra-group differences of 25%. For Kaplan-Meier survival curves, p values were calculated using log-rank (Mantel-Cox) testing. P values below an adjusted $p<0.017$ were deemed significant accounting for 3 pairwise comparisons. Statistical analysis of tumor flux was evaluated by ANOVA followed by Fisher post hoc testing to calculate p values and those less than 0.05 were quantified as statistically significant. For comparisons between mouse groups of unequal size, the mean value and SEM were used to allow for statistical analysis by ANOVA. Bar graph data represent averages ± SEM.

5. References

1. Chaffer CL, Weinberg RA. A perspective on cancer cell metastasis. Science. 2011;331(6024):1559-64. Epub 2011/03/26. doi: 10.1126/science.1203543. PubMed PMID: 21436443.

2. Chambers AF, Groom AC, MacDonald IC. Dissemination and growth of cancer cells in metastatic sites. Nat Rev Cancer. 2002;2(8):563-72. Epub 2002/08/03. doi: 10.1038/nrc865. PubMed PMID: 12154349.

3. Fidler IJ. The pathogenesis of cancer metastasis: the 'seed and soil' hypothesis revisited. Nat Rev Cancer. 2003;3(6):453-8. Epub 2003/06/05. doi: 10.1038/nrc1098. PubMed PMID: 12778135.

4. Seyfried TN, Huysentruyt LC. On the origin of cancer metastasis. Crit Rev Oncog. 2013;18(1-2):43-73. Epub 2012/12/15. doi: 10.1615/critrevoncog.v18.i1-2.40. PubMed PMID: 23237552; PMCID: PMC3597235.

5. Wei Q, Qian Y, Yu J, Wong CC. Metabolic rewiring in the promotion of cancer metastasis: mechanisms and therapeutic implications. Oncogene. 2020;39(39):6139-56. Epub 2020/08/26. doi: 10.1038/s41388-020-01432-7. PubMed PMID: 32839493; PMCID: PMC7515827.

6. Duncan JS, Whittle MC, Nakamura K, Abell AN, Midland AA, Zawistowski JS, Johnson NL, Granger DA, Jordan NV, Darr DB, Usary J, Kuan PF, Smalley DM, Major B, He X, Hoadley KA, Zhou B, Sharpless NE, Perou CM, Kim WY, Gomez SM, Chen X, Jin J, Frye SV, Earp HS, Graves LM, Johnson GL. Dynamic reprogramming of the kinome in response to targeted MEK inhibition in triple-negative breast cancer. Cell. 2012;149(2):307-21. Epub 2012/04/17. doi: 10.1016/j.cell.2012.02.053. PubMed PMID: 22500798; PMCID: PMC3328787.

7. Sharma SV, Lee, D. Y., Li, B., Quinlan, M. P., Takahashi, F., Maheswaran, S., McDermott, U., Azizian, N., Zou, L., Fischbach, M. A., Wong, K. K., Brandstetter, K., Wittner, B., Ramaswamy, S., Classon, M., & Settleman, J. . A chromatin-mediated reversible drug-tolerant state in cancer cell subpopulations. Cell. 2010;141(1):69-80.

8. Pavlova NN, Thompson CB. The Emerging Hallmarks of Cancer Metabolism. Cell Metab. 2016;23(1):27-47. Epub 2016/01/16. doi: 10.1016/j.cmet.2015.12.006. PubMed PMID: 26771115; PMCID: PMC4715268.

9. Chen X, Chen S, Yu D. Metabolic Reprogramming of Chemoresistant Cancer Cells and the Potential Significance of Metabolic Regulation in the Reversal of Cancer

Chemoresistance. Metabolites. 2020;10(7). Epub 2020/07/28. doi: 10.3390/metabo10070289. PubMed PMID: 32708822; PMCID: PMC7408410.

10. Jiang Z, Hsu JL, Li Y, Hortobagyi GN, Hung MC. Cancer Cell Metabolism Bolsters Immunotherapy Resistance by Promoting an Immunosuppressive Tumor Microenvironment. Front Oncol. 2020;10:1197. Epub 2020/08/11. doi: 10.3389/fonc.2020.01197. PubMed PMID: 32775303; PMCID: PMC7387712.

11. Lin J, Xia L, Liang J, Han Y, Wang H, Oyang L, Tan S, Tian Y, Rao S, Chen X, Tang Y, Su M, Luo X, Wang Y, Wang H, Zhou Y, Liao Q. The roles of glucose metabolic reprogramming in chemo- and radio-resistance. J Exp Clin Cancer Res. 2019;38(1):218. Epub 2019/05/28. doi: 10.1186/s13046-019-1214-z. PubMed PMID: 31122265; PMCID: PMC6533757.

12. Tang L, Wei F, Wu Y, He Y, Shi L, Xiong F, Gong Z, Guo C, Li X, Deng H, Cao K, Zhou M, Xiang B, Li X, Li Y, Li G, Xiong W, Zeng Z. Role of metabolism in cancer cell radioresistance and radiosensitization methods. J Exp Clin Cancer Res. 2018;37(1):87. Epub 2018/04/25. doi: 10.1186/s13046-018-0758-7. PubMed PMID: 29688867; PMCID: PMC5914062.

13. Koppenol WH, Bounds PL, Dang CV. Otto Warburg's contributions to current concepts of cancer metabolism. Nat Rev Cancer. 2011;11(5):325-37. Epub 2011/04/22. doi: 10.1038/nrc3038. PubMed PMID: 21508971.

14. DeBerardinis RJ, Chandel NS. Fundamentals of cancer metabolism. Sci Adv. 2016;2(5):e1600200. Epub 2016/07/08. doi: 10.1126/sciadv.1600200. PubMed PMID: 27386546; PMCID: PMC4928883.

15. Ganapathy-Kanniappan S, Geschwind JF. Tumor glycolysis as a target for cancer therapy: progress and prospects. Mol Cancer. 2013;12:152. Epub 2013/12/05. doi: 10.1186/1476-4598-12-152. PubMed PMID: 24298908; PMCID: PMC4223729.

16. Barthel A, Okino ST, Liao J, Nakatani K, Li J, Whitlock JP, Jr., Roth RA. Regulation of GLUT1 gene transcription by the serine/threonine kinase Akt1. J Biol Chem. 1999;274(29):20281-6. Epub 1999/07/10. doi: 10.1074/jbc.274.29.20281. PubMed PMID: 10400647.

17. Wieman HL, Wofford JA, Rathmell JC. Cytokine stimulation promotes glucose uptake via phosphatidylinositol-3 kinase/Akt regulation of Glut1 activity and trafficking. Mol Biol Cell. 2007;18(4):1437-46. Epub 2007/02/16. doi: 10.1091/mbc.e06-07-0593. PubMed PMID: 17301289; PMCID: PMC1838986.

18. Deprez J, Vertommen D, Alessi DR, Hue L, Rider MH. Phosphorylation and activation of heart 6-phosphofructo-2-kinase by protein kinase B and other protein kinases of the insulin signaling cascades. J Biol Chem. 1997;272(28):17269-75. Epub 1997/07/11. doi: 10.1074/jbc.272.28.17269. PubMed PMID: 9211863.

19. Gottlob K, Majewski N, Kennedy S, Kandel E, Robey RB, Hay N. Inhibition of early apoptotic events by Akt/PKB is dependent on the first committed step of glycolysis and mitochondrial hexokinase. Genes Dev. 2001;15(11):1406-18. Epub 2001/06/08. doi: 10.1101/gad.889901. PubMed PMID: 11390360; PMCID: PMC312709.

20. Kim JW, Zeller KI, Wang Y, Jegga AG, Aronow BJ, O'Donnell KA, Dang CV. Evaluation of myc E-box phylogenetic footprints in glycolytic genes by chromatin immunoprecipitation assays. Mol Cell Biol. 2004;24(13):5923-36. Epub 2004/06/17. doi: 10.1128/MCB.24.13.5923-5936.2004. PubMed PMID: 15199147; PMCID: PMC480875.

21. Gan L, Xiu R, Ren P, Yue M, Su H, Guo G, Xiao D, Yu J, Jiang H, Liu H, Hu G, Qing G. Metabolic targeting of oncogene MYC by selective activation of the proton-coupled monocarboxylate family of transporters. Oncogene. 2016;35(23):3037-48. Epub 2015/10/06. doi: 10.1038/onc.2015.360. PubMed PMID: 26434591.

22. Osthus RC, Shim H, Kim S, Li Q, Reddy R, Mukherjee M, Xu Y, Wonsey D, Lee LA, Dang CV. Deregulation of glucose transporter 1 and glycolytic gene expression by c-Myc. J Biol Chem. 2000;275(29):21797-800. Epub 2000/05/24. doi: 10.1074/jbc.C000023200. PubMed PMID: 10823814.

23. David CJ, Chen M, Assanah M, Canoll P, Manley JL. HnRNP proteins controlled by c-Myc deregulate pyruvate kinase mRNA splicing in cancer. Nature. 2010;463(7279):364-8. Epub 2009/12/17. doi: 10.1038/nature08697. PubMed PMID: 20010808; PMCID: PMC2950088.

24. Papandreou I, Cairns RA, Fontana L, Lim AL, Denko NC. HIF-1 mediates adaptation to hypoxia by actively downregulating mitochondrial oxygen consumption. Cell Metab. 2006;3(3):187-97. Epub 2006/03/07. doi: 10.1016/j.cmet.2006.01.012. PubMed PMID: 16517406.

25. Masoud GN, Li W. HIF-1alpha pathway: role, regulation and intervention for cancer therapy. Acta Pharm Sin B. 2015;5(5):378-89. Epub 2015/11/19. doi: 10.1016/j.apsb.2015.05.007. PubMed PMID: 26579469; PMCID: PMC4629436.

26. Gleadle JM, Ratcliffe PJ. Induction of hypoxia-inducible factor-1, erythropoietin, vascular endothelial growth factor, and glucose transporter-1 by hypoxia: evidence

against a regulatory role for Src kinase. Blood. 1997;89(2):503-9. Epub 1997/01/15. PubMed PMID: 9002952.

27. Mathupala SP, Rempel A, Pedersen PL. Glucose catabolism in cancer cells: identification and characterization of a marked activation response of the type II hexokinase gene to hypoxic conditions. J Biol Chem. 2001;276(46):43407-12. Epub 2001/09/15. doi: 10.1074/jbc.M108181200. PubMed PMID: 11557773.

28. Maxwell PH, Dachs GU, Gleadle JM, Nicholls LG, Harris AL, Stratford IJ, Hankinson O, Pugh CW, Ratcliffe PJ. Hypoxia-inducible factor-1 modulates gene expression in solid tumors and influences both angiogenesis and tumor growth. Proc Natl Acad Sci U S A. 1997;94(15):8104-9. Epub 1997/07/22. doi: 10.1073/pnas.94.15.8104. PubMed PMID: 9223322; PMCID: PMC21564.

29. Semenza GL, Jiang BH, Leung SW, Passantino R, Concordet JP, Maire P, Giallongo A. Hypoxia response elements in the aldolase A, enolase 1, and lactate dehydrogenase A gene promoters contain essential binding sites for hypoxia-inducible factor 1. J Biol Chem. 1996;271(51):32529-37. Epub 1996/12/20. doi: 10.1074/jbc.271.51.32529. PubMed PMID: 8955077.

30. Semenza GL, Roth PH, Fang HM, Wang GL. Transcriptional regulation of genes encoding glycolytic enzymes by hypoxia-inducible factor 1. J Biol Chem. 1994;269(38):23757-63. Epub 1994/09/23. PubMed PMID: 8089148.

31. Nagao A, Kobayashi M, Koyasu S, Chow CCT, Harada H. HIF-1-Dependent Reprogramming of Glucose Metabolic Pathway of Cancer Cells and Its Therapeutic Significance. Int J Mol Sci. 2019;20(2). Epub 2019/01/13. doi: 10.3390/ijms20020238. PubMed PMID: 30634433; PMCID: PMC6359724.

32. Canto C, Menzies KJ, Auwerx J. NAD(+) Metabolism and the Control of Energy Homeostasis: A Balancing Act between Mitochondria and the Nucleus. Cell Metab. 2015;22(1):31-53. Epub 2015/06/30. doi: 10.1016/j.cmet.2015.05.023. PubMed PMID: 26118927; PMCID: PMC4487780.

33. Golias T, Papandreou I, Sun R, Kumar B, Brown NV, Swanson BJ, Pai R, Jaitin D, Le QT, Teknos TN, Denko NC. Hypoxic repression of pyruvate dehydrogenase activity is necessary for metabolic reprogramming and growth of model tumours. Sci Rep. 2016;6:31146. Epub 2016/08/09. doi: 10.1038/srep31146. PubMed PMID: 27498883; PMCID: PMC4976358.

34. Annibaldi A, Dousse A, Martin S, Tazi J, Widmann C. Revisiting G3BP1 as a RasGAP binding protein: sensitization of tumor cells to chemotherapy by the RasGAP

317-326 sequence does not involve G3BP1. PLoS One. 2011;6(12):e29024. Epub 2011/12/30. doi: 10.1371/journal.pone.0029024. PubMed PMID: 22205990; PMCID: PMC3242762.

35. Murakami T, Nishiyama T, Shirotani T, Shinohara Y, Kan M, Ishii K, Kanai F, Nakazuru S, Ebina Y. Identification of two enhancer elements in the gene encoding the type 1 glucose transporter from the mouse which are responsive to serum, growth factor, and oncogenes. J Biol Chem. 1992;267(13):9300-6. Epub 1992/05/05. PubMed PMID: 1339457.

36. Minchenko O, Opentanova I, Caro J. Hypoxic regulation of the 6-phosphofructo-2-kinase/fructose-2,6-bisphosphatase gene family (PFKFB-1-4) expression in vivo. FEBS Lett. 2003;554(3):264-70. Epub 2003/11/19. doi: 10.1016/s0014-5793(03)01179-7. PubMed PMID: 14623077.

37. Tanner LB, Goglia AG, Wei MH, Sehgal T, Parsons LR, Park JO, White E, Toettcher JE, Rabinowitz JD. Four Key Steps Control Glycolytic Flux in Mammalian Cells. Cell Syst. 2018;7(1):49-62 e8. Epub 2018/07/02. doi: 10.1016/j.cels.2018.06.003. PubMed PMID: 29960885; PMCID: PMC6062487.

38. Sang N, Stiehl DP, Bohensky J, Leshchinsky I, Srinivas V, Caro J. MAPK signaling up-regulates the activity of hypoxia-inducible factors by its effects on p300. J Biol Chem. 2003;278(16):14013-9. Epub 2003/02/18. doi: 10.1074/jbc.M209702200. PubMed PMID: 12588875; PMCID: PMC4518846.

39. Semenza G. Signal transduction to hypoxia-inducible factor 1. Biochem Pharmacol. 2002;64(5-6):993-8. Epub 2002/09/06. doi: 10.1016/s0006-2952(02)01168-1. PubMed PMID: 12213597.

40. Martinez-Reyes I, Diebold LP, Kong H, Schieber M, Huang H, Hensley CT, Mehta MM, Wang T, Santos JH, Woychik R, Dufour E, Spelbrink JN, Weinberg SE, Zhao Y, DeBerardinis RJ, Chandel NS. TCA Cycle and Mitochondrial Membrane Potential Are Necessary for Diverse Biological Functions. Mol Cell. 2016;61(2):199-209. Epub 2016/01/05. doi: 10.1016/j.molcel.2015.12.002. PubMed PMID: 26725009; PMCID: PMC4724312.

41. Weinberg F, Hamanaka R, Wheaton WW, Weinberg S, Joseph J, Lopez M, Kalyanaraman B, Mutlu GM, Budinger GR, Chandel NS. Mitochondrial metabolism and ROS generation are essential for Kras-mediated tumorigenicity. Proc Natl Acad Sci U S A. 2010;107(19):8788-93. Epub 2010/04/28. doi: 10.1073/pnas.1003428107. PubMed PMID: 20421486; PMCID: PMC2889315.

42. Vasan K, Werner M, Chandel NS. Mitochondrial Metabolism as a Target for Cancer Therapy. Cell Metab. 2020;32(3):341-52. Epub 2020/07/16. doi: 10.1016/j.cmet.2020.06.019. PubMed PMID: 32668195; PMCID: PMC7483781.

43. Hensley CT, Wasti AT, DeBerardinis RJ. Glutamine and cancer: cell biology, physiology, and clinical opportunities. J Clin Invest. 2013;123(9):3678-84. Epub 2013/09/04. doi: 10.1172/JCI69600. PubMed PMID: 23999442; PMCID: PMC3754270.

44. Chandel NS, Maltepe E, Goldwasser E, Mathieu CE, Simon MC, Schumacker PT. Mitochondrial reactive oxygen species trigger hypoxia-induced transcription. Proc Natl Acad Sci U S A. 1998;95(20):11715-20. Epub 1998/09/30. doi: 10.1073/pnas.95.20.11715. PubMed PMID: 9751731; PMCID: PMC21706.

45. Cheung EC, Lee P, Ceteci F, Nixon C, Blyth K, Sansom OJ, Vousden KH. Opposing effects of TIGAR- and RAC1-derived ROS on Wnt-driven proliferation in the mouse intestine. Genes Dev. 2016;30(1):52-63. Epub 2015/12/19. doi: 10.1101/gad.271130.115. PubMed PMID: 26679840; PMCID: PMC4701978.

46. Irani K, Xia Y, Zweier JL, Sollott SJ, Der CJ, Fearon ER, Sundaresan M, Finkel T, Goldschmidt-Clermont PJ. Mitogenic signaling mediated by oxidants in Ras-transformed fibroblasts. Science. 1997;275(5306):1649-52. Epub 1997/03/14. doi: 10.1126/science.275.5306.1649. PubMed PMID: 9054359.

47. Porporato PE, Payen VL, Perez-Escuredo J, De Saedeleer CJ, Danhier P, Copetti T, Dhup S, Tardy M, Vazeille T, Bouzin C, Feron O, Michiels C, Gallez B, Sonveaux P. A mitochondrial switch promotes tumor metastasis. Cell Rep. 2014;8(3):754-66. Epub 2014/07/30. doi: 10.1016/j.celrep.2014.06.043. PubMed PMID: 25066121.

48. Chandel NS, Tuveson DA. The promise and perils of antioxidants for cancer patients. N Engl J Med. 2014;371(2):177-8. Epub 2014/07/10. doi: 10.1056/NEJMcibr1405701. PubMed PMID: 25006725.

49. Orr AL, Vargas L, Turk CN, Baaten JE, Matzen JT, Dardov VJ, Attle SJ, Li J, Quackenbush DC, Goncalves RL, Perevoshchikova IV, Petrassi HM, Meeusen SL, Ainscow EK, Brand MD. Suppressors of superoxide production from mitochondrial complex III. Nat Chem Biol. 2015;11(11):834-6. Epub 2015/09/15. doi: 10.1038/nchembio.1910. PubMed PMID: 26368590; PMCID: PMC4618194.

50. Duvel K, Yecies JL, Menon S, Raman P, Lipovsky AI, Souza AL, Triantafellow E, Ma Q, Gorski R, Cleaver S, Vander Heiden MG, MacKeigan JP, Finan PM, Clish CB, Murphy LO, Manning BD. Activation of a metabolic gene regulatory network

downstream of mTOR complex 1. Mol Cell. 2010;39(2):171-83. Epub 2010/07/31. doi: 10.1016/j.molcel.2010.06.022. PubMed PMID: 20670887; PMCID: PMC2946786.

51. Zaganjor E, Vyas S, Haigis MC. SIRT4 Is a Regulator of Insulin Secretion. Cell Chem Biol. 2017;24(6):656-8. Epub 2017/06/24. doi: 10.1016/j.chembiol.2017.06.002. PubMed PMID: 28644956.

52. Nikiforov MA, Chandriani S, O'Connell B, Petrenko O, Kotenko I, Beavis A, Sedivy JM, Cole MD. A functional screen for Myc-responsive genes reveals serine hydroxymethyltransferase, a major source of the one-carbon unit for cell metabolism. Mol Cell Biol. 2002;22(16):5793-800. Epub 2002/07/26. doi: 10.1128/mcb.22.16.5793-5800.2002. PubMed PMID: 12138190; PMCID: PMC133987.

53. Lucas S, Chen G, Aras S, Wang J. Serine catabolism is essential to maintain mitochondrial respiration in mammalian cells. Life Sci Alliance. 2018;1(2):e201800036. Epub 2018/11/21. doi: 10.26508/lsa.201800036. PubMed PMID: 30456347; PMCID: PMC6238390.

54. Morris JPt, Yashinskie JJ, Koche R, Chandwani R, Tian S, Chen CC, Baslan T, Marinkovic ZS, Sanchez-Rivera FJ, Leach SD, Carmona-Fontaine C, Thompson CB, Finley LWS, Lowe SW. alpha-Ketoglutarate links p53 to cell fate during tumour suppression. Nature. 2019;573(7775):595-9. Epub 2019/09/20. doi: 10.1038/s41586-019-1577-5. PubMed PMID: 31534224; PMCID: PMC6830448.

55. Miyashita T, Krajewski S, Krajewska M, Wang HG, Lin HK, Liebermann DA, Hoffman B, Reed JC. Tumor suppressor p53 is a regulator of bcl-2 and bax gene expression in vitro and in vivo. Oncogene. 1994;9(6):1799-805. Epub 1994/06/01. PubMed PMID: 8183579.

56. Czabotar PE, Lessene G, Strasser A, Adams JM. Control of apoptosis by the BCL-2 protein family: implications for physiology and therapy. Nat Rev Mol Cell Biol. 2014;15(1):49-63. Epub 2013/12/21. doi: 10.1038/nrm3722. PubMed PMID: 24355989.

57. Lagadinou ED, Sach A, Callahan K, Rossi RM, Neering SJ, Minhajuddin M, Ashton JM, Pei S, Grose V, O'Dwyer KM, Liesveld JL, Brookes PS, Becker MW, Jordan CT. BCL-2 inhibition targets oxidative phosphorylation and selectively eradicates quiescent human leukemia stem cells. Cell Stem Cell. 2013;12(3):329-41. Epub 2013/01/22. doi: 10.1016/j.stem.2012.12.013. PubMed PMID: 23333149; PMCID: PMC3595363.

58. Rysman E, Brusselmans K, Scheys K, Timmermans L, Derua R, Munck S, Van Veldhoven PP, Waltregny D, Daniels VW, Machiels J, Vanderhoydonc F, Smans K, Waelkens E, Verhoeven G, Swinnen JV. De novo lipogenesis protects cancer cells from

free radicals and chemotherapeutics by promoting membrane lipid saturation. Cancer Res. 2010;70(20):8117-26. Epub 2010/09/30. doi: 10.1158/0008-5472.CAN-09-3871. PubMed PMID: 20876798.

59. Vysochan A, Sengupta A, Weljie AM, Alwine JC, Yu Y. ACSS2-mediated acetyl-CoA synthesis from acetate is necessary for human cytomegalovirus infection. Proc Natl Acad Sci U S A. 2017;114(8):E1528-E35. Epub 2017/02/09. doi: 10.1073/pnas.1614268114. PubMed PMID: 28167750; PMCID: PMC5338361.

60. Yang C, Ko B, Hensley CT, Jiang L, Wasti AT, Kim J, Sudderth J, Calvaruso MA, Lumata L, Mitsche M, Rutter J, Merritt ME, DeBerardinis RJ. Glutamine oxidation maintains the TCA cycle and cell survival during impaired mitochondrial pyruvate transport. Mol Cell. 2014;56(3):414-24. Epub 2014/12/03. doi: 10.1016/j.molcel.2014.09.025. PubMed PMID: 25458842; PMCID: PMC4268166.

61. Eberle D, Hegarty B, Bossard P, Ferre P, Foufelle F. SREBP transcription factors: master regulators of lipid homeostasis. Biochimie. 2004;86(11):839-48. Epub 2004/12/14. doi: 10.1016/j.biochi.2004.09.018. PubMed PMID: 15589694.

62. Chajes V, Cambot M, Moreau K, Lenoir GM, Joulin V. Acetyl-CoA carboxylase alpha is essential to breast cancer cell survival. Cancer Res. 2006;66(10):5287-94. Epub 2006/05/19. doi: 10.1158/0008-5472.CAN-05-1489. PubMed PMID: 16707454.

63. Flavin R, Zadra G, Loda M. Metabolic alterations and targeted therapies in prostate cancer. J Pathol. 2011;223(2):283-94. Epub 2010/12/03. doi: 10.1002/path.2809. PubMed PMID: 21125681; PMCID: PMC3197856.

64. Migita T, Narita T, Nomura K, Miyagi E, Inazuka F, Matsuura M, Ushijima M, Mashima T, Seimiya H, Satoh Y, Okumura S, Nakagawa K, Ishikawa Y. ATP citrate lyase: activation and therapeutic implications in non-small cell lung cancer. Cancer Res. 2008;68(20):8547-54. Epub 2008/10/17. doi: 10.1158/0008-5472.CAN-08-1235. PubMed PMID: 18922930.

65. Milgraum LZ, Witters LA, Pasternack GR, Kuhajda FP. Enzymes of the fatty acid synthesis pathway are highly expressed in in situ breast carcinoma. Clin Cancer Res. 1997;3(11):2115-20. Epub 1998/11/17. PubMed PMID: 9815604.

66. Madison BB. Srebp2: A master regulator of sterol and fatty acid synthesis. J Lipid Res. 2016;57(3):333-5. Epub 2016/01/23. doi: 10.1194/jlr.C066712. PubMed PMID: 26798145; PMCID: PMC4766982.

67. Campion O, Al Khalifa T, Langlois B, Thevenard-Devy J, Salesse S, Savary K, Schneider C, Etique N, Dedieu S, Devy J. Contribution of the Low-Density Lipoprotein Receptor Family to Breast Cancer Progression. Front Oncol. 2020;10:882. Epub 2020/08/28. doi: 10.3389/fonc.2020.00882. PubMed PMID: 32850302; PMCID: PMC7406569.

68. Ricoult SJ, Yecies JL, Ben-Sahra I, Manning BD. Oncogenic PI3K and K-Ras stimulate de novo lipid synthesis through mTORC1 and SREBP. Oncogene. 2016;35(10):1250-60. Epub 2015/06/02. doi: 10.1038/onc.2015.179. PubMed PMID: 26028026; PMCID: PMC4666838.

69. Guo D, Reinitz F, Youssef M, Hong C, Nathanson D, Akhavan D, Kuga D, Amzajerdi AN, Soto H, Zhu S, Babic I, Tanaka K, Dang J, Iwanami A, Gini B, Dejesus J, Lisiero DD, Huang TT, Prins RM, Wen PY, Robins HI, Prados MD, Deangelis LM, Mellinghoff IK, Mehta MP, James CD, Chakravarti A, Cloughesy TF, Tontonoz P, Mischel PS. An LXR agonist promotes glioblastoma cell death through inhibition of an EGFR/AKT/SREBP-1/LDLR-dependent pathway. Cancer Discov. 2011;1(5):442-56. Epub 2011/11/08. doi: 10.1158/2159-8290.CD-11-0102. PubMed PMID: 22059152; PMCID: PMC3207317.

70. Owen OE, Kalhan SC, Hanson RW. The key role of anaplerosis and cataplerosis for citric acid cycle function. J Biol Chem. 2002;277(34):30409-12. Epub 2002/06/28. doi: 10.1074/jbc.R200006200. PubMed PMID: 12087111.

71. Altman BJ, Stine ZE, Dang CV. From Krebs to clinic: glutamine metabolism to cancer therapy. Nat Rev Cancer. 2016;16(11):749. Epub 2017/07/14. doi: 10.1038/nrc.2016.114. PubMed PMID: 28704361.

72. Bott AJ, Peng IC, Fan Y, Faubert B, Zhao L, Li J, Neidler S, Sun Y, Jaber N, Krokowski D, Lu W, Pan JA, Powers S, Rabinowitz J, Hatzoglou M, Murphy DJ, Jones R, Wu S, Girnun G, Zong WX. Oncogenic Myc Induces Expression of Glutamine Synthetase through Promoter Demethylation. Cell Metab. 2015;22(6):1068-77. Epub 2015/11/26. doi: 10.1016/j.cmet.2015.09.025. PubMed PMID: 26603296; PMCID: PMC4670565.

73. Dias MM, Adamoski D, Dos Reis LM, Ascencao CFR, de Oliveira KRS, Mafra ACP, da Silva Bastos AC, Quintero M, de GCC, Ferreira IM, Fidelis CHV, Rocco SA, Bajgelman MC, Stine Z, Berindan-Neagoe I, Calin GA, Ambrosio ALB, Dias SMG. GLS2 is protumorigenic in breast cancers. Oncogene. 2020;39(3):690-702. Epub 2019/09/22. doi: 10.1038/s41388-019-1007-z. PubMed PMID: 31541193.

74. Saha SK, Islam SMR, Abdullah-Al-Wadud M, Islam S, Ali F, Park KS. Multiomics Analysis Reveals that GLS and GLS2 Differentially Modulate the Clinical Outcomes of Cancer. J Clin Med. 2019;8(3). Epub 2019/03/16. doi: 10.3390/jcm8030355. PubMed PMID: 30871151; PMCID: PMC6463114.

75. Zhang J, Mao S, Guo Y, Wu Y, Yao X, Huang Y. Inhibition of GLS suppresses proliferation and promotes apoptosis in prostate cancer. Biosci Rep. 2019;39(6). Epub 2019/06/15. doi: 10.1042/BSR20181826. PubMed PMID: 31196962; PMCID: PMC6591571.

76. Qing G, Li B, Vu A, Skuli N, Walton ZE, Liu X, Mayes PA, Wise DR, Thompson CB, Maris JM, Hogarty MD, Simon MC. ATF4 regulates MYC-mediated neuroblastoma cell death upon glutamine deprivation. Cancer Cell. 2012;22(5):631-44. Epub 2012/11/17. doi: 10.1016/j.ccr.2012.09.021. PubMed PMID: 23153536; PMCID: PMC3510660.

77. Yoo HC, Yu YC, Sung Y, Han JM. Glutamine reliance in cell metabolism. Exp Mol Med. 2020;52(9):1496-516. Epub 2020/09/19. doi: 10.1038/s12276-020-00504-8. PubMed PMID: 32943735.

78. Son J, Lyssiotis CA, Ying H, Wang X, Hua S, Ligorio M, Perera RM, Ferrone CR, Mullarky E, Shyh-Chang N, Kang Y, Fleming JB, Bardeesy N, Asara JM, Haigis MC, DePinho RA, Cantley LC, Kimmelman AC. Glutamine supports pancreatic cancer growth through a KRAS-regulated metabolic pathway. Nature. 2013;496(7443):101-5. Epub 2013/03/29. doi: 10.1038/nature12040. PubMed PMID: 23535601; PMCID: PMC3656466.

79. Price GS, Page RL, Riviere JE, Cline JM, Thrall DE. Pharmacokinetics and toxicity of oral and intravenous lonidamine in dogs. Cancer Chemother Pharmacol. 1996;38(2):129-35. Epub 1996/01/01. doi: 10.1007/s002800050460. PubMed PMID: 8616902.

80. Ko YH, Smith BL, Wang Y, Pomper MG, Rini DA, Torbenson MS, Hullihen J, Pedersen PL. Advanced cancers: eradication in all cases using 3-bromopyruvate therapy to deplete ATP. Biochem Biophys Res Commun. 2004;324(1):269-75. Epub 2004/10/07. doi: 10.1016/j.bbrc.2004.09.047. PubMed PMID: 15465013.

81. Pedersen PL. The cancer cell's "power plants" as promising therapeutic targets: an overview. J Bioenerg Biomembr. 2007;39(1):1-12. Epub 2007/04/04. doi: 10.1007/s10863-007-9070-5. PubMed PMID: 17404823.

82. Ganapathy-Kanniappan S, Geschwind JF, Kunjithapatham R, Buijs M, Vossen JA, Tchernyshyov I, Cole RN, Syed LH, Rao PP, Ota S, Vali M. Glyceraldehyde-3-phosphate dehydrogenase (GAPDH) is pyruvylated during 3-bromopyruvate mediated cancer cell

death. Anticancer Res. 2009;29(12):4909-18. Epub 2010/01/02. PubMed PMID: 20044597; PMCID: PMC3743725.

83. Pereira da Silva AP, El-Bacha T, Kyaw N, dos Santos RS, da-Silva WS, Almeida FC, Da Poian AT, Galina A. Inhibition of energy-producing pathways of HepG2 cells by 3-bromopyruvate. Biochem J. 2009;417(3):717-26. Epub 2008/10/24. doi: 10.1042/BJ20080805. PubMed PMID: 18945211.

84. Jain RK, Munn LL, Fukumura D. Dissecting tumour pathophysiology using intravital microscopy. Nat Rev Cancer. 2002;2(4):266-76. Epub 2002/05/11. doi: 10.1038/nrc778. PubMed PMID: 12001988.

85. Le A, Stine ZE, Nguyen C, Afzal J, Sun P, Hamaker M, Siegel NM, Gouw AM, Kang BH, Yu SH, Cochran RL, Sailor KA, Song H, Dang CV. Tumorigenicity of hypoxic respiring cancer cells revealed by a hypoxia-cell cycle dual reporter. Proc Natl Acad Sci U S A. 2014;111(34):12486-91. Epub 2014/08/13. doi: 10.1073/pnas.1402012111. PubMed PMID: 25114222; PMCID: PMC4151727.

86. Rumsey WL, Schlosser C, Nuutinen EM, Robiolio M, Wilson DF. Cellular energetics and the oxygen dependence of respiration in cardiac myocytes isolated from adult rat. J Biol Chem. 1990;265(26):15392-402. Epub 1990/09/15. PubMed PMID: 2394731.

87. Pollak M. Overcoming Drug Development Bottlenecks With Repurposing: Repurposing biguanides to target energy metabolism for cancer treatment. Nat Med. 2014;20(6):591-3. Epub 2014/06/06. doi: 10.1038/nm.3596. PubMed PMID: 24901568.

88. Pollak M. The insulin and insulin-like growth factor receptor family in neoplasia: an update. Nat Rev Cancer. 2012;12(3):159-69. Epub 2012/02/18. doi: 10.1038/nrc3215. PubMed PMID: 22337149.

89. Weng TC, Yang YH, Lin SJ, Tai SH. A systematic review and meta-analysis on the therapeutic equivalence of statins. J Clin Pharm Ther. 2010;35(2):139-51. Epub 2010/05/12. doi: 10.1111/j.1365-2710.2009.01085.x. PubMed PMID: 20456733.

90. Kuoppala J, Lamminpaa A, Pukkala E. Statins and cancer: A systematic review and meta-analysis. Eur J Cancer. 2008;44(15):2122-32. Epub 2008/08/19. doi: 10.1016/j.ejca.2008.06.025. PubMed PMID: 18707867.

91. Gross MI, Demo SD, Dennison JB, Chen L, Chernov-Rogan T, Goyal B, Janes JR, Laidig GJ, Lewis ER, Li J, Mackinnon AL, Parlati F, Rodriguez ML, Shwonek PJ, Sjogren EB, Stanton TF, Wang T, Yang J, Zhao F, Bennett MK. Antitumor activity of the glutaminase inhibitor CB-839 in triple-negative breast cancer. Mol Cancer Ther.

2014;13(4):890-901. Epub 2014/02/14. doi: 10.1158/1535-7163.MCT-13-0870. PubMed PMID: 24523301.

92. Jacque N, Ronchetti AM, Larrue C, Meunier G, Birsen R, Willems L, Saland E, Decroocq J, Maciel TT, Lambert M, Poulain L, Hospital MA, Sujobert P, Joseph L, Chapuis N, Lacombe C, Moura IC, Demo S, Sarry JE, Recher C, Mayeux P, Tamburini J, Bouscary D. Targeting glutaminolysis has antileukemic activity in acute myeloid leukemia and synergizes with BCL-2 inhibition. Blood. 2015;126(11):1346-56. Epub 2015/07/19. doi: 10.1182/blood-2015-01-621870. PubMed PMID: 26186940; PMCID: PMC4608389.

93. Le A, Lane AN, Hamaker M, Bose S, Gouw A, Barbi J, Tsukamoto T, Rojas CJ, Slusher BS, Zhang H, Zimmerman LJ, Liebler DC, Slebos RJ, Lorkiewicz PK, Higashi RM, Fan TW, Dang CV. Glucose-independent glutamine metabolism via TCA cycling for proliferation and survival in B cells. Cell Metab. 2012;15(1):110-21. Epub 2012/01/10. doi: 10.1016/j.cmet.2011.12.009. PubMed PMID: 22225880; PMCID: PMC3345194.

94. Xiang Y, Stine ZE, Xia J, Lu Y, O'Connor RS, Altman BJ, Hsieh AL, Gouw AM, Thomas AG, Gao P, Sun L, Song L, Yan B, Slusher BS, Zhuo J, Ooi LL, Lee CG, Mancuso A, McCallion AS, Le A, Milone MC, Rayport S, Felsher DW, Dang CV. Targeted inhibition of tumor-specific glutaminase diminishes cell-autonomous tumorigenesis. J Clin Invest. 2015;125(6):2293-306. Epub 2015/04/29. doi: 10.1172/JCI75836. PubMed PMID: 25915584; PMCID: PMC4497742.

95. Yuneva MO, Fan TW, Allen TD, Higashi RM, Ferraris DV, Tsukamoto T, Mates JM, Alonso FJ, Wang C, Seo Y, Chen X, Bishop JM. The metabolic profile of tumors depends on both the responsible genetic lesion and tissue type. Cell Metab. 2012;15(2):157-70. Epub 2012/02/14. doi: 10.1016/j.cmet.2011.12.015. PubMed PMID: 22326218; PMCID: PMC3282107.

96. Wang JY. The capable ABL: what is its biological function? Mol Cell Biol. 2014;34(7):1188-97. Epub 2014/01/15. doi: 10.1128/MCB.01454-13. PubMed PMID: 24421390; PMCID: PMC3993570.

97. Gil-Henn H, Patsialou A, Wang Y, Warren MS, Condeelis JS, Koleske AJ. Arg/Abl2 promotes invasion and attenuates proliferation of breast cancer in vivo. Oncogene. 2013;32(21):2622-30. Epub 2012/07/11. doi: 10.1038/onc.2012.284. PubMed PMID: 22777352; PMCID: PMC3473103.

98. Gu JJ, Lavau CP, Pugacheva E, Soderblom EJ, Moseley MA, Pendergast AM. Abl family kinases modulate T cell-mediated inflammation and chemokine-induced

migration through the adaptor HEF1 and the GTPase Rap1. Sci Signal. 2012;5(233):ra51. Epub 2012/07/20. doi: 10.1126/scisignal.2002632. PubMed PMID: 22810897; PMCID: PMC3602906.

99. Gu JJ, Rouse C, Xu X, Wang J, Onaitis MW, Pendergast AM. Inactivation of ABL kinases suppresses non-small cell lung cancer metastasis. JCI Insight. 2016;1(21):e89647. Epub 2016/12/27. doi: 10.1172/jci.insight.89647. PubMed PMID: 28018973; PMCID: PMC5161211.

100. Hoj J.P. MB, Pendergast A.M. The ABL2 kinase regulates an HSF1-dependent transcriptional program required for lung adenocarcinoma brain metastasis. Proc Natl Acad Sci U S A. 2020.

101. Hoj JP MB, Pendergast AM. A TAZ-AXL-ABL2 Feed-Forward Signaling Axis Promotes Lung Adenocarcinoma Brain Metastasis. Cell Reports. 2019;29(11):3421-34. Epub 2019/12/12. doi: 10.1016/j.celrep.2019.11.018.

102. Imam SZ, Zhou Q, Yamamoto A, Valente AJ, Ali SF, Bains M, Roberts JL, Kahle PJ, Clark RA, Li S. Novel regulation of parkin function through c-Abl-mediated tyrosine phosphorylation: implications for Parkinson's disease. J Neurosci. 2011;31(1):157-63. Epub 2011/01/07. doi: 10.1523/JNEUROSCI.1833-10.2011. PubMed PMID: 21209200; PMCID: PMC3039694.

103. Khatri A, Kraft BD, Tata PR, Randell SH, Piantadosi CA, Pendergast AM. ABL kinase inhibition promotes lung regeneration through expansion of an SCGB1A1+ SPC+ cell population following bacterial pneumonia. Proc Natl Acad Sci U S A. 2019;116(5):1603-12. Epub 2019/01/19. doi: 10.1073/pnas.1816030116. PubMed PMID: 30655340; PMCID: PMC6358689.

104. Meirson T, Genna A, Lukic N, Makhnii T, Alter J, Sharma VP, Wang Y, Samson AO, Condeelis JS, Gil-Henn H. Targeting invadopodia-mediated breast cancer metastasis by using ABL kinase inhibitors. Oncotarget. 2018;9(31):22158-83. Epub 2018/05/19. doi: 10.18632/oncotarget.25243. PubMed PMID: 29774130; PMCID: PMC5955141.

105. Suh Y, Yoon CH, Kim RK, Lim EJ, Oh YS, Hwang SG, An S, Yoon G, Gye MC, Yi JM, Kim MJ, Lee SJ. Claudin-1 induces epithelial-mesenchymal transition through activation of the c-Abl-ERK signaling pathway in human liver cells. Oncogene. 2013;32(41):4873-82. Epub 2012/11/20. doi: 10.1038/onc.2012.505. PubMed PMID: 23160379.

106. Wang J, Rouse C, Jasper JS, Pendergast AM. ABL kinases promote breast cancer osteolytic metastasis by modulating tumor-bone interactions through TAZ and STAT5 signaling. Sci Signal. 2016;9(413):ra12. Epub 2016/02/04. doi: 10.1126/scisignal.aad3210. PubMed PMID: 26838548; PMCID: PMC4991033.

107. Wang J, Pendergast AM. The Emerging Role of ABL Kinases in Solid Tumors. Trends Cancer. 2015;1(2):110-23. Epub 2015/12/09. doi: 10.1016/j.trecan.2015.07.004. PubMed PMID: 26645050; PMCID: PMC4669955.

108. Bradley WD, Koleske AJ. Regulation of cell migration and morphogenesis by Abl-family kinases: emerging mechanisms and physiological contexts. J Cell Sci. 2009;122(Pt 19):3441-54. Epub 2009/09/18. doi: 10.1242/jcs.039859. PubMed PMID: 19759284; PMCID: PMC2746129.

109. Abelson HT, Rabstein LS. Lymphosarcoma: virus-induced thymic-independent disease in mice. Cancer Res. 1970;30(8):2213-22. Epub 1970/08/01. PubMed PMID: 4318922.

110. Ben-Neriah Y, Daley GQ, Mes-Masson AM, Witte ON, Baltimore D. The chronic myelogenous leukemia-specific P210 protein is the product of the bcr/abl hybrid gene. Science. 1986;233(4760):212-4. Epub 1986/07/11. doi: 10.1126/science.3460176. PubMed PMID: 3460176.

111. Greuber EK, Smith-Pearson P, Wang J, Pendergast AM. Role of ABL family kinases in cancer: from leukaemia to solid tumours. Nat Rev Cancer. 2013;13(8):559-71. Epub 2013/07/12. doi: 10.1038/nrc3563. PubMed PMID: 23842646; PMCID: PMC3935732.

112. Gu JJ, Hoj J, Rouse C, Pendergast AM. Mesenchymal stem cells promote metastasis through activation of an ABL-MMP9 signaling axis in lung cancer cells. PLoS One. 2020;15(10):e0241423. Epub 2020/10/30. doi: 10.1371/journal.pone.0241423. PubMed PMID: 33119681.

113. Khatri A, Gu JJ, McKernan CM, Xu X, Pendergast AM. ABL kinase inhibition sensitizes primary lung adenocarcinomas to chemotherapy by promoting tumor cell differentiation. Oncotarget. 2019;10(20):1874-86. Epub 2019/04/09. doi: 10.18632/oncotarget.26740. PubMed PMID: 30956771; PMCID: PMC6443011.

114. Ganguly SS, Fiore LS, Sims JT, Friend JW, Srinivasan D, Thacker MA, Cibull ML, Wang C, Novak M, Kaetzel DM, Plattner R. c-Abl and Arg are activated in human primary melanomas, promote melanoma cell invasion via distinct pathways, and drive metastatic progression. Oncogene. 2012;31(14):1804-16. Epub 2011/09/06. doi: 10.1038/onc.2011.361. PubMed PMID: 21892207; PMCID: PMC3235241.

115. Jain A, Tripathi R, Turpin CP, Wang C, Plattner R. Abl kinase regulation by BRAF/ERK and cooperation with Akt in melanoma. Oncogene. 2017;36(32):4585-96. Epub 2017/04/04. doi: 10.1038/onc.2017.76. PubMed PMID: 28368422; PMCID: PMC5552414.

116. Tripathi R, Fiore LS, Richards DL, Yang Y, Liu J, Wang C, Plattner R. Abl and Arg mediate cysteine cathepsin secretion to facilitate melanoma invasion and metastasis. Sci Signal. 2018;11(518). Epub 2018/02/22. doi: 10.1126/scisignal.aao0422. PubMed PMID: 29463776; PMCID: PMC6642731.

117. Yoon CH, Kim MJ, Park MJ, Park IC, Hwang SG, An S, Choi YH, Yoon G, Lee SJ. Claudin-1 acts through c-Abl-protein kinase Cdelta (PKCdelta) signaling and has a causal role in the acquisition of invasive capacity in human liver cells. J Biol Chem. 2010;285(1):226-33. Epub 2009/11/10. doi: 10.1074/jbc.M109.054189. PubMed PMID: 19897486; PMCID: PMC2804169.

118. Kruh GD, Perego R, Miki T, Aaronson SA. The complete coding sequence of arg defines the Abelson subfamily of cytoplasmic tyrosine kinases. Proc Natl Acad Sci U S A. 1990;87(15):5802-6. Epub 1990/08/01. doi: 10.1073/pnas.87.15.5802. PubMed PMID: 2198571; PMCID: PMC54416.

119. Colicelli J. ABL tyrosine kinases: evolution of function, regulation, and specificity. Sci Signal. 2010;3(139):re6. Epub 2010/09/16. doi: 10.1126/scisignal.3139re6. PubMed PMID: 20841568; PMCID: PMC2954126.

120. Kurochkina N, Guha U. SH3 domains: modules of protein-protein interactions. Biophys Rev. 2013;5(1):29-39. Epub 2013/03/01. doi: 10.1007/s12551-012-0081-z. PubMed PMID: 28510178; PMCID: PMC5418429.

121. Sparks AB, Rider JE, Hoffman NG, Fowlkes DM, Quillam LA, Kay BK. Distinct ligand preferences of Src homology 3 domains from Src, Yes, Abl, Cortactin, p53bp2, PLCgamma, Crk, and Grb2. Proc Natl Acad Sci U S A. 1996;93(4):1540-4. Epub 1996/02/20. doi: 10.1073/pnas.93.4.1540. PubMed PMID: 8643668; PMCID: PMC39976.

122. Hoj JP, Mayro B, Pendergast AM. The ABL2 kinase regulates an HSF1-dependent transcriptional program required for lung adenocarcinoma brain metastasis. Proc Natl Acad Sci U S A. 2020;117(52):33486-95. Epub 2020/12/16. doi: 10.1073/pnas.2007991117. PubMed PMID: 33318173.

123. Pluk H, Dorey K, Superti-Furga G. Autoinhibition of c-Abl. Cell. 2002;108(2):247-59. Epub 2002/02/08. doi: 10.1016/s0092-8674(02)00623-2. PubMed PMID: 11832214.

124. Hantschel O, Nagar B, Guettler S, Kretzschmar J, Dorey K, Kuriyan J, Superti-Furga G. A myristoyl/phosphotyrosine switch regulates c-Abl. Cell. 2003;112(6):845-57. Epub 2003/03/26. doi: 10.1016/s0092-8674(03)00191-0. PubMed PMID: 12654250.

125. Ren R, Ye ZS, Baltimore D. Abl protein-tyrosine kinase selects the Crk adapter as a substrate using SH3-binding sites. Genes Dev. 1994;8(7):783-95. Epub 1994/04/01. doi: 10.1101/gad.8.7.783. PubMed PMID: 7926767.

126. Henderson BR, Eleftheriou A. A comparison of the activity, sequence specificity, and CRM1-dependence of different nuclear export signals. Exp Cell Res. 2000;256(1):213-24. Epub 2000/03/31. doi: 10.1006/excr.2000.4825. PubMed PMID: 10739668.

127. Wen ST, Jackson PK, Van Etten RA. The cytostatic function of c-Abl is controlled by multiple nuclear localization signals and requires the p53 and Rb tumor suppressor gene products. EMBO J. 1996;15(7):1583-95. Epub 1996/04/01. PubMed PMID: 8612582; PMCID: PMC450068.

128. McWhirter JR, Wang JY. An actin-binding function contributes to transformation by the Bcr-Abl oncoprotein of Philadelphia chromosome-positive human leukemias. EMBO J. 1993;12(4):1533-46. Epub 1993/04/01. PubMed PMID: 8467803; PMCID: PMC413366.

129. Miller AL, Wang Y, Mooseker MS, Koleske AJ. The Abl-related gene (Arg) requires its F-actin-microtubule cross-linking activity to regulate lamellipodial dynamics during fibroblast adhesion. J Cell Biol. 2004;165(3):407-19. Epub 2004/05/13. doi: 10.1083/jcb.200308055. PubMed PMID: 15138293; PMCID: PMC2172189.

130. Van Etten RA, Jackson PK, Baltimore D, Sanders MC, Matsudaira PT, Janmey PA. The COOH terminus of the c-Abl tyrosine kinase contains distinct F- and G-actin binding domains with bundling activity. J Cell Biol. 1994;124(3):325-40. Epub 1994/02/01. doi: 10.1083/jcb.124.3.325. PubMed PMID: 8294516; PMCID: PMC2119935.

131. Wang Y, Miller AL, Mooseker MS, Koleske AJ. The Abl-related gene (Arg) nonreceptor tyrosine kinase uses two F-actin-binding domains to bundle F-actin. Proc Natl Acad Sci U S A. 2001;98(26):14865-70. Epub 2001/12/26. doi: 10.1073/pnas.251249298. PubMed PMID: 11752434; PMCID: PMC64950.

132. Cancer Genome Atlas N. Comprehensive molecular portraits of human breast tumours. Nature. 2012;490(7418):61-70. Epub 2012/09/25. doi: 10.1038/nature11412. PubMed PMID: 23000897; PMCID: PMC3465532.

133. Cerami E, Gao J, Dogrusoz U, Gross BE, Sumer SO, Aksoy BA, Jacobsen A, Byrne CJ, Heuer ML, Larsson E, Antipin Y, Reva B, Goldberg AP, Sander C, Schultz N. The cBio cancer genomics portal: an open platform for exploring multidimensional cancer genomics data. Cancer Discov. 2012;2(5):401-4. Epub 2012/05/17. doi: 10.1158/2159-8290.CD-12-0095. PubMed PMID: 22588877; PMCID: PMC3956037.

134. Simpson L, He X, Pins M, Huang X, Campbell SC, Yang XJ, Perlman EJ, Bergan RC. Renal medullary carcinoma and ABL gene amplification. J Urol. 2005;173(6):1883-8. Epub 2005/05/10. doi: 10.1097/01.ju.0000158448.56888.09. PubMed PMID: 15879768.

135. Sos ML, Michel K, Zander T, Weiss J, Frommolt P, Peifer M, Li D, Ullrich R, Koker M, Fischer F, Shimamura T, Rauh D, Mermel C, Fischer S, Stuckrath I, Heynck S, Beroukhim R, Lin W, Winckler W, Shah K, LaFramboise T, Moriarty WF, Hanna M, Tolosi L, Rahnenfuhrer J, Verhaak R, Chiang D, Getz G, Hellmich M, Wolf J, Girard L, Peyton M, Weir BA, Chen TH, Greulich H, Barretina J, Shapiro GI, Garraway LA, Gazdar AF, Minna JD, Meyerson M, Wong KK, Thomas RK. Predicting drug susceptibility of non-small cell lung cancers based on genetic lesions. J Clin Invest. 2009;119(6):1727-40. Epub 2009/05/20. doi: 10.1172/JCI37127. PubMed PMID: 19451690; PMCID: PMC2689116.

136. Sonoshita M, Itatani Y, Kakizaki F, Sakimura K, Terashima T, Katsuyama Y, Sakai Y, Taketo MM. Promotion of colorectal cancer invasion and metastasis through activation of NOTCH-DAB1-ABL-RHOGEF protein TRIO. Cancer Discov. 2015;5(2):198-211. Epub 2014/11/30. doi: 10.1158/2159-8290.CD-14-0595. PubMed PMID: 25432929.

137. Xing QT, Qu CM, Wang G. Overexpression of Abl2 predicts poor prognosis in hepatocellular carcinomas and is associated with cancer cell migration and invasion. Onco Targets Ther. 2014;7:881-5. Epub 2014/06/19. doi: 10.2147/OTT.S62348. PubMed PMID: 24940071; PMCID: PMC4051810.

138. Allington TM, Galliher-Beckley AJ, Schiemann WP. Activated Abl kinase inhibits oncogenic transforming growth factor-beta signaling and tumorigenesis in mammary tumors. FASEB J. 2009;23(12):4231-43. Epub 2009/08/20. doi: 10.1096/fj.09-138412. PubMed PMID: 19690215; PMCID: PMC2812049.

139. Srinivasan D, Sims JT, Plattner R. Aggressive breast cancer cells are dependent on activated Abl kinases for proliferation, anchorage-independent growth and survival. Oncogene. 2008;27(8):1095-105. Epub 2007/08/19. doi: 10.1038/sj.onc.1210714. PubMed PMID: 17700528.

140. Li X, Ma Q, Wang J, Liu X, Yang Y, Zhao H, Wang Y, Jin Y, Zeng J, Li J, Song L, Li X, Li P, Qian X, Cao C. c-Abl and Arg tyrosine kinases regulate lysosomal degradation of the oncoprotein Galectin-3. Cell Death Differ. 2010;17(8):1277-87. Epub 2010/02/13. doi: 10.1038/cdd.2010.8. PubMed PMID: 20150913.

141. Sourbier C, Ricketts CJ, Matsumoto S, Crooks DR, Liao PJ, Mannes PZ, Yang Y, Wei MH, Srivastava G, Ghosh S, Chen V, Vocke CD, Merino M, Srinivasan R, Krishna MC, Mitchell JB, Pendergast AM, Rouault TA, Neckers L, Linehan WM. Targeting ABL1-mediated oxidative stress adaptation in fumarate hydratase-deficient cancer. Cancer Cell. 2014;26(6):840-50. Epub 2014/12/10. doi: 10.1016/j.ccell.2014.10.005. PubMed PMID: 25490448; PMCID: PMC4386283.

142. Krebs AM, Mitschke J, Losada ML, Schmalhofer O, Boerries M, Busch H, Boettcher M, Mougiakakos D, Reichardt W, Bronsert P. The EMT-activator Zeb1 is a key factor for cell plasticity and promotes metastasis in pancreatic cancer. Nature cell biology. 2017;19(5):518-29.

143. Tsai Jeff H, Donaher Joana L, Murphy Danielle A, Chau S, Yang J. Spatiotemporal Regulation of Epithelial-Mesenchymal Transition Is Essential for Squamous Cell Carcinoma Metastasis. Cancer Cell. 2012;22(6):725-36. doi: 10.1016/j.ccr.2012.09.022.

144. Yang J, Mani SA, Donaher JL, Ramaswamy S, Itzykson RA, Come C, Savagner P, Gitelman I, Richardson A, Weinberg RA. Twist, a Master Regulator of Morphogenesis, Plays an Essential Role in Tumor Metastasis. Cell. 2004;117(7):927-39. doi: 10.1016/j.cell.2004.06.006.

145. Zheng X, Carstens JL, Kim J, Scheible M, Kaye J, Sugimoto H, Wu C-C, LeBleu VS, Kalluri R. Epithelial-to-mesenchymal transition is dispensable for metastasis but induces chemoresistance in pancreatic cancer. Nature. 2015;527(7579):525-30.

146. Bartucci M, Dattilo R, Moriconi C, Pagliuca A, Mottolese M, Federici G, Benedetto AD, Todaro M, Stassi G, Sperati F, Amabile MI, Pilozzi E, Patrizii M, Biffoni M, Maugeri-Sacca M, Piccolo S, De Maria R. TAZ is required for metastatic activity and chemoresistance of breast cancer stem cells. Oncogene. 2015;34(6):681-90. Epub 2014/02/18. doi: 10.1038/onc.2014.5. PubMed PMID: 24531710.

147. Lei QY, Zhang H, Zhao B, Zha ZY, Bai F, Pei XH, Zhao S, Xiong Y, Guan KL. TAZ promotes cell proliferation and epithelial-mesenchymal transition and is inhibited by the hippo pathway. Mol Cell Biol. 2008;28(7):2426-36. Epub 2008/01/30. doi: 10.1128/MCB.01874-07. PubMed PMID: 18227151; PMCID: PMC2268418.

148. Yamaguchi H, Taouk GM. A Potential Role of YAP/TAZ in the Interplay Between Metastasis and Metabolic Alterations. Front Oncol. 2020;10:928. Epub 2020/07/01. doi: 10.3389/fonc.2020.00928. PubMed PMID: 32596154; PMCID: PMC7300268.

149. Brabletz T, Jung A, Reu S, Porzner M, Hlubek F, Kunz-Schughart LA, Knuechel R, Kirchner T. Variable beta-catenin expression in colorectal cancers indicates tumor progression driven by the tumor environment. Proc Natl Acad Sci U S A. 2001;98(18):10356-61. Epub 2001/08/30. doi: 10.1073/pnas.171610498. PubMed PMID: 11526241; PMCID: PMC56965.

150. Sanchez-Tillo E, de Barrios O, Siles L, Cuatrecasas M, Castells A, Postigo A. beta-catenin/TCF4 complex induces the epithelial-to-mesenchymal transition (EMT)-activator ZEB1 to regulate tumor invasiveness. Proc Natl Acad Sci U S A. 2011;108(48):19204-9. Epub 2011/11/15. doi: 10.1073/pnas.1108977108. PubMed PMID: 22080605; PMCID: PMC3228467.

151. Wang F, Hou W, Chitsike L, Xu Y, Bettler C, Perera A, Bank T, Cotler SJ, Dhanarajan A, Denning MF, Ding X, Breslin P, Qiang W, Li J, Koleske AJ, Qiu W. ABL1, Overexpressed in Hepatocellular Carcinomas, Regulates Expression of NOTCH1 and Promotes Development of Liver Tumors in Mice. Gastroenterology. 2020;159(1):289-305 e16. Epub 2020/03/17. doi: 10.1053/j.gastro.2020.03.013. PubMed PMID: 32171747; PMCID: PMC7387191.

152. Yang L, Lin C, Liu ZR. P68 RNA helicase mediates PDGF-induced epithelial mesenchymal transition by displacing Axin from beta-catenin. Cell. 2006;127(1):139-55. Epub 2006/10/05. doi: 10.1016/j.cell.2006.08.036. PubMed PMID: 17018282.

153. Barnes K, McIntosh E, Whetton AD, Daley GQ, Bentley J, Baldwin SA. Chronic myeloid leukaemia: an investigation into the role of Bcr-Abl-induced abnormalities in glucose transport regulation. Oncogene. 2005;24(20):3257-67. Epub 2005/03/01. doi: 10.1038/sj.onc.1208461. PubMed PMID: 15735728.

154. Gottschalk S, Anderson N, Hainz C, Eckhardt SG, Serkova NJ. Imatinib (STI571)-mediated changes in glucose metabolism in human leukemia BCR-ABL-positive cells. Clin Cancer Res. 2004;10(19):6661-8. Epub 2004/10/12. doi: 10.1158/1078-0432.CCR-04-0039. PubMed PMID: 15475456.

155. Kumar S, Bharti A, Mishra NC, Raina D, Kharbanda S, Saxena S, Kufe D. Targeting of the c-Abl tyrosine kinase to mitochondria in the necrotic cell death response

to oxidative stress. J Biol Chem. 2001;276(20):17281-5. Epub 2001/05/15. doi: 10.1074/jbc.M101414200. PubMed PMID: 11350980.

156. Kurosu T, Ohki M, Wu N, Kagechika H, Miura O. Sorafenib induces apoptosis specifically in cells expressing BCR/ABL by inhibiting its kinase activity to activate the intrinsic mitochondrial pathway. Cancer Res. 2009;69(9):3927-36. Epub 2009/04/16. doi: 10.1158/0008-5472.CAN-08-2978. PubMed PMID: 19366808.

157. Kurmi K, Hitosugi S, Yu J, Boakye-Agyeman F, Wiese EK, Larson TR, Dai Q, Machida YJ, Lou Z, Wang L, Boughey JC, Kaufmann SH, Goetz MP, Karnitz LM, Hitosugi T. Tyrosine Phosphorylation of Mitochondrial Creatine Kinase 1 Enhances a Druggable Tumor Energy Shuttle Pathway. Cell Metab. 2018;28(6):833-47 e8. Epub 2018/09/04. doi: 10.1016/j.cmet.2018.08.008. PubMed PMID: 30174304; PMCID: PMC6281770.

158. Beran M, Cao X, Estrov Z, Jeha S, Jin G, Brien S, Talpaz M, Arlinghaus RB, Lydon NB, Kantarjian H. Selective inhibition of cell proliferation and BCR-ABL phosphorylation in acute lymphoblastic leukemia cells expressing Mr 190,000 BCR-ABL protein by a tyrosine kinase inhibitor (CGP-57148). Clinical Cancer Research. 1998;4(7):1661.

159. Deininger M, Buchdunger E, Druker BJ. The development of imatinib as a therapeutic agent for chronic myeloid leukemia. Blood. 2005;105(7):2640-53. Epub 2004/12/25. doi: 10.1182/blood-2004-08-3097. PubMed PMID: 15618470.

160. Gambacorti-Passerini C, le Coutre P, Mologni L, Fanelli M, Bertazzoli C, Marchesi E, Di Nicola M, Biondi A, Corneo GM, Belotti D, Pogliani E, Lydon NB. Inhibition of the ABL Kinase Activity Blocks the Proliferation of BCR/ABL+Leukemic Cells and Induces Apoptosis. Blood Cells, Molecules, and Diseases. 1997;23(3):380-94. doi: https://doi.org/10.1006/bcmd.1997.0155.

161. Okada M, Adachi S, Imai T, Watanabe K, Toyokuni SY, Ueno M, Zervos AS, Kroemer G, Nakahata T. A novel mechanism for imatinib mesylate-induced cell death of BCR-ABL-positive human leukemic cells: caspase-independent, necrosis-like programmed cell death mediated by serine protease activity. Blood. 2004;103(6):2299-307. Epub 2003/12/03. doi: 10.1182/blood-2003-05-1605. PubMed PMID: 14645012.

162. O'Hare T, Zabriskie MS, Eiring AM, Deininger MW. Pushing the limits of targeted therapy in chronic myeloid leukaemia. Nat Rev Cancer. 2012;12(8):513-26. Epub 2012/07/25. doi: 10.1038/nrc3317. PubMed PMID: 22825216.

163. Eide CA, O'Hare T. Chronic myeloid leukemia: advances in understanding disease biology and mechanisms of resistance to tyrosine kinase inhibitors. Current hematologic malignancy reports. 2015;10(2):158-66.

164. Pemovska T, Johnson E, Kontro M, Repasky GA, Chen J, Wells P, Cronin CN, McTigue M, Kallioniemi O, Porkka K, Murray BW, Wennerberg K. Axitinib effectively inhibits BCR-ABL1(T315I) with a distinct binding conformation. Nature. 2015;519(7541):102-5. doi: 10.1038/nature14119.

165. Sim MW, Cohen MS. The discovery and development of vandetanib for the treatment of thyroid cancer. Expert Opinion on Drug Discovery. 2014;9(1):105-14. doi: 10.1517/17460441.2014.866942.

166. Hennequin LF, Stokes ESE, Thomas AP, Johnstone C, Plé PA, Ogilvie DJ, Dukes M, Wedge SR, Kendrew J, Curwen JO. Novel 4-Anilinoquinazolines with C-7 Basic Side Chains: Design and Structure Activity Relationship of a Series of Potent, Orally Active, VEGF Receptor Tyrosine Kinase Inhibitors. Journal of Medicinal Chemistry. 2002;45(6):1300-12. doi: 10.1021/jm011022e.

167. Modi S, Seidman AD, Dickler M, Moasser M, D'Andrea G, Moynahan ME, Menell J, Panageas KS, Tan LK, Norton L. A phase II trial of imatinib mesylate monotherapy in patients with metastatic breast cancer. Breast cancer research and treatment. 2005;90(2):157-63.

168. Cristofanilli M, Morandi P, Krishnamurthy S, Reuben J, Lee B-N, Francis D, Booser DJ, Green M, Arun BK, Pusztai L. Imatinib mesylate (Gleevec®) in advanced breast cancer-expressing C-Kit or PDGFR-β: clinical activity and biological correlations. Annals of oncology. 2008;19(10):1713-9.

169. Carvajal RD, Lawrence DP, Weber JS, Gajewski TF, Gonzalez R, Lutzky J, O'Day SJ, Hamid O, Wolchok JD, Chapman PB, Sullivan RJ, Teitcher JB, Ramaiya N, Giobbie-Hurder A, Antonescu CR, Heinrich MC, Bastian BC, Corless CL, Fletcher JA, Hodi FS. Phase II Study of Nilotinib in Melanoma Harboring KIT Alterations Following Progression to Prior KIT Inhibition. Clin Cancer Res. 2015;21(10):2289-96. Epub 2015/02/20. doi: 10.1158/1078-0432.CCR-14-1630. PubMed PMID: 25695690; PMCID: PMC5013827.

170. Guo J, Carvajal RD, Dummer R, Hauschild A, Daud A, Bastian BC, Markovic SN, Queirolo P, Arance A, Berking C, Camargo V, Herchenhorn D, Petrella TM, Schadendorf D, Sharfman W, Testori A, Novick S, Hertle S, Nourry C, Chen Q, Hodi FS. Efficacy and safety of nilotinib in patients with KIT-mutated metastatic or inoperable melanoma: final

results from the global, single-arm, phase II TEAM trial. Ann Oncol. 2017;28(6):1380-7. Epub 2017/03/23. doi: 10.1093/annonc/mdx079. PubMed PMID: 28327988; PMCID: PMC5452069.

171. Wei X, Mao L, Chi Z, Sheng X, Cui C, Kong Y, Dai J, Wang X, Li S, Tang B, Lian B, Yan X, Bai X, Zhou L, Guo J, Si L. Efficacy Evaluation of Imatinib for the Treatment of Melanoma: Evidence From a Retrospective Study. Oncol Res. 2019;27(4):495-501. Epub 2018/08/05. doi: 10.3727/096504018X15331163433914. PubMed PMID: 30075827.

172. Bauman JE, Eaton KD, Wallace SG, Carr LL, Lee SJ, Jones DV, Arias-Pulido H, Cerilli LA, Martins RG. A Phase II study of pulse dose imatinib mesylate and weekly paclitaxel in patients aged 70 and over with advanced non-small cell lung cancer. BMC Cancer. 2012;12:449. Epub 2012/10/05. doi: 10.1186/1471-2407-12-449. PubMed PMID: 23033932; PMCID: PMC3517479.

173. Chew HK, Barlow WE, Albain K, Lew D, Gown A, Hayes DF, Gralow J, Hortobagyi GN, Livingston R. A phase II study of imatinib mesylate and capecitabine in metastatic breast cancer: Southwest Oncology Group Study 0338. Clin Breast Cancer. 2008;8(6):511-5. Epub 2008/12/17. doi: 10.3816/CBC.2008.n.062. PubMed PMID: 19073506; PMCID: PMC3510680.

174. Dy GK, Miller AA, Mandrekar SJ, Aubry MC, Langdon RM, Jr., Morton RF, Schild SE, Jett JR, Adjei AA. A phase II trial of imatinib (ST1571) in patients with c-kit expressing relapsed small-cell lung cancer: a CALGB and NCCTG study. Ann Oncol. 2005;16(11):1811-6. Epub 2005/08/10. doi: 10.1093/annonc/mdi365. PubMed PMID: 16087693.

175. Johnson BE, Fischer T, Fischer B, Dunlop D, Rischin D, Silberman S, Kowalski MO, Sayles D, Dimitrijevic S, Fletcher C, Hornick J, Salgia R, Le Chevalier T. Phase II study of imatinib in patients with small cell lung cancer. Clin Cancer Res. 2003;9(16 Pt 1):5880-7. Epub 2003/12/17. PubMed PMID: 14676110.

176. Tsao AS, Liu S, Fujimoto J, Wistuba, II, Lee JJ, Marom EM, Charnsangavej C, Fossella FV, Tran HT, Blumenschein GR, Papadimitrakopoulou V, Kies MS, Hong WK, Stewart DJ. Phase II trials of imatinib mesylate and docetaxel in patients with metastatic non-small cell lung cancer and head and neck squamous cell carcinoma. J Thorac Oncol. 2011;6(12):2104-11. Epub 2011/09/06. doi: 10.1097/JTO.0b013e31822e7256. PubMed PMID: 21892101.

177. Packer LM, Rana S, Hayward R, O'Hare T, Eide CA, Rebocho A, Heidorn S, Zabriskie MS, Niculescu-Duvaz I, Druker BJ, Springer C, Marais R. Nilotinib and MEK

inhibitors induce synthetic lethality through paradoxical activation of RAF in drug-resistant chronic myeloid leukemia. Cancer Cell. 2011;20(6):715-27. Epub 2011/12/16. doi: 10.1016/j.ccr.2011.11.004. PubMed PMID: 22169110; PMCID: PMC3951999.

178. Zhang J, Adrián FJ, Jahnke W, Cowan-Jacob SW, Li AG, Iacob RE, Sim T, Powers J, Dierks C, Sun F, Guo G-R, Ding Q, Okram B, Choi Y, Wojciechowski A, Deng X, Liu G, Fendrich G, Strauss A, Vajpai N, Grzesiek S, Tuntland T, Liu Y, Bursulaya B, Azam M, Manley PW, Engen JR, Daley GQ, Warmuth M, Gray NS. Targeting Bcr–Abl by combining allosteric with ATP-binding-site inhibitors. Nature. 2010;463(7280):501-6. doi: 10.1038/nature08675.

179. Wylie AA, Schoepfer J, Jahnke W, Cowan-Jacob SW, Loo A, Furet P, Marzinzik AL, Pelle X, Donovan J, Zhu W, Buonamici S, Hassan AQ, Lombardo F, Iyer V, Palmer M, Berellini G, Dodd S, Thohan S, Bitter H, Branford S, Ross DM, Hughes TP, Petruzzelli L, Vanasse KG, Warmuth M, Hofmann F, Keen NJ, Sellers WR. The allosteric inhibitor ABL001 enables dual targeting of BCR–ABL1. Nature. 2017;543(7647):733-7. doi: 10.1038/nature21702.

180. Hochhaus Aea. Efficacy and Safety Results from ASCEMBL, a Multicenter, Open-Label, Phase 3 Study of Asciminib, a First-in-Class STAMP Inhibitor, vs Bosutinib (BOS) in Patients (Pts) with Chronic Myeloid Leukemia in Chronic Phase (CML-CP) Previously Treated with ≥2 Tyrosine Kinase Inhibitors (TKIs). . Blood. 2020;136. doi: 10.1182/blood-2020-143816.

181. Wertheim JA, Forsythe K, Druker BJ, Hammer D, Boettiger D, Pear WS. BCR-ABL-induced adhesion defects are tyrosine kinase-independent. Blood. 2002;99(11):4122-30. Epub 2002/05/16. doi: 10.1182/blood.v99.11.4122. PubMed PMID: 12010816.

182. Hamilton A, Helgason GV, Schemionek M, Zhang B, Myssina S, Allan EK, Nicolini FE, Müller-Tidow C, Bhatia R, Brunton VG, Koschmieder S, Holyoake TL. Chronic myeloid leukemia stem cells are not dependent on Bcr-Abl kinase activity for their survival. Blood. 2012;119(6):1501-10. Epub 2011/12/21. doi: 10.1182/blood-2010-12-326843. PubMed PMID: 22184410; PMCID: PMC3286213.

183. Sakamoto KM, Kim KB, Kumagai A, Mercurio F, Crews CM, Deshaies RJ. Protacs: chimeric molecules that target proteins to the Skp1-Cullin-F box complex for ubiquitination and degradation. Proc Natl Acad Sci U S A. 2001;98(15):8554-9. Epub 2001/07/05. doi: 10.1073/pnas.141230798. PubMed PMID: 11438690; PMCID: PMC37474.

184. Zhao Q, Ren C, Liu L, Chen J, Shao Y, Sun N, Sun R, Kong Y, Ding X, Zhang X, Xu Y, Yang B, Yin Q, Yang X, Jiang B. Discovery of SIAIS178 as an Effective BCR-ABL

Degrader by Recruiting Von Hippel–Lindau (VHL) E3 Ubiquitin Ligase. Journal of Medicinal Chemistry. 2019;62(20):9281-98. doi: 10.1021/acs.jmedchem.9b01264.

185. Burslem GM, Schultz AR, Bondeson DP, Eide CA, Savage Stevens SL, Druker BJ, Crews CM. Targeting BCR-ABL1 in Chronic Myeloid Leukemia by PROTAC-Mediated Targeted Protein Degradation. Cancer Research. 2019;79(18):4744. doi: 10.1158/0008-5472.CAN-19-1236.

186. Lai AC, Toure M, Hellerschmied D, Salami J, Jaime-Figueroa S, Ko E, Hines J, Crews CM. Modular PROTAC Design for the Degradation of Oncogenic BCR-ABL. Angewandte Chemie (International ed in English). 2016;55(2):807-10. Epub 2015/11/23. doi: 10.1002/anie.201507634. PubMed PMID: 26593377.

187. Dong Y, Tu R, Liu H, Qing G. Regulation of cancer cell metabolism: oncogenic MYC in the driver's seat. Signal Transduct Target Ther. 2020;5(1):124. Epub 2020/07/12. doi: 10.1038/s41392-020-00235-2. PubMed PMID: 32651356; PMCID: PMC7351732.

188. Jin N, Bi A, Lan X, Xu J, Wang X, Liu Y, Wang T, Tang S, Zeng H, Chen Z, Tan M, Ai J, Xie H, Zhang T, Liu D, Huang R, Song Y, Leung EL, Yao X, Ding J, Geng M, Lin SH, Huang M. Identification of metabolic vulnerabilities of receptor tyrosine kinases-driven cancer. Nat Commun. 2019;10(1):2701. Epub 2019/06/22. doi: 10.1038/s41467-019-10427-2. PubMed PMID: 31221965; PMCID: PMC6586626.

189. Pupo E, Avanzato D, Middonti E, Bussolino F, Lanzetti L. KRAS-Driven Metabolic Rewiring Reveals Novel Actionable Targets in Cancer. Front Oncol. 2019;9:848. Epub 2019/09/24. doi: 10.3389/fonc.2019.00848. PubMed PMID: 31544066; PMCID: PMC6730590.

190. Tarrado-Castellarnau M, de Atauri P, Cascante M. Oncogenic regulation of tumor metabolic reprogramming. Oncotarget. 2016;7(38):62726-53. Epub 2017/01/04. doi: 10.18632/oncotarget.10911. PubMed PMID: 28040803; PMCID: PMC5308762.

191. Zong WX, Rabinowitz JD, White E. Mitochondria and Cancer. Mol Cell. 2016;61(5):667-76. Epub 2016/03/05. doi: 10.1016/j.molcel.2016.02.011. PubMed PMID: 26942671; PMCID: PMC4779192.

192. Hoj JP, Mayro B, Pendergast AM. A TAZ-AXL-ABL2 Feed-Forward Signaling Axis Promotes Lung Adenocarcinoma Brain Metastasis. Cell Rep. 2019;29(11):3421-34 e8. Epub 2019/12/12. doi: 10.1016/j.celrep.2019.11.018. PubMed PMID: 31825826.

193. Herbst RS, Morgensztern D, Boshoff C. The biology and management of non-small cell lung cancer. Nature. 2018;553(7689):446-54. Epub 2018/01/25. doi: 10.1038/nature25183. PubMed PMID: 29364287.

194. Deng X, Okram B, Ding Q, Zhang J, Choi Y, Adrian FJ, Wojciechowski A, Zhang G, Che J, Bursulaya B, Cowan-Jacob SW, Rummel G, Sim T, Gray NS. Expanding the diversity of allosteric bcr-abl inhibitors. J Med Chem. 2010;53(19):6934-46. Epub 2010/09/11. doi: 10.1021/jm100555f. PubMed PMID: 20828158; PMCID: PMC2951064.

195. Zhang J, Adrian FJ, Jahnke W, Cowan-Jacob SW, Li AG, Iacob RE, Sim T, Powers J, Dierks C, Sun F, Guo GR, Ding Q, Okram B, Choi Y, Wojciechowski A, Deng X, Liu G, Fendrich G, Strauss A, Vajpai N, Grzesiek S, Tuntland T, Liu Y, Bursulaya B, Azam M, Manley PW, Engen JR, Daley GQ, Warmuth M, Gray NS. Targeting Bcr-Abl by combining allosteric with ATP-binding-site inhibitors. Nature. 2010;463(7280):501-6. Epub 2010/01/15. doi: 10.1038/nature08675. PubMed PMID: 20072125; PMCID: PMC2901986.

196. Reck M, Rabe KF. Precision Diagnosis and Treatment for Advanced Non-Small-Cell Lung Cancer. N Engl J Med. 2017;377(9):849-61. Epub 2017/08/31. doi: 10.1056/NEJMra1703413. PubMed PMID: 28854088.

197. Perillo B, Di Donato M, Pezone A, Di Zazzo E, Giovannelli P, Galasso G, Castoria G, Migliaccio A. ROS in cancer therapy: the bright side of the moon. Exp Mol Med. 2020;52(2):192-203. Epub 2020/02/16. doi: 10.1038/s12276-020-0384-2. PubMed PMID: 32060354; PMCID: PMC7062874.

198. Zorov DB, Juhaszova M, Sollott SJ. Mitochondrial reactive oxygen species (ROS) and ROS-induced ROS release. Physiol Rev. 2014;94(3):909-50. Epub 2014/07/06. doi: 10.1152/physrev.00026.2013. PubMed PMID: 24987008; PMCID: PMC4101632.

199. Lin KH, Xie A, Rutter JC, Ahn YR, Lloyd-Cowden JM, Nichols AG, Soderquist RS, Koves TR, Muoio DM, MacIver NJ, Lamba JK, Pardee TS, McCall CM, Rizzieri DA, Wood KC. Systematic Dissection of the Metabolic-Apoptotic Interface in AML Reveals Heme Biosynthesis to Be a Regulator of Drug Sensitivity. Cell Metab. 2019;29(5):1217-31 e7. Epub 2019/02/19. doi: 10.1016/j.cmet.2019.01.011. PubMed PMID: 30773463; PMCID: PMC6506362.

200. Karr S. Epidemiology and management of hyperlipidemia. Am J Manag Care. 2017;23(9 Suppl):S139-S48. Epub 2017/10/06. PubMed PMID: 28978219.

201. Demidenko E, Miller TW. Statistical determination of synergy based on Bliss definition of drugs independence. PLoS One. 2019;14(11):e0224137. Epub 2019/11/26. doi: 10.1371/journal.pone.0224137. PubMed PMID: 31765385; PMCID: PMC6876842.

202. Chou CW, Lin CH, Hsiao TH, Lo CC, Hsieh CY, Huang CC, Sher YP. Therapeutic effects of statins against lung adenocarcinoma via p53 mutant-mediated apoptosis. Sci Rep. 2019;9(1):20403. Epub 2020/01/02. doi: 10.1038/s41598-019-56532-6. PubMed PMID: 31892709; PMCID: PMC6938497.

203. Otahal A, Aydemir D, Tomasich E, Minichsdorfer C. Delineation of cell death mechanisms induced by synergistic effects of statins and erlotinib in non-small cell lung cancer cell (NSCLC) lines. Sci Rep. 2020;10(1):959. Epub 2020/01/24. doi: 10.1038/s41598-020-57707-2. PubMed PMID: 31969600; PMCID: PMC6976657.

204. Han JY, Lee SH, Yoo NJ, Hyung LS, Moon YJ, Yun T, Kim HT, Lee JS. A randomized phase II study of gefitinib plus simvastatin versus gefitinib alone in previously treated patients with advanced non-small cell lung cancer. Clin Cancer Res. 2011;17(6):1553-60. Epub 2011/03/18. doi: 10.1158/1078-0432.CCR-10-2525. PubMed PMID: 21411446.

205. Lee Y, Lee KH, Lee GK, Lee SH, Lim KY, Joo J, Go YJ, Lee JS, Han JY. Randomized Phase II Study of Afatinib Plus Simvastatin Versus Afatinib Alone in Previously Treated Patients with Advanced Nonadenocarcinomatous Non-small Cell Lung Cancer. Cancer Res Treat. 2017;49(4):1001-11. Epub 2017/01/24. doi: 10.4143/crt.2016.546. PubMed PMID: 28111428; PMCID: PMC5654166.

206. Seckl MJ, Ottensmeier CH, Cullen M, Schmid P, Ngai Y, Muthukumar D, Thompson J, Harden S, Middleton G, Fife KM, Crosse B, Taylor P, Nash S, Hackshaw A. Multicenter, Phase III, Randomized, Double-Blind, Placebo-Controlled Trial of Pravastatin Added to First-Line Standard Chemotherapy in Small-Cell Lung Cancer (LUNGSTAR). J Clin Oncol. 2017;35(14):1506-14. Epub 2017/02/28. doi: 10.1200/JCO.2016.69.7391. PubMed PMID: 28240967; PMCID: PMC5455702.

207. Warren CFA, Wong-Brown MW, Bowden NA. BCL-2 family isoforms in apoptosis and cancer. Cell Death Dis. 2019;10(3):177. Epub 2019/02/23. doi: 10.1038/s41419-019-1407-6. PubMed PMID: 30792387; PMCID: PMC6384907.

208. Garrido C, Galluzzi L, Brunet M, Puig PE, Didelot C, Kroemer G. Mechanisms of cytochrome c release from mitochondria. Cell Death Differ. 2006;13(9):1423-33. Epub 2006/05/06. doi: 10.1038/sj.cdd.4401950. PubMed PMID: 16676004.

209. Thurnher M, Nussbaumer O, Gruenbacher G. Novel aspects of mevalonate pathway inhibitors as antitumor agents. Clin Cancer Res. 2012;18(13):3524-31. Epub 2012/04/25. doi: 10.1158/1078-0432.CCR-12-0489. PubMed PMID: 22529099.

210. Konstantinopoulos PA, Papavassiliou AG. Multilevel modulation of the mevalonate and protein-prenylation circuitries as a novel strategy for anticancer therapy. Trends Pharmacol Sci. 2007;28(1):6-13. Epub 2006/12/08. doi: 10.1016/j.tips.2006.11.005. PubMed PMID: 17150261.

211. Lobell RB, Liu D, Buser CA, Davide JP, DePuy E, Hamilton K, Koblan KS, Lee Y, Mosser S, Motzel SL, Abbruzzese JL, Fuchs CS, Rowinsky EK, Rubin EH, Sharma S, Deutsch PJ, Mazina KE, Morrison BW, Wildonger L, Yao SL, Kohl NE. Preclinical and clinical pharmacodynamic assessment of L-778,123, a dual inhibitor of farnesyl:protein transferase and geranylgeranyl:protein transferase type-I. Mol Cancer Ther. 2002;1(9):747-58. Epub 2002/12/14. PubMed PMID: 12479371.

212. Munoz MA, Jurczyluk J, Mehr S, Chai RC, Arts RJW, Sheu A, McMahon C, Center JR, Singh-Grewal D, Chaitow J, Campbell DE, Quinn JMW, Alexandrov K, Tnimov Z, Tangye SG, Simon A, Phan TG, Rogers MJ. Defective protein prenylation is a diagnostic biomarker of mevalonate kinase deficiency. J Allergy Clin Immunol. 2017;140(3):873-5 e6. Epub 2017/05/16. doi: 10.1016/j.jaci.2017.02.033. PubMed PMID: 28501347.

213. Kelly WJ, Shah NJ, Subramaniam DS. Management of Brain Metastases in Epidermal Growth Factor Receptor Mutant Non-Small-Cell Lung Cancer. Front Oncol. 2018;8:208. Epub 2018/07/19. doi: 10.3389/fonc.2018.00208. PubMed PMID: 30018881; PMCID: PMC6037690.

214. Yang H, Liang SQ, Schmid RA, Peng RW. New Horizons in KRAS-Mutant Lung Cancer: Dawn After Darkness. Front Oncol. 2019;9:953. Epub 2019/10/16. doi: 10.3389/fonc.2019.00953. PubMed PMID: 31612108; PMCID: PMC6773824.

215. Hughes TP, Mauro MJ, Cortes JE, Minami H, Rea D, DeAngelo DJ, Breccia M, Goh YT, Talpaz M, Hochhaus A, le Coutre P, Ottmann O, Heinrich MC, Steegmann JL, Deininger MWN, Janssen J, Mahon FX, Minami Y, Yeung D, Ross DM, Tallman MS, Park JH, Druker BJ, Hynds D, Duan Y, Meille C, Hourcade-Potelleret F, Vanasse KG, Lang F, Kim DW. Asciminib in Chronic Myeloid Leukemia after ABL Kinase Inhibitor Failure. N Engl J Med. 2019;381(24):2315-26. Epub 2019/12/12. doi: 10.1056/NEJMoa1902328. PubMed PMID: 31826340.

216. Wood WG, Eckert GP, Igbavboa U, Muller WE. Statins and neuroprotection: a prescription to move the field forward. Ann N Y Acad Sci. 2010;1199:69-76. Epub 2010/07/17. doi: 10.1111/j.1749-6632.2009.05359.x. PubMed PMID: 20633110; PMCID: PMC2909025.

217. Merck. Zocor (simvastatin)2020.

218. Barter PJ. High- Versus Low-Dose Statin: Effects on Cardiovascular Events and All-Cause Death. Circulation. 2018;137(19):2013-5. Epub 2018/05/08. doi: 10.1161/CIRCULATIONAHA.118.034407. PubMed PMID: 29735589.

219. Bjorkhem-Bergman L, Lindh JD, Bergman P. What is a relevant statin concentration in cell experiments claiming pleiotropic effects? Br J Clin Pharmacol. 2011;72(1):164-5. Epub 2011/01/13. doi: 10.1111/j.1365-2125.2011.03907.x. PubMed PMID: 21223360; PMCID: PMC3141200.

220. Hu M, Cheung BM, Tomlinson B. Safety of statins: an update. Ther Adv Drug Saf. 2012;3(3):133-44. Epub 2012/06/01. doi: 10.1177/2042098612439884. PubMed PMID: 25083232; PMCID: PMC4110822.

221. Kienast Y, von Baumgarten L, Fuhrmann M, Klinkert WE, Goldbrunner R, Herms J, Winkler F. Real-time imaging reveals the single steps of brain metastasis formation. Nat Med. 2010;16(1):116-22. Epub 2009/12/22. doi: 10.1038/nm.2072. PubMed PMID: 20023634.

222. Valiente M, Ahluwalia MS, Boire A, Brastianos PK, Goldberg SB, Lee EQ, Le Rhun E, Preusser M, Winkler F, Soffietti R. The Evolving Landscape of Brain Metastasis. Trends Cancer. 2018;4(3):176-96. Epub 2018/03/07. doi: 10.1016/j.trecan.2018.01.003. PubMed PMID: 29506669; PMCID: PMC6602095.

223. Clendening JW, Pandyra A, Boutros PC, El Ghamrasni S, Khosravi F, Trentin GA, Martirosyan A, Hakem A, Hakem R, Jurisica I, Penn LZ. Dysregulation of the mevalonate pathway promotes transformation. Proc Natl Acad Sci U S A. 2010;107(34):15051-6. Epub 2010/08/11. doi: 10.1073/pnas.0910258107. PubMed PMID: 20696928; PMCID: PMC2930553.

224. Moon SH, Huang CH, Houlihan SL, Regunath K, Freed-Pastor WA, Morris JPt, Tschaharganeh DF, Kastenhuber ER, Barsotti AM, Culp-Hill R, Xue W, Ho YJ, Baslan T, Li X, Mayle A, de Stanchina E, Zender L, Tong DR, D'Alessandro A, Lowe SW, Prives C. p53 Represses the Mevalonate Pathway to Mediate Tumor Suppression. Cell. 2019;176(3):564-80 e19. Epub 2018/12/26. doi: 10.1016/j.cell.2018.11.011. PubMed PMID: 30580964; PMCID: PMC6483089.

225. Villa GR, Hulce JJ, Zanca C, Bi J, Ikegami S, Cahill GL, Gu Y, Lum KM, Masui K, Yang H, Rong X, Hong C, Turner KM, Liu F, Hon GC, Jenkins D, Martini M, Armando AM, Quehenberger O, Cloughesy TF, Furnari FB, Cavenee WK, Tontonoz P, Gahman TC, Shiau AK, Cravatt BF, Mischel PS. An LXR-Cholesterol Axis Creates a Metabolic Co-Dependency for Brain Cancers. Cancer Cell. 2016;30(5):683-93. Epub 2016/10/18. doi: 10.1016/j.ccell.2016.09.008. PubMed PMID: 27746144; PMCID: PMC5479636.

226. Wang X, Huang Z, Wu Q, Prager BC, Mack SC, Yang K, Kim LJY, Gimple RC, Shi Y, Lai S, Xie Q, Miller TE, Hubert CG, Song A, Dong Z, Zhou W, Fang X, Zhu Z, Mahadev V, Bao S, Rich JN. MYC-Regulated Mevalonate Metabolism Maintains Brain Tumor-Initiating Cells. Cancer Res. 2017;77(18):4947-60. Epub 2017/07/22. doi: 10.1158/0008-5472.CAN-17-0114. PubMed PMID: 28729418; PMCID: PMC5600855.

227. Wang M, Casey PJ. Protein prenylation: unique fats make their mark on biology. Nat Rev Mol Cell Biol. 2016;17(2):110-22. Epub 2016/01/23. doi: 10.1038/nrm.2015.11. PubMed PMID: 26790532.

228. Howe EN, Burnette MD, Justice ME, Schnepp PM, Hedrick V, Clancy JW, Guldner IH, Lamere AT, Li J, Aryal UK, D'Souza-Schorey C, Zartman JJ, Zhang S. Rab11b-mediated integrin recycling promotes brain metastatic adaptation and outgrowth. Nat Commun. 2020;11(1):3017. Epub 2020/06/17. doi: 10.1038/s41467-020-16832-2. PubMed PMID: 32541798; PMCID: PMC7295786.

229. De Pinieux G, Chariot P, Ammi-Said M, Louarn F, Lejonc JL, Astier A, Jacotot B, Gherardi R. Lipid-lowering drugs and mitochondrial function: effects of HMG-CoA reductase inhibitors on serum ubiquinone and blood lactate/pyruvate ratio. Br J Clin Pharmacol. 1996;42(3):333-7. Epub 1996/09/01. doi: 10.1046/j.1365-2125.1996.04178.x. PubMed PMID: 8877024; PMCID: PMC2042680.

230. Deichmann R, Lavie C, Andrews S. Coenzyme q10 and statin-induced mitochondrial dysfunction. Ochsner J. 2010;10(1):16-21. Epub 2011/05/24. PubMed PMID: 21603349; PMCID: PMC3096178.

231. Qu H, Guo M, Chai H, Wang WT, Gao ZY, Shi DZ. Effects of Coenzyme Q10 on Statin-Induced Myopathy: An Updated Meta-Analysis of Randomized Controlled Trials. J Am Heart Assoc. 2018;7(19):e009835. Epub 2018/10/30. doi: 10.1161/JAHA.118.009835. PubMed PMID: 30371340; PMCID: PMC6404871.

232. Schirris TJ, Renkema GH, Ritschel T, Voermans NC, Bilos A, van Engelen BG, Brandt U, Koopman WJ, Beyrath JD, Rodenburg RJ, Willems PH, Smeitink JA, Russel FG. Statin-Induced Myopathy Is Associated with Mitochondrial Complex III Inhibition.

Cell Metab. 2015;22(3):399-407. Epub 2015/09/04. doi: 10.1016/j.cmet.2015.08.002. PubMed PMID: 26331605.

233. Lee JS, Roberts A, Juarez D, Vo TT, Bhatt S, Herzog LO, Mallya S, Bellin RJ, Agarwal SK, Salem AH, Xu T, Jia J, Li L, Hanna JR, Davids MS, Fleischman AG, O'Brien S, Lam LT, Leverson JD, Letai A, Schatz JH, Fruman DA. Statins enhance efficacy of venetoclax in blood cancers. Sci Transl Med. 2018;10(445). Epub 2018/06/15. doi: 10.1126/scitranslmed.aaq1240. PubMed PMID: 29899021; PMCID: PMC6336198.

234. Hebert-Chatelain E, Jose C, Gutierrez Cortes N, Dupuy JW, Rocher C, Dachary-Prigent J, Letellier T. Preservation of NADH ubiquinone-oxidoreductase activity by Src kinase-mediated phosphorylation of NDUFB10. Biochim Biophys Acta. 2012;1817(5):718-25. Epub 2012/02/11. doi: 10.1016/j.bbabio.2012.01.014. PubMed PMID: 22321370.

235. Ogura M, Yamaki J, Homma MK, Homma Y. Mitochondrial c-Src regulates cell survival through phosphorylation of respiratory chain components. Biochem J. 2012;447(2):281-9. Epub 2012/07/25. doi: 10.1042/BJ20120509. PubMed PMID: 22823520; PMCID: PMC3459221.

236. Plattner R, Kadlec L, DeMali KA, Kazlauskas A, Pendergast AM. c-Abl is activated by growth factors and Src family kinases and has a role in the cellular response to PDGF. Genes Dev. 1999;13(18):2400-11. Epub 1999/09/29. doi: 10.1101/gad.13.18.2400. PubMed PMID: 10500097; PMCID: PMC317022.

237. Cardwell CR, Mc Menamin U, Hughes CM, Murray LJ. Statin use and survival from lung cancer: a population-based cohort study. Cancer Epidemiol Biomarkers Prev. 2015;24(5):833-41. Epub 2015/05/03. doi: 10.1158/1055-9965.EPI-15-0052. PubMed PMID: 25934831.

238. Khurana V, Bejjanki HR, Caldito G, Owens MW. Statins reduce the risk of lung cancer in humans: a large case-control study of US veterans. Chest. 2007;131(5):1282-8. Epub 2007/05/15. doi: 10.1378/chest.06-0931. PubMed PMID: 17494779.

239. Wang J, Li C, Tao H, Cheng Y, Han L, Li X, Hu Y. Statin use and risk of lung cancer: a meta-analysis of observational studies and randomized controlled trials. PLoS One. 2013;8(10):e77950. Epub 2013/11/10. doi: 10.1371/journal.pone.0077950. PubMed PMID: 24205041; PMCID: PMC3808274.

240. Cristofanilli M, Morandi P, Krishnamurthy S, Reuben JM, Lee BN, Francis D, Booser DJ, Green MC, Arun BK, Pusztai L, Lopez A, Islam R, Valero V, Hortobagyi GN. Imatinib mesylate (Gleevec) in advanced breast cancer-expressing C-Kit or PDGFR-beta: clinical activity and biological correlations. Ann Oncol. 2008;19(10):1713-9. Epub

2008/06/03. doi: 10.1093/annonc/mdn352. PubMed PMID: 18515258; PMCID: PMC2735063.

241. Skora L, Mestan J, Fabbro D, Jahnke W, Grzesiek S. NMR reveals the allosteric opening and closing of Abelson tyrosine kinase by ATP-site and myristoyl pocket inhibitors. Proc Natl Acad Sci U S A. 2013;110(47):E4437-45. Epub 2013/11/06. doi: 10.1073/pnas.1314712110. PubMed PMID: 24191057; PMCID: PMC3839726.

242. Nayak L, Lee EQ, Wen PY. Epidemiology of brain metastases. Curr Oncol Rep. 2012;14(1):48-54. Epub 2011/10/21. doi: 10.1007/s11912-011-0203-y. PubMed PMID: 22012633.

243. Wefel JS, Parsons MW, Gondi V, Brown PD. Neurocognitive aspects of brain metastasis. Handb Clin Neurol. 2018;149:155-65. Epub 2018/01/09. doi: 10.1016/B978-0-12-811161-1.00012-8. PubMed PMID: 29307352.

244. Greene-Schloesser D, Robbins ME, Peiffer AM, Shaw EG, Wheeler KT, Chan MD. Radiation-induced brain injury: A review. Front Oncol. 2012;2:73. Epub 2012/07/27. doi: 10.3389/fonc.2012.00073. PubMed PMID: 22833841; PMCID: PMC3400082.

245. Patchell RA, Tibbs PA, Walsh JW, Dempsey RJ, Maruyama Y, Kryscio RJ, Markesbery WR, Macdonald JS, Young B. A randomized trial of surgery in the treatment of single metastases to the brain. N Engl J Med. 1990;322(8):494-500. Epub 1990/02/22. doi: 10.1056/NEJM199002223220802. PubMed PMID: 2405271.

246. Mahajan A, Ahmed S, McAleer MF, Weinberg JS, Li J, Brown P, Settle S, Prabhu SS, Lang FF, Levine N, McGovern S, Sulman E, McCutcheon IE, Azeem S, Cahill D, Tatsui C, Heimberger AB, Ferguson S, Ghia A, Demonte F, Raza S, Guha-Thakurta N, Yang J, Sawaya R, Hess KR, Rao G. Post-operative stereotactic radiosurgery versus observation for completely resected brain metastases: a single-centre, randomised, controlled, phase 3 trial. Lancet Oncol. 2017;18(8):1040-8. Epub 2017/07/09. doi: 10.1016/S1470-2045(17)30414-X. PubMed PMID: 28687375; PMCID: PMC5560102.

247. Lockman PR, Mittapalli RK, Taskar KS, Rudraraju V, Gril B, Bohn KA, Adkins CE, Roberts A, Thorsheim HR, Gaasch JA, Huang S, Palmieri D, Steeg PS, Smith QR. Heterogeneous blood-tumor barrier permeability determines drug efficacy in experimental brain metastases of breast cancer. Clin Cancer Res. 2010;16(23):5664-78. Epub 2010/09/11. doi: 10.1158/1078-0432.CCR-10-1564. PubMed PMID: 20829328; PMCID: PMC2999649.

248. Xie L, Nagpal S, Wakelee HA, Li G, Soltys SG, Neal JW. Osimertinib for EGFR-Mutant Lung Cancer with Brain Metastases: Results from a Single-Center Retrospective

Study. Oncologist. 2019;24(6):836-43. Epub 2018/08/22. doi: 10.1634/theoncologist.2018-0264. PubMed PMID: 30126856; PMCID: PMC6656518.

249. Soria JC, Ohe Y, Vansteenkiste J, Reungwetwattana T, Chewaskulyong B, Lee KH, Dechaphunkul A, Imamura F, Nogami N, Kurata T, Okamoto I, Zhou C, Cho BC, Cheng Y, Cho EK, Voon PJ, Planchard D, Su WC, Gray JE, Lee SM, Hodge R, Marotti M, Rukazenkov Y, Ramalingam SS, Investigators F. Osimertinib in Untreated EGFR-Mutated Advanced Non-Small-Cell Lung Cancer. N Engl J Med. 2018;378(2):113-25. Epub 2017/11/21. doi: 10.1056/NEJMoa1713137. PubMed PMID: 29151359.

250. Marcus HJ, Carpenter KL, Price SJ, Hutchinson PJ. In vivo assessment of high-grade glioma biochemistry using microdialysis: a study of energy-related molecules, growth factors and cytokines. J Neurooncol. 2010;97(1):11-23. Epub 2009/08/29. doi: 10.1007/s11060-009-9990-5. PubMed PMID: 19714445.

251. Ishiuchi S, Tsuzuki K, Yoshida Y, Yamada N, Hagimura N, Okado H, Miwa A, Kurihara H, Nakazato Y, Tamura M, Sasaki T, Ozawa S. Blockage of Ca(2+)-permeable AMPA receptors suppresses migration and induces apoptosis in human glioblastoma cells. Nat Med. 2002;8(9):971-8. Epub 2002/08/13. doi: 10.1038/nm746. PubMed PMID: 12172541.

252. Buckingham SC, Campbell SL, Haas BR, Montana V, Robel S, Ogunrinu T, Sontheimer H. Glutamate release by primary brain tumors induces epileptic activity. Nat Med. 2011;17(10):1269-74. Epub 2011/09/13. doi: 10.1038/nm.2453. PubMed PMID: 21909104; PMCID: PMC3192231.

253. Yuen TI, Morokoff AP, Bjorksten A, D'Abaco G, Paradiso L, Finch S, Wong D, Reid CA, Powell KL, Drummond KJ, Rosenthal MA, Kaye AH, O'Brien TJ. Glutamate is associated with a higher risk of seizures in patients with gliomas. Neurology. 2012;79(9):883-9. Epub 2012/07/31. doi: 10.1212/WNL.0b013e318266fa89. PubMed PMID: 22843268.

254. Robert SM, Buckingham SC, Campbell SL, Robel S, Holt KT, Ogunrinu-Babarinde T, Warren PP, White DM, Reid MA, Eschbacher JM, Berens ME, Lahti AC, Nabors LB, Sontheimer H. SLC7A11 expression is associated with seizures and predicts poor survival in patients with malignant glioma. Sci Transl Med. 2015;7(289):289ra86. Epub 2015/05/29. doi: 10.1126/scitranslmed.aaa8103. PubMed PMID: 26019222; PMCID: PMC4503260.

255. Brahmachari S, Ge P, Lee SH, Kim D, Karuppagounder SS, Kumar M, Mao X, Shin JH, Lee Y, Pletnikova O, Troncoso JC, Dawson VL, Dawson TM, Ko HS. Activation

of tyrosine kinase c-Abl contributes to alpha-synuclein-induced neurodegeneration. J Clin Invest. 2016;126(8):2970-88. Epub 2016/06/28. doi: 10.1172/JCI85456. PubMed PMID: 27348587; PMCID: PMC4966315.

256. Heyburn L, Hebron ML, Smith J, Winston C, Bechara J, Li Z, Lonskaya I, Burns MP, Harris BT, Moussa CE. Tyrosine kinase inhibition reverses TDP-43 effects on synaptic protein expression, astrocytic function and amino acid dis-homeostasis. J Neurochem. 2016;139(4):610-23. Epub 2016/08/11. doi: 10.1111/jnc.13763. PubMed PMID: 27507246.

257. Brahmachari S, Karuppagounder SS, Ge P, Lee S, Dawson VL, Dawson TM, Ko HS. c-Abl and Parkinson's Disease: Mechanisms and Therapeutic Potential. J Parkinsons Dis. 2017;7(4):589-601. Epub 2017/11/06. doi: 10.3233/JPD-171191. PubMed PMID: 29103051; PMCID: PMC5676866.

258. Karuppagounder SS, Brahmachari S, Lee Y, Dawson VL, Dawson TM, Ko HS. The c-Abl inhibitor, nilotinib, protects dopaminergic neurons in a preclinical animal model of Parkinson's disease. Sci Rep. 2014;4:4874. Epub 2014/05/03. doi: 10.1038/srep04874. PubMed PMID: 24786396; PMCID: PMC4007078.

259. Lee WJ, Moon J, Kim TJ, Jun JS, Lee HS, Ryu YJ, Lee ST, Jung KH, Park KI, Jung KY, Kim M, Lee SK, Chu K. The c-Abl inhibitor, nilotinib, as a potential therapeutic agent for chronic cerebellar ataxia. J Neuroimmunol. 2017;309:82-7. Epub 2017/06/12. doi: 10.1016/j.jneuroim.2017.05.015. PubMed PMID: 28601294.

260. Katsumata R, Ishigaki S, Katsuno M, Kawai K, Sone J, Huang Z, Adachi H, Tanaka F, Urano F, Sobue G. c-Abl inhibition delays motor neuron degeneration in the G93A mouse, an animal model of amyotrophic lateral sclerosis. PLoS One. 2012;7(9):e46185. Epub 2012/10/11. doi: 10.1371/journal.pone.0046185. PubMed PMID: 23049975; PMCID: PMC3458026.

261. Ji X, Qian J, Rahman SMJ, Siska PJ, Zou Y, Harris BK, Hoeksema MD, Trenary IA, Heidi C, Eisenberg R, Rathmell JC, Young JD, Massion PP. xCT (SLC7A11)-mediated metabolic reprogramming promotes non-small cell lung cancer progression. Oncogene. 2018;37(36):5007-19. Epub 2018/05/24. doi: 10.1038/s41388-018-0307-z. PubMed PMID: 29789716; PMCID: PMC6127081.

262. Timmerman LA, Holton T, Yuneva M, Louie RJ, Padro M, Daemen A, Hu M, Chan DA, Ethier SP, van 't Veer LJ, Polyak K, McCormick F, Gray JW. Glutamine sensitivity analysis identifies the xCT antiporter as a common triple-negative breast

tumor therapeutic target. Cancer Cell. 2013;24(4):450-65. Epub 2013/10/08. doi: 10.1016/j.ccr.2013.08.020. PubMed PMID: 24094812; PMCID: PMC3931310.

263. Lanzardo S, Conti L, Rooke R, Ruiu R, Accart N, Bolli E, Arigoni M, Macagno M, Barrera G, Pizzimenti S, Aurisicchio L, Calogero RA, Cavallo F. Immunotargeting of Antigen xCT Attenuates Stem-like Cell Behavior and Metastatic Progression in Breast Cancer. Cancer Res. 2016;76(1):62-72. Epub 2015/11/15. doi: 10.1158/0008-5472.CAN-15-1208. PubMed PMID: 26567138.

264. Dixon SJ, Lemberg KM, Lamprecht MR, Skouta R, Zaitsev EM, Gleason CE, Patel DN, Bauer AJ, Cantley AM, Yang WS, Morrison B, 3rd, Stockwell BR. Ferroptosis: an iron-dependent form of nonapoptotic cell death. Cell. 2012;149(5):1060-72. Epub 2012/05/29. doi: 10.1016/j.cell.2012.03.042. PubMed PMID: 22632970; PMCID: PMC3367386.

265. Stockwell BR, Friedmann Angeli JP, Bayir H, Bush AI, Conrad M, Dixon SJ, Fulda S, Gascon S, Hatzios SK, Kagan VE, Noel K, Jiang X, Linkermann A, Murphy ME, Overholtzer M, Oyagi A, Pagnussat GC, Park J, Ran Q, Rosenfeld CS, Salnikow K, Tang D, Torti FM, Torti SV, Toyokuni S, Woerpel KA, Zhang DD. Ferroptosis: A Regulated Cell Death Nexus Linking Metabolism, Redox Biology, and Disease. Cell. 2017;171(2):273-85. Epub 2017/10/07. doi: 10.1016/j.cell.2017.09.021. PubMed PMID: 28985560; PMCID: PMC5685180.

266. Stockwell BR, Jiang X, Gu W. Emerging Mechanisms and Disease Relevance of Ferroptosis. Trends Cell Biol. 2020;30(6):478-90. Epub 2020/05/16. doi: 10.1016/j.tcb.2020.02.009. PubMed PMID: 32413317; PMCID: PMC7230071.

267. Ursini F, Maiorino M, Valente M, Ferri L, Gregolin C. Purification from pig liver of a protein which protects liposomes and biomembranes from peroxidative degradation and exhibits glutathione peroxidase activity on phosphatidylcholine hydroperoxides. Biochim Biophys Acta. 1982;710(2):197-211. Epub 1982/02/15. doi: 10.1016/0005-2760(82)90150-3. PubMed PMID: 7066358.

268. Zilka O, Shah R, Li B, Friedmann Angeli JP, Griesser M, Conrad M, Pratt DA. On the Mechanism of Cytoprotection by Ferrostatin-1 and Liproxstatin-1 and the Role of Lipid Peroxidation in Ferroptotic Cell Death. ACS Cent Sci. 2017;3(3):232-43. Epub 2017/04/08. doi: 10.1021/acscentsci.7b00028. PubMed PMID: 28386601; PMCID: PMC5364454.

269. Habib E, Linher-Melville K, Lin HX, Singh G. Expression of xCT and activity of system xc(-) are regulated by NRF2 in human breast cancer cells in response to oxidative

stress. Redox Biol. 2015;5:33-42. Epub 2015/04/02. doi: 10.1016/j.redox.2015.03.003. PubMed PMID: 25827424; PMCID: PMC4392061.

270. Yang WH, Ding CC, Sun T, Rupprecht G, Lin CC, Hsu D, Chi JT. The Hippo Pathway Effector TAZ Regulates Ferroptosis in Renal Cell Carcinoma. Cell Rep. 2019;28(10):2501-8 e4. Epub 2019/09/05. doi: 10.1016/j.celrep.2019.07.107. PubMed PMID: 31484063.

271. Hasegawa M, Takahashi H, Rajabi H, Alam M, Suzuki Y, Yin L, Tagde A, Maeda T, Hiraki M, Sukhatme VP, Kufe D. Functional interactions of the cystine/glutamate antiporter, CD44v and MUC1-C oncoprotein in triple-negative breast cancer cells. Oncotarget. 2016;7(11):11756-69. doi: 10.18632/oncotarget.7598. PubMed PMID: 26930718; PMCID: PMC4914246.

272. Tsuchihashi K, Okazaki S, Ohmura M, Ishikawa M, Sampetrean O, Onishi N, Wakimoto H, Yoshikawa M, Seishima R, Iwasaki Y, Morikawa T, Abe S, Takao A, Shimizu M, Masuko T, Nagane M, Furnari FB, Akiyama T, Suematsu M, Baba E, Akashi K, Saya H, Nagano O. The EGF Receptor Promotes the Malignant Potential of Glioma by Regulating Amino Acid Transport System xc(-). Cancer Res. 2016;76(10):2954-63. Epub 2016/03/17. doi: 10.1158/0008-5472.CAN-15-2121. PubMed PMID: 26980765; PMCID: PMC4873328.

273. Tanos B, Pendergast AM. Abl tyrosine kinase regulates endocytosis of the epidermal growth factor receptor. J Biol Chem. 2006;281(43):32714-23. doi: 10.1074/jbc.M603126200. PubMed PMID: 16943190.

274. Gorrini C, Harris IS, Mak TW. Modulation of oxidative stress as an anticancer strategy. Nat Rev Drug Discov. 2013;12(12):931-47. Epub 2013/11/30. doi: 10.1038/nrd4002. PubMed PMID: 24287781.

275. Zeng Q, Michael IP, Zhang P, Saghafinia S, Knott G, Jiao W, McCabe BD, Galvan JA, Robinson HPC, Zlobec I, Ciriello G, Hanahan D. Synaptic proximity enables NMDAR signalling to promote brain metastasis. Nature. 2019;573(7775):526-31. Epub 2019/09/20. doi: 10.1038/s41586-019-1576-6. PubMed PMID: 31534217; PMCID: PMC6837873.

276. Rowan CG, Brunelli SM, Munson J, Flory J, Reese PP, Hennessy S, Lewis J, Mines D, Barrett JS, Bilker W, Strom BL. Clinical importance of the drug interaction between statins and CYP3A4 inhibitors: a retrospective cohort study in The Health Improvement Network. Pharmacoepidemiol Drug Saf. 2012;21(5):494-506. Epub 2012/03/17. doi: 10.1002/pds.3199. PubMed PMID: 22422642; PMCID: PMC3890414.

277. Jacobson TA. Comparative pharmacokinetic interaction profiles of pravastatin, simvastatin, and atorvastatin when coadministered with cytochrome P450 inhibitors. Am J Cardiol. 2004;94(9):1140-6. Epub 2004/11/03. doi: 10.1016/j.amjcard.2004.07.080. PubMed PMID: 15518608.

278. Murphy MP. How mitochondria produce reactive oxygen species. Biochem J. 2009;417(1):1-13. Epub 2008/12/09. doi: 10.1042/BJ20081386. PubMed PMID: 19061483; PMCID: PMC2605959.

279. Martinez-Reyes I, Cardona LR, Kong H, Vasan K, McElroy GS, Werner M, Kihshen H, Reczek CR, Weinberg SE, Gao P, Steinert EM, Piseaux R, Budinger GRS, Chandel NS. Mitochondrial ubiquinol oxidation is necessary for tumour growth. Nature. 2020;585(7824):288-92. Epub 2020/07/10. doi: 10.1038/s41586-020-2475-6. PubMed PMID: 32641834; PMCID: PMC7486261.

280. Bommi-Reddy A, Kaelin WG, Jr. Slaying RAS with a synthetic lethal weapon. Cell Res. 2010;20(2):119-21. Epub 2010/02/02. doi: 10.1038/cr.2010.16. PubMed PMID: 20118966.

281. Berndt N, Hamilton AD, Sebti SM. Targeting protein prenylation for cancer therapy. Nat Rev Cancer. 2011;11(11):775-91. Epub 2011/10/25. doi: 10.1038/nrc3151. PubMed PMID: 22020205; PMCID: PMC4037130.

282. Storck EM, Morales-Sanfrutos J, Serwa RA, Panyain N, Lanyon-Hogg T, Tolmachova T, Ventimiglia LN, Martin-Serrano J, Seabra MC, Wojciak-Stothard B, Tate EW. Dual chemical probes enable quantitative system-wide analysis of protein prenylation and prenylation dynamics. Nat Chem. 2019;11(6):552-61. Epub 2019/04/03. doi: 10.1038/s41557-019-0237-6. PubMed PMID: 30936521; PMCID: PMC6544531.

283. Gu B, Huang YZ, He XP, Joshi RB, Jang W, McNamara JO. A Peptide Uncoupling BDNF Receptor TrkB from Phospholipase Cgamma1 Prevents Epilepsy Induced by Status Epilepticus. Neuron. 2015;88(3):484-91. Epub 2015/10/21. doi: 10.1016/j.neuron.2015.09.032. PubMed PMID: 26481038; PMCID: PMC4636438.

284. Rix U, Hantschel O, Dürnberger G, Remsing Rix LL, Planyavsky M, Fernbach NV, Kaupe I, Bennett KL, Valent P, Colinge J, Köcher T, Superti-Furga G. Chemical proteomic profiles of the BCR-ABL inhibitors imatinib, nilotinib, and dasatinib reveal novel kinase and nonkinase targets. Blood. 2007;110(12):4055-63. doi: 10.1182/blood-2007-07-102061.

285. Araujo J, Logothetis C. Dasatinib: A potent SRC inhibitor in clinical development for the treatment of solid tumors. Cancer Treatment Reviews. 2010;36(6):492-500. doi: https://doi.org/10.1016/j.ctrv.2010.02.015.

286. Montero JC, Seoane S, Ocaña A, Pandiella A. Inhibition of Src Family Kinases and Receptor Tyrosine Kinases by Dasatinib: Possible Combinations in Solid Tumors. Clinical Cancer Research. 2011;17(17):5546. doi: 10.1158/1078-0432.CCR-10-2616.

287. Puttini M, Coluccia AM, Boschelli F, Cleris L, Marchesi E, Donella-Deana A, Ahmed S, Redaelli S, Piazza R, Magistroni V, Andreoni F, Scapozza L, Formelli F, Gambacorti-Passerini C. In vitro and in vivo activity of SKI-606, a novel Src-Abl inhibitor, against imatinib-resistant Bcr-Abl+ neoplastic cells. Cancer Res. 2006;66(23):11314-22. Epub 2006/11/23. doi: 10.1158/0008-5472.Can-06-1199. PubMed PMID: 17114238.

288. Remsing Rix LL, Rix U, Colinge J, Hantschel O, Bennett KL, Stranzl T, Müller A, Baumgartner C, Valent P, Augustin M, Till JH, Superti-Furga G. Global target profile of the kinase inhibitor bosutinib in primary chronic myeloid leukemia cells. Leukemia. 2009;23(3):477-85. doi: 10.1038/leu.2008.334.

289. Golas JM, Arndt K, Etienne C, Lucas J, Nardin D, Gibbons J, Frost P, Ye F, Boschelli DH, Boschelli F. SKI-606, a 4-Anilino-3-quinolinecarbonitrile Dual Inhibitor of Src and Abl Kinases, Is a Potent Antiproliferative Agent against Chronic Myelogenous Leukemia Cells in Culture and Causes Regression of K562 Xenografts in Nude Mice. Cancer Research. 2003;63(2):375.

290. O'Hare T, Shakespeare WC, Zhu X, Eide CA, Rivera VM, Wang F, Adrian LT, Zhou T, Huang W-S, Xu Q, Metcalf CA, Tyner JW, Loriaux MM, Corbin AS, Wardwell S, Ning Y, Keats JA, Wang Y, Sundaramoorthi R, Thomas M, Zhou D, Snodgrass J, Commodore L, Sawyer TK, Dalgarno DC, Deininger MWN, Druker BJ, Clackson T. AP24534, a Pan-BCR-ABL Inhibitor for Chronic Myeloid Leukemia, Potently Inhibits the T315I Mutant and Overcomes Mutation-Based Resistance. Cancer Cell. 2009;16(5):401-12. doi: https://doi.org/10.1016/j.ccr.2009.09.028.

291. Gozgit JM, Wong MJ, Wardwell S, Tyner JW, Loriaux MM, Mohemmad QK, Narasimhan NI, Shakespeare WC, Wang F, Druker BJ, Clackson T, Rivera VM. Potent Activity of Ponatinib (AP24534) in Models of FLT3-Driven Acute Myeloid Leukemia and Other Hematologic Malignancies. Molecular Cancer Therapeutics. 2011;10(6):1028. doi: 10.1158/1535-7163.MCT-10-1044.

292. Canning P, Tan L, Chu K, Lee SW, Gray NS, Bullock AN. Structural mechanisms determining inhibition of the collagen receptor DDR1 by selective and multi-targeted type II kinase inhibitors. Journal of molecular biology. 2014;426(13):2457-70. Epub 2014/04/23. doi: 10.1016/j.jmb.2014.04.014. PubMed PMID: 24768818.

293. Lierman E, Smits S, Cools J, Dewaele B, Debiec-Rychter M, Vandenberghe P. Ponatinib is active against imatinib-resistant mutants of FIP1L1-PDGFRA and KIT, and against FGFR1-derived fusion kinases. Leukemia. 2012;26(7):1693-5. doi: 10.1038/leu.2012.8.

294. Pemovska T, Johnson E, Kontro M, Repasky GA, Chen J, Wells P, Cronin CN, McTigue M, Kallioniemi O, Porkka K, Murray BW, Wennerberg K. Axitinib effectively inhibits BCR-ABL1(T315I) with a distinct binding conformation. Nature. 2015;519(7541):102-5. Epub 2015/02/18. doi: 10.1038/nature14119. PubMed PMID: 25686603.

295. Carlomagno F, Vitagliano D, Guida T, Ciardiello F, Tortora G, Vecchio G, Ryan AJ, Fontanini G, Fusco A, Santoro M. ZD6474, an Orally Available Inhibitor of KDR Tyrosine Kinase Activity, Efficiently Blocks Oncogenic RET Kinases. Cancer Research. 2002;62(24):7284.

296. Valiente M, Obenauf AC, Jin X, Chen Q, Zhang XH, Lee DJ, Chaft JE, Kris MG, Huse JT, Brogi E, Massague J. Serpins promote cancer cell survival and vascular co-option in brain metastasis. Cell. 2014;156(5):1002-16. Epub 2014/03/04. doi: 10.1016/j.cell.2014.01.040. PubMed PMID: 24581498; PMCID: PMC3988473.

297. Cortot AB, Repellin CE, Shimamura T, Capelletti M, Zejnullahu K, Ercan D, Christensen JG, Wong KK, Gray NS, Janne PA. Resistance to irreversible EGF receptor tyrosine kinase inhibitors through a multistep mechanism involving the IGF1R pathway. Cancer Res. 2013;73(2):834-43. Epub 2012/11/23. doi: 10.1158/0008-5472.CAN-12-2066. PubMed PMID: 23172312; PMCID: PMC3994895.

298. Vicent S, Luis-Ravelo D, Anton I, Garcia-Tunon I, Borras-Cuesta F, Dotor J, De Las Rivas J, Lecanda F. A novel lung cancer signature mediates metastatic bone colonization by a dual mechanism. Cancer Res. 2008;68(7):2275-85. Epub 2008/04/03. doi: 10.1158/0008-5472.CAN-07-6493. PubMed PMID: 18381434.

299. Shalem O, Sanjana NE, Hartenian E, Shi X, Scott DA, Mikkelson T, Heckl D, Ebert BL, Root DE, Doench JG, Zhang F. Genome-scale CRISPR-Cas9 knockout screening in human cells. Science. 2014;343(6166):84-7. Epub 2013/12/18. doi: 10.1126/science.1247005. PubMed PMID: 24336571; PMCID: PMC4089965.

Biography

Jillian Hattaway Luttman graduated summa cum laude from North Carolina State University majoring in Biological Sciences with a minor in Biotechnology. As an undergraduate, she conducted research in the lab of Dr. Nanette Nascone-Yoder at the North Carolina State University Veterinary school in the Department of Molecular Biomedical Sciences where she studied the molecular mechanisms of gastrointestinal tract development in *Xenopus Laevis*. She matriculated into Duke University through the Developmental and Stem Cell Biology Training Program and ultimately joined the Molecular Cancer Biology degree granting program. She performed research in the lab of Ann Marie Pendergast studying metabolic vulnerabilities in tumors treated with ABL kinase inhibitors. She has presented her research findings at multiple national and regional conferences.

Dr. Luttman's innovative research resulted in the filing of two patents: "Compositions and methods for the treatment of cancer and CNS disorders" (No.PCT/US2020/046569) and "Methods for the Prevention and Treatment of Cancer Using ABL Inhibitors and Cholestero-Modifying Agents" (Provisional Patent Appln No. 63/134,991). Her graduate work was funded by multiple grants including the NSF Graduate Research Fellowship (DGE 1644868), Duke Department of Pharmacology and Cancer Biology Industry Internship Awardee, and the Duke Proteomics and Metabolomics Grant Recipient. Her undergraduate research was funded by the ACCIAC

Research Fellowship, NSF Interdisciplinary Training in Biological and Mathematical Sciences Award, and the Goodnight Scholars Undergraduate Research Grant. Dr. Luttman has received numerous awards and scholarships such as the Duke Scholar in Molecular Medicine- Oncology and Regenerative Medicine track, Fitzgerald Academic Achievement Award, Gordon G. Hammes Faculty Teaching Award Committee, NC State University Goodnight Full-Ride Scholarship, Albert G. Myers Undergraduate Scholarship, Clyde and Dezaree Brackett Undergraduate Scholarship, Sallie Southall Cotton Undergraduate Scholarship.

During her time at Duke, Dr. Luttman was focused on mentorship and scientific advancement activities such as being the Program Director for the Duke SURPH program, participant in the Triangle ComSciCon Workshop, organizer for the Duke DSCB Program Student Recruitment, representative of the Duke University Graduate and Professional Student Council, and coordinator for the Triangle Developmental Biology Symposium. Further, she also worked a science educator through being a course developer and instructor for Girls Exploring Science and Technology, teaching assistant for the Duke Responsible Conduct of Research retreat, volunteer for the Duke FEMMES Saturday Program and Capstone, and educational outreach volunteer for the Schiele Museum.

Finally, Dr. Luttman's research initiatives have resulted in the following publications: "Luttman, JH., Lin, K., Hoj, J., Nichols, A., MacIver, N., Wood, K., Pendergast, AM. ABL allosteric inhibitors synergize with statins to promote lung cancer cell apoptosis. *Cell Reports*, (2021).", "Luttman, JH., Colemon, A., Mayro, B. et al. Role of the ABL tyrosine kinases in the epithelial–mesenchymal transition and the metastatic cascade. *Cell Communication and Signaling* 19, 59 (2021).", and "Luttman, JH., Crizer, K., Wring, S. Serotonin as a causative agent and target for treatment of idiopathic pulmonary fibrosis. In preparation.".